CENTRO DE INVESTIGACIÓN Y DE ESTUDIOS AVANZADOS DEL INSTITUTO POLITÉCNICO NACIONAL

UNIDAD ZACATENCO

DEPARTAMENTO DE CONTROL AUTOMÁTICO

"Estabilidad, control y robustez de sistemas con retardo: aplicaciones a sistemas de tráfico"

Tesis que presenta

M.C. LUIS JUÁREZ RAMIRO

Para obtener el grado de

DOCTOR EN CIENCIAS

En la especialidad de

CONTROL AUTOMÁTICO

Director de tesis

Dra. Sabine Marie Sylvie Mondié Cuzange

Ciudad de México, México Octubre 2020

CENTRO DE INVESTIGACIÓN Y DE ESTUDIOS AVANZADOS DEL INSTITUTO POLITÉCNICO NACIONAL

UNIDAD ZACATENCO

DEPARTAMENTO DE CONTROL AUTOMÁTICO

"Stability, control and robustness of delay systems: applications to traffic systems"

T H E S I S

Presented by

LUIS JUÁREZ RAMIRO

To obtain the degree of

DOCTOR OF PHILOSOPHY

In the field of

AUTOMATIC CONTROL

Thesis advisor

Prof. Sabine Marie Sylvie Mondié Cuzange

Mexico, Mexico City October 2020

Dedicado a mi Madre Olga
que siempre me ha apoyado

A mi hija Itziar

En memoria de mi hermano Gelacio

Acknowledgments

I would like to thank my thesis advisor Prof. Sabine Mondié Cuzange for her understanding and consistent support. There are no words to express my sincere gratitude for all her patience and outstanding mentorship.

I would also like to thank my committee members, Prof. Moisés Bonilla Estrada, Prof. Carlos Cuvas Castillo, Prof. Wen Yu, Prof. Alexander Poznyak Gorbatch, for their constructive remarks on the contents of this manuscript.

I'm very grateful to my family for their unconditional support and the affection with which they valued and promoted this dream. All of you are always present in my thoughts.

This research project has been supported by the National Council for Science and Technology (CONACyT), Grant 180725 and PNPC 552811.

Last but not least, I would like to thank to the community of the DCA for creating a very pleasant environment during my research. In particular to Jesús Tavares and Salvador Ortíz for their friendship during this journey.

Notations

Simbols

d_i	Headway vehicle i.
d^*, v^*	Equilibrium point values.
$h_{i,i-1}$	Communications or sensing delays.
l_i	Length vehicle i.
s_i	Position vehicle i.
$U(\tau)$	Delay Lyapunov Matrix.
v_i	Velocity vehicle i.
$\alpha_{i,i-1}$, $\beta_{i,j}$	Control gains.
σ	Exponential Decay.

Acronyms

ACC	Adaptive cruise control.
CCC	Connected cruise control.
CACC	Cooperative adaptive cruise control.
DDE	Differential difference equation.
ECACC	Extended cooperative adaptive cruise control
FDE	Functional differential equation.
LIDAR	Laser imaging detection and ranging.
V2I	Communication vehicle to infrastructure.
V2V	Communication vehicle to vehicle.

Contents

Resumen

En el presente trabajo de investigación se estudia el control de los sistemas de tráfico tomando en cuenta la problemática de retardos. En estos sistemas, los retardos son más notables principalmente en las comunicaciones inter-vehiculares y en el tiempo de reacción de los conductores, generando numerosos problemas como colisiones y estancamiento del flujo vehicular. Por estas razones, en esta tesis se realiza el control de estos procesos, asegurando un flujo de vehículos, continuo y veloz. Estos procesos se modelan por medio de sistemas con retardos concentrados o distribuidos.

Por simplicidad y para hacer el problema tratable, en el presente trabajo, se considera una cadena de vehículos terrestres siguiendo a un líder, en un escenario donde sólamente existe un carril, es decir no se consideran cambios de carril ni rebases. Tomando como base modelos de tráfico recientes, se desarrollan tres representaciones para la cadena de vehículos: i) dos que involucran retardos concentrados, ii) una que involucra retardos distribuidos.

En esta tesis se estudia una clase de controladores dinámicos predictivos cuando se aplican a sistemas lineales con retardo en el estado y en la entrada. Estos algoritmos de control compensan los retardos del sistema, dando como resultado un sistema libre de retardos y así mejorando su desempeño. En el dominio del tiempo, la estabilidad del sistema con retardos en lazo cerrado con el controlador dinámico predictivo, es equivalente a la estabilidad de un sistema con retardos concentrados y distribuidos. Por lo tanto, empleando la matriz de Lyapunov de tipo retardada en el marco de funcionales de Lyapunov-Krasovskii se derivan tres resultados i) teoría para analizar la estabilidad de sistemas con retardos concentrados y distribuidos, ii) una metodología para construir el controlador dinámico predictivo, iii) teoría para analizar la robustez de sistemas con retardos concentrados y distribuidos.

Cabe señalar que existen resultados teóricos sobre controladores dinámicos predictivos en el dominio de la frecuencia, sin embargo estos no permiten realizar un análisis detallado de robustez, mientras que éste es posible bajo el enfoque temporal.

En general, como se muestra al principio de este trabajo, un sistema de tráfico con retardos posee una respuesta más lenta y oscilatoria, el cual es un comportamiento no deseado. Los resultados obtenidos de la simulación de cadenas de vehículos confirman la efectividad del controlador dinámico predictivo, ya que compensa retardos que incluso podrían causar inestabilidad en el sistema. En la práctica, la implementación de esta clase de controladores está comprobada.

La obtención de cotas exactas de estabilidad para incertidumbre en matrices y retardos en sistemas con retardos concentrados y distribuidos, finalizan este trabajo. Algunos ejemplos académicos ilustran los resultados obtenidos.

Se espera que los resultados de este trabajo sean un punto de partida para coadyuvar a disminuir los problemas de tráfico como los embotellamientos, accidentes, la reducción en el consumo de gasolina y la emisión de contaminantes.

Abstract

This research work studies the control of traffic systems, considering delay issues. To mention just a few examples, in these systems, delays are mainly in the communications between vehicles and in the reaction time of the drivers, generating numerous problems, such as crashes and flow stagnation. For these reasons, in this thesis the control of traffic processes, ensuring a continuous and fast vehicles flow, is addressed. These processes are modeled by concentrated or distributed delay systems.

For simplicity, in the present work, a chain of ground vehicles following a leader, in a scenery where exists only a lane, and without changing lanes, are considered. On the basis of recent models, three representations for the chain of vehicles are obtained: i) two of these involving concentrated delays, and ii) one with distributed delays.

In this thesis a class of dynamic predictive controllers for linear systems with input and state delays are studied. The function of these control algorithms is to compensate the system delays, giving as a result a delay-free system, and hence improving its performance. Under the time-domain approach, the stability of the delay system in closed-loop with the dynamic predictive control is functionally equivalent to the stability of a system with concentrated and distributed delays. Therefore, by using the delay Lyapunov matrix on the Lyapunov-Krasovskii approach, three results are derived: i) a theoretical result for the stability analysis of systems with concentrated and distributed delays, ii) a methodology for constructing the dynamic predictive controller, iii) theoretical results for the robust stability analysis of systems with concentrated and distributed delays.

It is worth noting that exist theoretical results for dynamic predictive controllers on the frequency-domain approach, however these do not deeply allow a robust analysis, whereas it is possible on the time-domain.

In general, as it is shown at the beginning of the work, traffic systems with delays have a slower and oscillatory response, which is an undesired behavior. Simulated results of the chain of vehicles validate the effectiveness of the dynamic predictive controller, compensating delays even for instable systems. In practice, the implementation of this

class of controllers is verified.

Finally, in this work, exact stability bounds for matrix and delay uncertainties of linear systems with pointwise and distributed delays are obtained. Some academic examples illustrate our approach.

It is expected that the results of this work will be a starting point for reducing traffic problems such as congestion, accidents, the reduction in gasoline consumption and the emission of pollutants.

Chapter 1

Introduction

This chapter gives first a brief overview of the topics addressed in this thesis, time-delay systems, traffic systems, and their control strategies. The remainder of this chapter presents the main objectives of the work, a general overview of the thesis, and the publications that have been the result of this research.

1.1 Time-delay systems

To observe the physical phenomena of nature, the differential equations either linear or non-linear have demonstrated to be useful to determinate the state as well as the subsequent behavior of the state of the phenomena. The simplest general form is

$$\dot{x}(t) = g(x, t), \quad x(0) = c,$$

in this sense, the behavior of the solutions of these equations with constant or variable coefficients, and the stability of solutions of linear and non-linear differential equations, existence and uniqueness of solutions, are common problems. As observed, these systems depend only on the present state and can be subject to various types of initial, two-point, and multipoint boundary conditions.

Contrary to systems represented by differential equations, delay systems take account of the fact that the rate of change of physical systems depends not only on their present state, but also on their past history. According to (Bellman & Cooke, 1963; Hale & Lunel, 2013) a delay system may be mathematically described by the so called Differential-Difference Equations (DDEs) or Functional Differential Equations (FDEs) whose simplest representation is

$$B_0\dot{u}(t) + B_1\dot{u}(t-h) + A_0u(t) + A_1u(t-h) = 0, \tag{1.1}$$

where B_0, B_1, A_0, A_1 are matrix $n \times n$ coefficients, $t > 0$ is the time, and $h > 0$ is the delay. $u(t) \in R^n$ is the output of the equation. Based on the presence of the matrix coefficients, equation (1.1) result in systems of *neutral, advanced or retarded type*, respectively.

Definition 1.1. *(Bellman & Cooke, 1963)*

- Neutral type $B_0\dot{u}(t) + B_1\dot{u}(t-h) + A_0u(t) + A_1u(t-h) = 0$,
- Advanced type $B_0\dot{u}(t) + A_0u(t) + A_1u(t+h) = 0$,
- Retarded type $B_0\dot{u}(t) + A_0u(t) + A_1u(t-h) = 0$.

To know the $u(t)$ output involves past, present and future information. Systems represented by these equations belong to the class of infinite dimensional systems. The main subject of study of the time-delay systems is the stability analysis. Two approaches for the stability analysis of these systems are the frequency and time domain framework.

Frequency framework: it is restricted to linear systems, and is based on the characteristic quasipolinomial and the Nyquist stability criterion. The most common approach is the D-decomposition method developed by Neimark (1949).

Time-domain framework: this technique generalizes the Lyapunov theorem using Lyapunov - Krasovskii functionals and Lyapunov - Razumikhin functionals (Kolmanovskii, 1967; Krasovskii, 1956). Non-linear and uncertainty systems can be also addressed under this approach in particular. Complete type functionals (Kharitonov & Zhabko, 2001) are fundamental to test stability.

1.2 Traffic systems

In 1975 the National Highway traffic Safety Administration (NHTSA) developed the data system, the Fatality Analysis Reporting System (FARS) which contains data on the most severe traffic crashes, those in which someone was killed (Administration *et al.*, 2016). Based on the data, the number of young drivers 16 to 20 years old involved in fatal crashes increased by 10 percent since 2014. Other issues related to traffic systems are the fuel consumption and CO_2 emission (Suthaputchakun, Sun & Dianati, 2012), safety with respect to collision avoidance (Caveney, 2010), changing lanes (Sepulcre & Gozalvez, 2012), to name a few. These are many reasons to devote time to the study of traffic systems.

1.2.1 Mathematical models

To begin the study of traffic systems, empirical data are obtained on public roads and highways applying different sampling techniques (Chandler, Herman & Montroll, 1958; Helbing, 2001; Rothery, Gartner, Messner & Rathi, 1998). The next step is to elaborate a model that involves the desired physical variables. These models seek to capture parameters defining the traffic flow and the behaviors of the drivers and vehicles. The existing models are divided into three main types:

- Microscopic (particled-based) (Bose & Ioannou, 2003; Pipes, 1953; Treiber, Hennecke & Helbing, 2000),
- Mesoscopic (gas-kinetic) (Helbing & Treiber, 1998),
- Macroscopic (fluid-dynamic) (Treiber & Helbing, 1999).

A classical example of microscopic model is the Car Following Model where the driver follows his neighboring vehicle. Nevertheless, these mathematical models may consider some common aspects such as changing lane, single and multiple lanes, memory effects on human driving, delays, on-off ramps and vehicle dynamics.

To facilitate the modeling of traffic flow, most authors consider a platooning system with a type behavior of follow the leader, the scenario is a single lane without lane changing (Pipes, 1953; Swaroop, 1997)

1.2.2 Time-delay effects in traffic flow models

Numerous studies have been developed in order to know the origin of the time-delay in traffic dynamics. According to (Sipahi & Niculescu, 2009) the time-delay $\tau(t)$ in traffic dynamics can be classified into three main components:

- Physiological lag,
- Mechanical time lag,
- Delay time of vehicle motion,

in this way, the time-delays are included in mathematical models. Moreover, the *physiological lag* can be classified as: sensing, perception, response selection and programming and movement time. The delay contribution is introduced for human operators and information flow.

Several works where mathematical models involve different type of delays can be seen on (Bando, Hasebe, Nakanishi & Nakayama, 1998; Orosz, Krauskopf & Wilson, 2005; Orosz, Wilson & Krauskopf, 2004; Sipahi, Atay & Niculescu, 2007; Sipahi & Niculescu, 2008, 2010; Sipahi, Niculescu & Delice, 2009; Treiber, Kesting & Helbing, 2006).

1.2.3 Traffic control strategies

The common objectives of a vehicle platoon is to reduce the inter-vehicle spacings or headway. Taking advantage of this idea, automated controllers have been implemented to compensate these spacings. To name a few, control strategies are: optimal control (Jin & Orosz, 2015), adaptive control (Swaroop, Hedrick & Choi, 2001), nonlinear spacing controllers (Zhou & Peng, 2005) and decentralized control (Stankovic, Stanojevic & Siljak, 2000).

The implementation of control strategies have been possible thanks to the wireless communication vehicle to vehicle (V2V) or vehicle to infrastructure (V2I) (Caveney, 2010; Sepulcre & Gozalvez, 2012; Suthaputchakun, Sun & Dianati, 2012; Wang, Wang & Wang, 2016).

Nowadays, Adaptive cruise control (ACC) (Ioannou & Chien, 1993; Rajamani & Zhu, 2002; Shladover, 1991) allows to achieve longitudinal control on vehicle platoon. This strategy considers the motion of the vehicle immediately ahead, which is captured by using range sensor (radar, LIDAR (Laser Imaging Detection and Ranging) or camera). The disadvantage of this technology is the use of range sensor as all vehicles need to be equipped. Wireless communication, particularly the one dedicated short range communication (DSRC) (Kenney, 2011) allows the control strategy called Cooperative Adaptive cruise control (CACC) (Desjardins & Chaib-Draa, 2011; Milanés, Shladover, Spring, Nowakowski, Kawazoe & Nakamura, 2014; Naus, Vugts, Ploeg, van de Molengraft & Steinbuch, 2010). In this control strategy, range sensors monitor the vehicle ahead and a prescribed leader by wireless communication too. These technologies have been implemented in the US since the beginning of the PATH program and the SARTRE project and in Europe in the Gran Cooperative Driving Challenge. The limitation of ACC and CACC is the low penetration of automated vehicles. Taking advantage of these ideas, the Connected Cruise Control (CCC) (Orosz, 2016) arises as an alternative showing more flexibility. In this strategy, in addition to the information of the prescribed leader, the transmitted data of multiple vehicles ahead, is considered. Moreover, these vehicles can be equipped or not, allowing human drivers into the platoon. A list of studies using the

CCC control strategy comprise communication delays (Zhang & Orosz, 2013), stochastic communication delays (Qin, Gomez & Orosz, 2017), headway dynamics as acceleration (Jin & Orosz, 2014), connectivity structures (Zhang & Orosz, 2016) and uncertainties in control gains and delays (Hajdu, Zhang, Insperger & Orosz, 2016).

The stability analysis of the vehicle platoon is twofold, *plant stability* and *string stability*. The capacity of a vehicle to achieve the steady state while no disturbances occur is called *plant stability* and the ability to attenuate disturbances of vehicles ahead is named *car string stability*. The most used approach to test stability is the frequency domain (Jin & Orosz, 2014; Qin, Gomez & Orosz, 2017; Zhang & Orosz, 2016), giving rise to a variety of transfer functions to be computed and analyzed. As platoon members are added, the complexity of the analysis clearly increases.

1.3 Problem statement

In this work, the stability, control and robustness of delay systems, modeling traffic systems are addressed. The main object of study is a vehicle platoon where the scenario is a single lane. Our aim is to synchronize all followers with the leader's speed, and to keep the inter-vehicle spacing into a secure distance, as well as, to consider the time-delay generated by the data sharing. The traffic dynamics is described by means of microscopic mathematical models. The following questions are of special interest:

- How to consider the presence of delays affects stability region of platoon traffic systems?.
- How the delay compensation, using prediction schemes, affects the platoon stability?.

In light of the time-domain approach for delay systems, the above problem is carried out by using theory for linear systems with multiple pointwise and distributed delays. Moreover, this approach requires to adapt methodologies as the construction of the delay Lyapunov matrix, the dynamic predictor-based delay compensation, and the robust stability conditions for the proposed systems. Therefore, in this thesis, the main problem is:

"to develop new methodologies for the stability analysis, the input delay compensation, and the robust stability analysis for linear systems with multiple pointwise and distributed delays, which model the above problem of traffic systems".

1.4 Objectives

According to the findings in traffic systems in previous sections, it is observed that the time-delay is inherent to vehicle platoons and should not be omitted. In contrast with the use of the frequency domain approach adopted by researchers in the field, the stability analysis on the Lyapunov-Krasovskii approach in time domain framework is carried out applying functionals of complete type (Egorov, Cuvas & Mondié, 2017; Egorov & Mondié, 2014). These techniques allow us to test stability, and at the same time analyze the robustness of the system with respect to time variant perturbations. However, the implementation of the above algorithms requires new compact representations of the vehicle platoon. Next, the objectives of the present work are summarized.

Objective 1. The primary objective is to develop microscopic mathematical models, describing the traffic dynamics (velocity, position and inter-vehicle spacing), communication delays, and the driver's memory effects. In regard to the traffic scenario, it is considered to be a follow the leader type where vehicles transit in a single lane.

Objective 2. The second objective is to develop a methodology to test stability of linear systems with multiple concentrated and distributed delays.

Objective 3. The third objective is to develop a methodology to compensate the time-delay of linear systems with input and state delays. In order to achieve that objective, dynamic controllers are applied.

Objective 4. The fourth objective is to develop a methodology to test robustness of linear systems with multiple concentrated and distributed delays.

Objective 5. Finally, the last objective is to apply the above methods on the schemes obtained in the objective 1.

1.5 Outline of the thesis

A summary of the thesis is presented as follows:

Chapter 2 presents three microscopic mathematical models for the vehicle platoon. At first, a compact representation of the complete chain of vehicles, including the leader, is obtained. Based on the CCC strategy, this model is the result of a linearization of a non linear model, where the equilibrium point is defined as the constant velocity of the leader. The second representation is an extension of the ECACC strategy, which consists in introducing a complete delayed control action. Lastly, the driver's memory effects are represented by using the uniform distribution, giving rise to the third model which is also based on the ECACC strategy. Overall, the two first models are linear systems with concentrated delays, and the last one is a linear system with concentrated and distributed delays.

Chapter 3 gives a methodology for testing the stability of linear systems with multiple concentrated and distributed delays. The stability test in the time-domain is based on the Lyapunov-Krasovskii approach and the so-called delay Lyapunov matrix. Under these perspectives, the results of this chapter are summarized in a theorem, which allows the construction of a delay-free system of matrix equations. Such system is crucial for obtaining the delay Lyapunov matrix. Finally, an example illustrates how this delay matrix allows to apply stability conditions.

Chapter 4 explains the procedure for compensating the time-delay of systems with input and state delays. More specifically, this technique uses dynamic predictive controllers to compensate delays, giving rise to linear systems with multiple concentrated and distributed delays. Using the results developed in Chapter 3, an illustrative example is given.

Chapter 5 presents a methodology for testing the robustness of linear systems with multiple concentrated and distributed delays. Considering the time-domain framework, a functional which is not of complete type is used to obtain exact robust stability conditions. These conditions include both matrix parameters and delay uncertainties. For illustrative purposes, two examples are presented.

Chapter 6 shows three examples which illustrate the methods of analysis proposed in Chapters 3 and 4. For simplicity without loss of generality, including the leader, the examples are based on the models of Chapter 2 and consider three and five vehicle chains. On these scenarios, using the Lyapunov-Krasovskii approach, stability charts are constructed. In general, to limit the stability regions for previously defined space of parameters, the D-partition method is also applied. Following the results, to validate the obtained regions, numerical simulations for pairs of parameters within and out are carried out. Lastly, some concluding remarks are given.

A description of each Appendix which includes preliminary results that support this work, is listed below.

Appendix A gives the mathematical representation and necessary stability conditions for linear systems with pointwise and distributed delays.

Appendix B presents the change of variable used for σ-stabilization.

Appendix C proves the robust stability conditions for systems with multiple concentrated delays.

Appendix D reminds the definition of Kronecker product of matrices.

Finally, a summary of theoretical contributions of this study is discussed, as well as its limitations and further research directions.

1.6 Publications

This introductory part ends with a summary of the scientific contributions derived from this work, publications in journal papers, book chapters and conferences papers.

Journal Publications

1. L. Juárez, S. Mondié, and C. Cuvas. "Connected cruise control of a car platoon: A time-domain stability analysis". *Proceedings of the Institution of Mechanical Engineers, Part I: Journal of Systems and Control Engineering*, 232(6), 672-682, 2018.

2. L. Juárez, and S. Mondié. "Dynamic Predictor-based Controls: A Time-domain Stability Analysis". *IEEE Latin America Transactions*, page 1207, Vol. 17, No. 7, July 2019.

3. L. Juárez, S. Mondié, and Vladimir L. Kharitonov. "Dynamic predictor for systems with state and input delay: A time-domain robust stability analysis". *Int J Robust Nonlinear Control*. 2020;1–15.

4. L. Juárez, I. V. Alexandrova, and S. Mondié. "Robust Stability Analysis for Linear Systems with Distributed Delays: a Time-Domain Approach". Accepted to the *Int J Robust Nonlinear Control*, 2020.

Book chapters

1. C. Cuvas, A. Ramírez, L. Juárez and S. Mondié. "Scanning the Space of Parameters for Stability Regions of a Class of Time-Delay Systems; A Lyapunov Matrix Approach." Delays and Interconnections: Methodology, Algorithms and Applications. Springer, Cham, 2019. 153-167.

Conference publications

1. C. Cuvas, A. Ramírez, L. Juárez, and S. Mondié. "Scanning the space of parameters for stability regions of time-delay systems: a Lyapunov matrix approach". *Congreso Nacional de Control Automático, Querétaro, México, Septiembre 28-30, 2016.*

2. L. Juárez-Ramiro, S. Mondié, and C. Cuvas. Stability analysis of a car platoon with communication delays and headway compensation. *In 2017 4th International Conference on Control, Decision and Information Technologies (CoDIT)*, pages 0012 -0017, April 2017, Barcelona, Spain. doi: 10.1109/CoDIT.2017.8102559.

3. L. Juárez, and S. Mondié. "Lyapunov matrices for the stability analysis of a multiple distributed time-delay system with repeated piecewise function kernel". *Congreso Nacional de Control Automático, San Luis Potosí, México, 10-12 de Octubre de 2018.*

4. L. Juárez and S. Mondié. "Lyapunov matrices for the stability analysis of a system with state and input delays and dynamic predictor control". *15th International Conference on Electrical Engineering, Computing Science and Automatic Control (CCE).* Mexico City, Mexico September 5-7, 2018

5. L. Juárez and S. Mondié. "Lyapunov matrices for the stability analysis of a multiple distributed time-delay system with piecewise-function kernel". *IEEE Conference on Decision and Control (CDC), Miami Beach, FL, USA, Dec. 17-19, 2018*

6. L. Juárez, S. Mondié, and L. Vite. "Nested Stabilization for Connected Cruise Control via the Delay Lyapunov Matrix". *16th International Conference on Electrical Engineering, Computing Science and Automatic Control (CCE), Mexico City, Mexico September 11-13, 2019*

7. L. Juárez, and S. Mondié. "Dynamic Predictor-based Extended Cooperative Adaptive Cruise Control". *15th IFAC Workshop on Time Delay Systems Sinaia, Romania, September 9-11, 2019.*

8. L. Juárez, and S. Mondié. "Assisted Cooperative Adaptive Cruise Control with human memory effects". *6th International Conference on Control, Decision and Information Technologies (CoDIT'19), Paris, France, April 23-26, 2019.*

Chapter 2

Microscopic vehicle platoon models

In this chapter, three representations for chain of vehicles in closed-loop with novel control strategies, are presented. For simplicity, the scenario is a single lane, and considers all vehicles as particles. The main objective of the group is to maintain a constant velocity with a secure inter-vehicle space. In this context, the data sharing (velocity, position, acceleration, etc.) for all vehicles, including the leader, can be done downstream, upstream or both ways. The communication among vehicles can be easily done in practice, if each vehicle is equipped with the V2V wireless communication or its equivalent, but significant delays are introduced.

2.1 Model "A" based on the CCC Strategy

This representation is based on the leader following scheme and the ideas presented in (Li & Orosz, 2016). The previous work in (Li & Orosz, 2016) introduces a transfer function for each pair o vehicles, giving rise to a group of transfer functions for all the chain of vehicles. In this work, in order to apply time-domain stability approaches, a compact representation including all the vehicles is constructed.

Modeling framework. First, consider that all vehicles are CCC equipped except the leader, who only transmits communication signals. The dynamic of the leading vehicle, called vehicle 0, is considered as the input of the platoon and is modeled by

$$\dot{s}_0(t) = v_0.$$

The number of vehicles in the platoon is represented by n in Figure 2.1, and for each i-th vehicle, where $i = \overline{1, n}$, we define a dynamical representation. The main variables are:

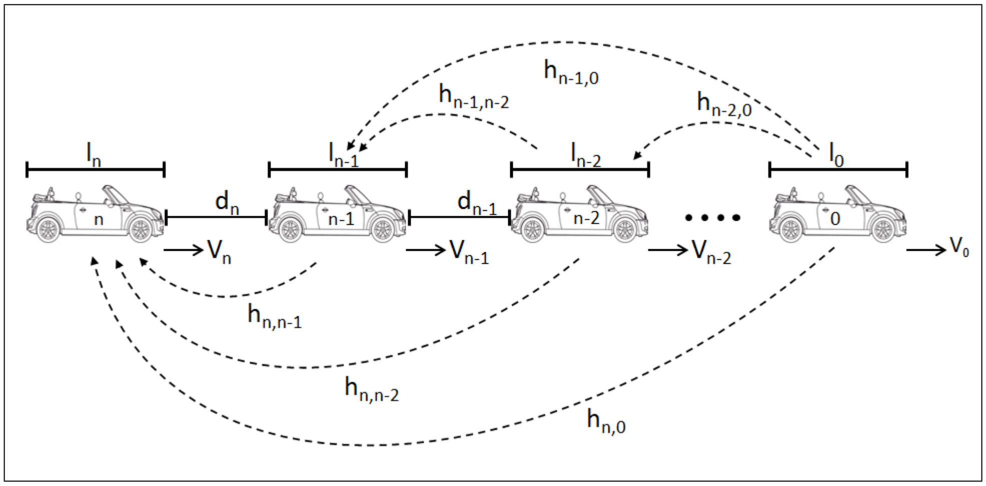

Figure 2.1: Connected vehicles system

$h_{i,i-1}$: communications or sensing delays, v_i: velocity of the vehicle i, l_i: length of the vehicle i, d_i: headway of the vehicle i, s_i: position of the vehicle i. The distance between vehicles i and $i-1$ is

$$d_i(t) = s_{i-1}(t) - s_i(t) - l_i.$$

The CCC is a consensus problem whose objective is to minimize speed differences. It is described by the non-linear system

$$\begin{aligned} \dot{d}_i(t) &= v_{i-1}(t) - v_i(t), \\ \dot{v}_i(t) &= \alpha_{i,i-1}\left(V_i(d_i(t-h_{i,i-1})) - v_i(t-h_{i,i-1})\right) + \sum_{j=0}^{i-1} \beta_{i,j}\left(v_j(t-h_{i,j}) - v_i(t-h_{i,j})\right). \end{aligned} \tag{2.1}$$

The purpose of the non-linear function $V(d)$ is to keep a gap between vehicles and a soft response. The parameters $\alpha_{i,i-1}$, $\beta_{i,j}$ are control gains.

$$V(d) = \begin{cases} 0, & d \leq d_{st} & \text{(2.2a)} \\ \dfrac{V_{max}}{2}[1 - cos(\pi(\dfrac{d - d_{st}}{d_{go} - d_{st}}))], & d_{st} \leq d \leq d_{go} & \text{(2.2b)} \\ V_{max}, & d \geq d_{go}. & \text{(2.2c)} \end{cases}$$

Real traffic parameters in (2.2) are set to be $d_{st} = 5[m]$, $d_{go} = 35[m]$, $V_{max} = 30[m/s]$, (Orosz, Wilson & Stépán, 2010). The change of variables

$$\tilde{d}_i(t) = d_i(t) - d^*, \quad \tilde{v}_i(t) = v_i(t) - v^*,$$

where the equilibrium is given by

$$d_i(t) \equiv d^*, \qquad v_i(t) \equiv v^* = V_i(d^*),$$

allows to study the system in the vicinity of the origin. By defining the variables $\tilde{x}_i(t) = [\tilde{d}_i(t) \quad \tilde{v}_i(t)]^T$, $\tilde{x}_0(t) = [0 \quad \tilde{v}_0(t)]^T$ and linearizing (2.1), we obtain

$$\dot{\tilde{x}}_i(t) = A_0^i \tilde{x}_i(t) + A_{i,i-1}\tilde{x}_i(t-h_{i,i-1}) + \sum_{j=0}^{i-1}(B_{i,j}\tilde{x}_i(t-h_{i,j}) + C_{i,j}\tilde{x}_j(t-h_{i,j})) + D_{i-1}\tilde{x}_{i-1}(t), \tag{2.3}$$

where

$$\begin{aligned} A_0^i &= \begin{bmatrix} 0 & -1 \\ 0 & 0 \end{bmatrix}, \ A_{i,i-1} = \begin{bmatrix} 0 & 0 \\ \psi_{i,i-1} & -\alpha_{i,i-1} \end{bmatrix}, \ B_{i,j} = \begin{bmatrix} 0 & 0 \\ 0 & -\beta_{i,j} \end{bmatrix}, \\ C_{i,j} &= \begin{bmatrix} 0 & 0 \\ 0 & \beta_{i,j} \end{bmatrix}, \ D_{i-1} = \begin{bmatrix} 0 & 1 \\ 0 & 0 \end{bmatrix}, \quad \psi_{i,i-1} = \alpha_{i,i-1}V_i'(d^*). \end{aligned}$$

Then, we can model a platoon dynamics by defining $x(t) = [\tilde{x}_1(t) \quad \tilde{x}_2(t) \quad \ldots \quad \tilde{x}_n(t)]^T$:

$$\begin{aligned} \dot{x}(t) = {} & \mathcal{A}_{0,0}x(t) + \mathcal{A}_{1,0}x(t-h_{1,0}) + \mathcal{A}_{2,0}x(t-h_{2,0}) + \mathcal{A}_{2,1}x(t-h_{2,1}) + \mathcal{A}_{3,0}x(t-h_{3,0}) \\ & + \mathcal{A}_{3,1}x(t-h_{3,1}) + \mathcal{A}_{3,2}x(t-h_{3,2}) + \ldots + \mathcal{A}_{n,0}x(t-h_{n,0}) + \mathcal{A}_{n,1}x(t-h_{n,1}) + \ldots \\ & + \mathcal{A}_{n,n-1}x(t-h_{n,n-1}) + \mathcal{B}_0\tilde{x}_0(t) + \mathcal{B}_1\tilde{x}_0(t-h_{1,0}) + \ldots + \mathcal{B}_n\tilde{x}_0(t-h_{n,0}), \end{aligned} \tag{2.4}$$

where, n : tail car, $\mathcal{A}_{0,0}, \ \mathcal{A}_{1,0}, \ \ldots, \mathcal{A}_{n,n-1}$ and $\mathcal{B}_0, \ \mathcal{B}_1, \ \ldots, \mathcal{B}_n$: are appropriate matrices which include the right-hand terms of $\dot{\tilde{x}}_1(t)$ to $\dot{\tilde{x}}_n(t)$.

The obtained model is the result of a linearization, carried out at the operating point where the platoon keeps a constant velocity. The dynamic of each vehicle can be analyzed under the desired equilibrium conditions. This leads to what is known as a head-to-tail dynamic representation where the input is the velocity of the leader $\tilde{v}_0(t)$ vehicle.

In conclusion, the mathematical model (2.4) represents a time-delay system with multiple concentrated delays. For a better understanding of the general structure of this delay system, the reader is referred to Appendix A.1.

2.2 Model "B" based on the ECACC strategy

This model arises in the extended cooperative adaptive cruise control introduced in (Montanaro *et al.*, 2014) where each vehicle considers a local and a delayed network control

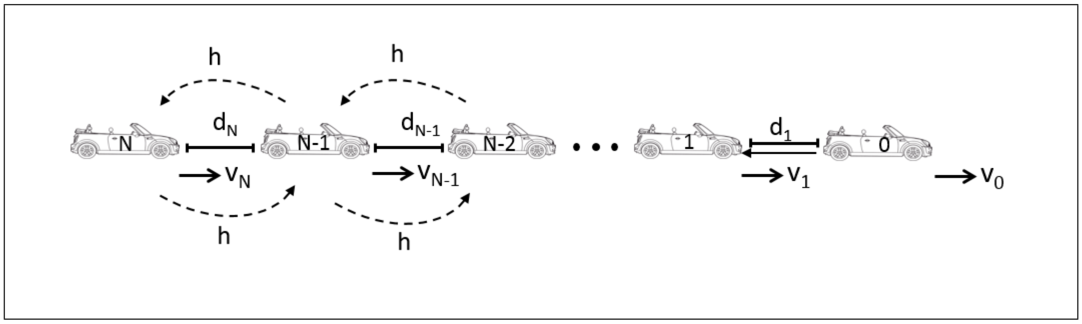

Figure 2.2: Platoon of $N+1$ vehicles. The variable d and v are the inter-vehicle distance and the velocity of the vehicle, respectively. The variable h is the transmission delay.

action. The novelty in this work, is to consider that all states are delayed, and to apply later a delay compensator.

Modeling framework. We consider a platoon of N+1 vehicles as shown in Figure 2.2. For robustness, the network communication structure uses bidirectionally information between vehicles. The leader's dynamic is described by

$$\dot{r}_0(t) = v_0(t),$$

where $r_0(t)$ and $v_0(t)$ are the known position and velocity of the leader; the i-th follower dynamics is

$$\begin{aligned}\dot{r}_i(t) =& v_i(t),\\ \dot{v}_i(t) =& u_i(t-h),\end{aligned}$$

the position, velocity and acceleration of the i-th vehicle, $i = 1, ..., N$, are $r_i(t)$, $v_i(t)$ and $u_i(t)$, respectively and $h > 0$ is the delay introduced by the actuators. Montanaro *et al.* (2014) explain that control actions $u_i(t-h)$ are produced by the low level vehicle controllers which control the engines. The control objective is to maintain a defined inter-vehicle distance for all followers and the same velocity as the leader. The tracking errors are defined as

$$e_i(t) = d_i(t) - \hat{d}_i(t),$$

where $d_i(t) = r_{i-1}(t) - r_i(t) - L_i$ is the spacing between two consecutive vehicles, L_i is the length of the i-th vehicle. Here, $\hat{d}_i(t) = \delta_i + p_i v_i$ is the desired inter-vehicle distance, $\delta_i > 0$ is the stopping secure distance, $p_i > 0$ is the time headway which is defined as the time to stop the vehicles according to the quality of the brake, wheels, and road conditions, to name a few. The fleet dynamics are

$$\begin{aligned} \dot{e}_i(t) =& v_{i-1}(t) - v_i(t) - p_i\dot{v}_i(t), && (2.5)\\ \dot{v}_i(t) =& u_i(t-h). && (2.6) \end{aligned}$$

In contrast with the extended cooperative adaptive cruise control where the control action is divided into local and delayed network strategies, we consider here the worst case scenario where the complete control action (2.6) is delayed. The control is given by

$$\begin{aligned} u_i(t-h) =& \frac{1}{p_i}(v_{i-1}(t-h) - v_i(t-h)) + \frac{1}{p_i}k_i e_i(t-h)\\ &+ \frac{1}{p_i}\sum_{j=1}^{N} a_{ij}k_{ij}e_j(t-h), \qquad (2.7) \end{aligned}$$

where k_i and k_{ij} are constant gains, corresponding to local and neighboring vehicle errors, respectively. As mentioned before, the wireless communication among the vehicles of the fleet defines a network communication structure. This structure can be represented by means of graph theory. Each vehicle transmits the tracking error information with delay to other neighboring vehicles, resulting in a dynamic network of agents. We use the adjacency matrix $\mathcal{A} = [a_{ij}]_{N\times N}$ in order to represent the inter-vehicle communication. If the vehicle i obtains information from vehicle j, $a_{ij} = 1$, zero otherwise. Self-information is not allowed ($a_{ii} = 0$).

The control action $u_1(t)$ which belongs to the first vehicle is a special case. This is because the velocity $v_0(t)$ of the leader acts as the input of the fleet. We consider that this velocity does not have delay, provided that vehicle 1 is equipped with sensors that practically do not introduce delays as radars when the information of the leader vehicle is obtained.

Substituting the control law (2.7) into (2.5-2.6) gives the model

$$\dot{x}(t) = Ax(t) + Bu(t-h) + Dv_0(t) \qquad (2.8)$$

with $x(t) = [e_1(t)\ v_1(t)\ e_2(t)\ v_2(t)\ \dots\ e_N(t)\ v_N(t)]^T$. Here, A and B are respectively $(2N\times 2N)$ and $(2N\times N)$ real matrices that describe the network configuration structure. The matrix D is a real $(2N\times 1)$ matrix equal to

$$D = \begin{bmatrix} 0\\ 1/p_1\\ 0\\ \vdots\\ 0 \end{bmatrix},$$

and is generated by the velocity $v_0(t)$ of the leading vehicle which in turn is the input of the system (2.8).

2.3 Model "C" based on the ECACC strategy (driver's memory effects)

In this section, the extended cooperative adaptive cruise control proposed in (Montanaro *et al.*, 2014) is used again. In contrast with the control action used in (Montanaro *et al.*, 2014), here the delayed reactions of drivers are modeled by distributed delays, as presented in (Sipahi & Niculescu, 2010). The resulting closed-loop is a linear system with multiple concentrated and distributed delays.

Modeling framework. To start with, we consider a fleet of $n+1$ vehicles as shown in Figure 2.3. The leader dynamic is expressed by

$$\dot{r}_0(t) = v_0(t),$$

where $r_0(t)$ and $v_0(t)$ are the leader position and velocity, respectively. The dynamics of the *i-th* follower is given by

$$\dot{r}_i(t) = v_i(t),$$
$$\dot{v}_i(t) = u_i(t),$$

where $r_i(t)$, $v_i(t)$ and $u_i(t)$ are the position, velocity and acceleration (acting as control action) of the *i-th* vehicle with $i = 1, \ldots, n$. The spacing policy between two consecutive vehicles is shown in Figure 2.4. It is defined as

$$d_i(t) = r_{i-1}(t) - r_i(t) - l_i,$$

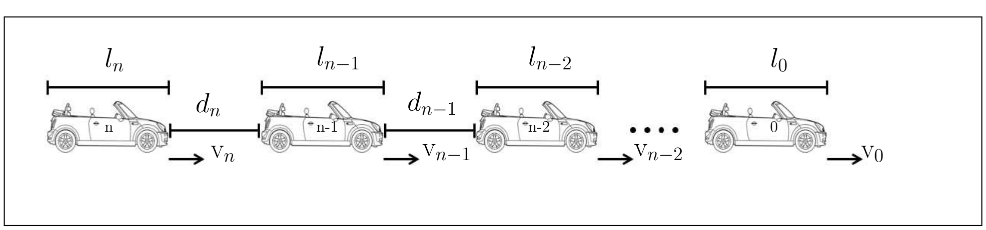

Figure 2.3: Platoon of vehicles

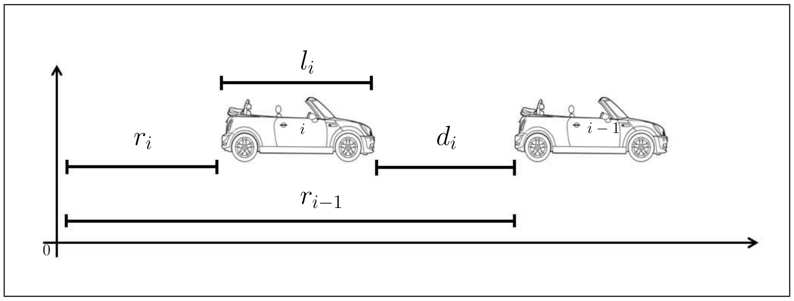

Figure 2.4: Spacing policy between two vehicles

where l_i is the vehicle length. The aim is to fix a secure reference or inter-vehicular distance

$$\hat{d}_i(t) = \delta_i + p_i v_i(t),$$

where δ_i is the stopping distance, p_i is the time headway. Defining the tracking error as $e(t) = d_i(t) - \hat{d}_i(t)$, the dynamic of the platoon is:

$$\begin{aligned} \dot{e}_i(t) &= \dot{d}_i(t) - \dot{\hat{d}}_i(t), \\ &= v_{i-1}(t) - v_i(t) - p_i u_i(t), \\ \dot{v}_i(t) &= u_i(t). \end{aligned} \tag{2.9}$$

The control strategy in (Montanaro *et al.*, 2014) with local and network control action is defined as $u_i(t) = u_{li}(t) + u_{wi}(t)$, where

$$\begin{aligned} u_{li}(t) &= u_{li}(r_i(t), r_{i-1}(t), v_i(t), v_{i-1}(t)), \\ u_{wi}(t) &= \sum_{j \in N}^{N} u_{ij}(e_j(t - h_{ij}(t)), \dot{e}_j(t - h_{ij}(t))). \end{aligned}$$

We propose a control strategy with human memory as follows

$$\begin{aligned} u_{li}(t) &= \frac{1}{p_i}(v_{i-1}(t) - v_i(t)) + \frac{k_i}{p_i}\int_0^\infty f_i(\tau) e_i(t-\tau) d\tau, \\ u_{wi}(t) &= \frac{1}{h_i}\sum_{j=1}^{n} a_{ij} k_{ij} e_j(t - h_{ij}(t)). \end{aligned} \tag{2.10}$$

Replacing (2.10) in (2.9) the dynamics of the fleet can be written as

$$\dot{e}_i(t) = -k_i \int_0^\infty f_i(\tau) e_i(t-\tau) d\tau - \sum_{j=1}^{n} k_{ij} a_{ij} e_j(t - h_{ij}(t)), \tag{2.11}$$

where $i = 1, \ldots, n$ and k_{ij} are control gains and represent the weight that the vehicle i gives to the communication link. As explained in (Sipahi & Niculescu, 2010), the gains k_i can be seen as a measure of the driver's aggressiveness per unit of vehicle mas. The distributed function $f_i(\tau)$ is the uniform distribution. We point out that other forms of distributions can be used for the analysis, but there is no evidence on which distribution better represents the memory effects. The uniform distribution depicted in Figure 2.5 models the short-term memory of the drivers as follows

$$f_i(\tau) = \begin{cases} \frac{1}{\xi_i}, & h_i \leq \tau \leq h_i + \xi_i \\ 0, & \text{otherwise}, \end{cases}$$

h_i = is known as the gap (length of time after which the memory with size ξ_i becomes effective).
ξ_i = size of the driver's memory.
τ = is the average of the memory window,

$$\tau = h_i + \frac{\xi_i}{2}.$$

Then, system (2.11) can be rewritten as

$$\dot{e}_i(t) = -\frac{k_i}{\xi_i} \int_{-\xi_i}^{0} e_i(t + \theta - h_i) d\theta - \sum_{j=1}^{n} k_{ij} a_{ij} e_j(t - h_{ij}(t)). \tag{2.12}$$

The driver's decision is captured by the integral term in the above equation. For simplicity, we consider the driver's decision parameters as equals, that is, $\xi_i = \xi$ and $h_i = h$. Then,

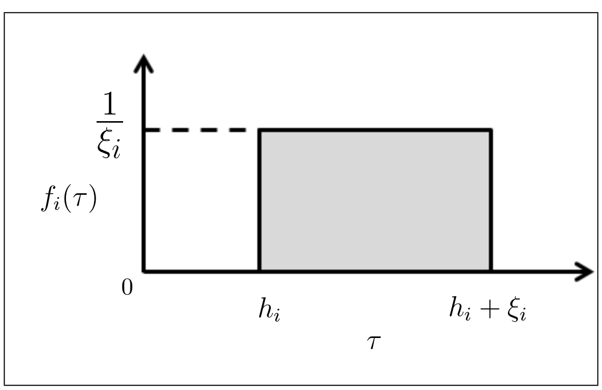

Figure 2.5: Uniform distribution for modeling the short-term memory of the human drivers (Figure taken from (Sipahi & Niculescu, 2010)).

defining $e = [e_1(t)\ e_2(t)\ \ldots\ e_n(t)]^T$, the dynamic of the fleet can be represented as

$$\dot{e}(t) = \sum_{i=1}^{n}\sum_{j=1}^{n} A_{ij} e(t - h_{ij}(t)) + \int_{-\xi}^{0} Ge(t + \theta - h)d\theta, \tag{2.13}$$

where A_{ij} are $(n \times n)$ real matrices, so that the element of the matrix

$$[A_{ij}]_{p,q} = \begin{cases} -k_{ij} & \text{if } (p,q) = (i,j) \\ 0 & \text{otherwise,} \end{cases}$$

and matrix G =diag$\{-k_1/\xi\ \ -k_2/\xi\ \ \ldots\ \ -k_n/\xi\}$. Note that system (2.13) is a linear system with multiple concentrated and distributed delays.

2.4 Conclusions

This chapter presents three microscopic models for the chain of vehicles. It is worth noting that the first two models are linear systems with concentrated delays while the third one is a linear system with multiple concentrated and distributed delays. Not surprisingly, the mathematical tools for the stability analysis are not the same. While in general, recent results in the time-domain based on the delay Lyapunov matrix allow the stability analysis of systems with concentrated delays, mathematical tools for analyzing systems with distributed delays are not completely available. Similarly, the use of delay compensators for systems with concentrated delays, as will be shown, produces systems with distributed delays. Therefore, an extension of the Lyapunov-Krasovskii theory is needed and is presented in the next chapter.

Chapter 3

Stability analysis strategy

In traffic systems, as explained in the previous chapter, the driver's memory effects introduce distributed delays (Sipahi & Niculescu, 2010) and as will be shown later, dynamic predictor controllers give rise to linear systems with multiple concentrated and distributed delays. In view of the above, it is clear that the stability analysis for this class of linear systems must be addressed.

In this chapter, a methodology for the stability analysis of linear systems with multiple concentrated and distributed delays, is presented. The stability of systems with only concentrated delays has been well studied in the time-domain, by using the delay Lyapunov matrix, for more details, the reader is referred to Appendix A.1. The same approach for distributed delay systems with predefined kernels, has been applied in (Aliseyko, 2019; Cuvas, Mondié & Ochoa, 2015; Kharitonov, 2006) for constructing the delay Lyapunov matrix, and in (Cuvas, Mondié & Ochoa, 2015) for testing stability.

Here, we generalize the stability analysis of distributed delay systems to a class of piecewise function kernels. The key element of our work is the delay Lyapunov matrix of the distributed linear system, as discussed later, it reduces to the computation of the solutions of a delay-free system of matrix equations (Kharitonov, 2012). Once the delay Lyapunov matrix is obtained, the analysis can be performed with the help of the necessary and sufficient stability conditions (Egorov, Cuvas & Mondié, 2017) reminded in Appendix A.2
.

3.1 Multiple distributed time-delay systems

Consider the linear system with multiple constant pointwise delays and multiple distributed delays with piecewise-function kernel described by

$$\begin{aligned}\dot{x}(t) &= \sum_{j=0}^{m} A_j x(t-jh) + \sum_{j=0}^{m-1} \int_{-(j+1)h}^{-jh} G_j(\theta) x(t+\theta) d\theta, \\ &= \sum_{j=0}^{m} A_j x(t-jh) + \sum_{j=0}^{m-1} \int_{-h}^{0} G_j(\theta - jh) x(t+\theta-jh) d\theta,\end{aligned} \tag{3.1}$$

where $A_0, \ldots, A_m$ are $n \times n$ constant matrices, h is the basic delay and $mh = H$ is the maximum delay. For an initial function $\varphi \in PC([-H, 0], \mathbb{R}^n)$ the restriction of the solution $x(t, \varphi)$ to the interval $[t-H, t]$ is denoted by $x_t(\varphi)$. We represent the kernel $G_j(\theta - jh)$ as follows,

$$G_j(\theta - jh) = \sum_{i=0}^{k_j} g_{j,i}(\theta) C_{j,i}, \tag{3.2}$$

where $g_{j,i}(\theta)$ are scalar functions and $C_{j,i}$ are $n \times n$ constant matrices. The scalar functions g are assumed to satisfy

$$g'_{j,i}(\theta) = \sum_{k=0}^{k_j} \alpha_{j,i}^{k} g_{j,k}, \quad j = 0, 1, \ldots, m-1. \tag{3.3}$$

The above restriction is the primary condition to construct the delay-free system of matrix equations which allows the Lyapunov matrix construction.

3.2 Lyapunov matrix construction

In this section, the Lyapunov matrix is constructed. The dynamic, symmetric and algebraic properties are extended to the class of systems addressed in this work. Then, the auxiliary matrices are defined according to the form of the kernel of the distributed term. As a result, a delay-free system of matrix equations subjects to a two points boundary value problem is obtained. Its solution gives the delay Lyapunov matrix $U(\tau)$ in the interval $\tau \in [0, H]$.

3.2.1 Properties of $U(\tau)$

For systems with multiple distributed delays, the Lyapunov matrix is $U(\tau)$ associated to a constant symmetric positive definite matrix W, was shown (Kharitonov, 2012) to satisfy:

1.- the dynamic property for $\tau > 0$

$$U'(\tau) = \sum_{j=0}^{m} U(\tau - jh)A_j + \sum_{j=0}^{m-1} \int_{-h}^{0} U(\tau + \theta - jh)G_j(\theta - jh)d\theta, \tag{3.4}$$

2.- the symmetry property, for $\tau \geq 0$

$$U(-\tau) = U^T(\tau), \tag{3.5}$$

3.- the algebraic property,

$$U'(+0) - U'(-0) = -W. \tag{3.6}$$

For $\tau < 0$, the dynamic property is given by

$$U'(\tau) = -[U'(-\tau)]^T = -\sum_{j=0}^{m} A_j^T U(\tau + jh) - \sum_{j=0}^{m-1} \int_{-h}^{0} G_j(\theta - jh)^T U(\tau - \theta + jh)d\theta. \tag{3.7}$$

The algebraic property can be rewritten as

$$\begin{aligned} -W = \sum_{j=0}^{m} \left[U(-jh)A_0 + A_j^T U(jh)\right] + \sum_{j=0}^{m-1} \Bigg\{ &\int_{-h}^{0} U(\theta - jh)G_j(\theta - jh)d\theta \\ + &\int_{-h}^{0} G_j(\theta - jh)^T U(-\theta + jh)d\theta \Bigg\}. \end{aligned} \tag{3.8}$$

If the Lyapunov condition holds (the characteristic equation of (3.1) has no eigenvalues that are symmetric with respect to the origin) then the Lyapunov matrix is the unique solution of the two points boundary problem, defined by properties (3.4-3.8).

3.2.2 Delay-free auxiliary system

This section is devoted to the semi-analytic construction of the Lyapunov matrix for kernels of the form (3.2) which fulfill the condition (3.3).

We define $2m$ auxiliary matrices corresponding to the multiple constant delays,

$$Y_i(\tau) = U(\tau + ih), \qquad -m \leq i \leq m-1. \tag{3.9}$$

We also assume that all functions $g_{j,i}(\theta)$ are different and define the following auxiliary matrices,

$$\begin{aligned} Z_{j,i,p}(\tau) &= \int_{-h}^{0} g_{j,i}(\theta)U(\tau + \theta + ph)d\theta, \quad 0 \leq i \leq k_j, \quad -j \leq p \leq (m-1) - j, \\ J_{j,i,p}(\tau) &= \int_{-h}^{0} g_{j,i}(\theta)U(\tau - \theta + ph)d\theta, \quad 0 \leq i \leq k_j, \quad -(m-j) \leq p \leq -1 + j, \end{aligned} \tag{3.10}$$

where $0 \le j \le m-1$.

The number of auxiliary matrices is $2m(1 + \sum_{j=0}^{m-1}(k_j+1))$.

Lemma 1. *Let $U(t)$ be a Lyapunov matrix of system (3.1), associated with a symmetric matrix W. Then the auxiliary matrices (3.10) satisfy the system of linear differential equations,*

$$\begin{cases} Y_i'(\tau) = \sum_{j=0}^{m} Y_{i-j}(\tau)A_j + \sum_{p=0}^{m-1}\left(\sum_{j=0}^{k_p} Z_{p,j,i-p}(\tau)C_{p,j}\right), \quad 0 \le i \le m-1, \\ Y_i'(\tau) = -\sum_{j=0}^{m} A_j^T Y_{i+j}(\tau) - \sum_{p=0}^{m-1}\left(\sum_{j=0}^{k_p} C_{p,j}^T J_{p,j,i+p}(\tau)\right), \quad -m \le i \le -1, \\ Z_{j,i,p}'(\tau) = g_{j,i}(0)Y_p(\tau) - g_{j,i}(-h)Y_{p-1}(\tau) - \sum_{k=0}^{k_j}\alpha_{j,i}^k Z_{j,k,p}(\tau), \\ 0 \le j \le m-1, \quad 0 \le i \le k_j, \quad -j \le p \le (m-1)-j, \\ J_{j,i,p}'(\tau) = -g_{j,i}(0)Y_p(\tau) + g_{j,i}(-h)Y_{p+1}(\tau) + \sum_{k=0}^{k_j}\alpha_{j,i}^k J_{j,k,p}(\tau), \\ 0 \le j \le m-1, \quad 0 \le i \le k_j, \qquad -(m-j) \le p \le -1+j, \end{cases} \tag{3.11}$$

and the boundary conditions

$$\begin{cases} Y_i(0) = Y_{i-1}(h), \qquad -m+1 \le i \le m-1, \\ Z_{j,i,p}(0) = Z_{j,i,p-1}(h), \quad 0 \le j \le m-1, \quad 0 \le i \le k_j, \quad 1-j \le p \le (m-1)-j, \\ J_{j,i,p}(0) = J_{j,i,p-1}(h), \quad 0 \le j \le m-1, \quad 0 \le i \le k_j, \quad -(m-1)+j \le p \le -1+j, \\ Z_{j,i,-j}(0) = J_{j,i,-1+j}^T(h), \quad 0 \le j \le m-1, \quad 0 \le i \le k_j \\ Z_{j,i,0}(0) = \int_0^h g_{j,i}(\theta-h)Y_{-1}(\theta)d\theta, \qquad 0 \le j \le m-1, \quad 0 \le i \le k_j, \\ J_{j,i,0}(0) = \int_0^h g_{j,i}(-\theta)Y_0(\theta)d\theta, \qquad 1 \le j \le m-1, \quad 0 \le i \le k_j, \\ \sum_{j=0}^{m}\left[Y_{-j}(0)A_0 + A_j^T Y_{j-1}(h)\right] + \sum_{j=0}^{m-1}\left\{\sum_{i=0}^{k_j} Z_{j,i,-j}(0)C_{j,i} + \sum_{i=0}^{k_j} C_{j,i}^T J_{j,i,j-1}(h)\right\} = -W. \end{cases} \tag{3.12}$$

Proof. The system of equations (3.11) follows from the dynamic properties (3.4), (3.7) and definitions (3.9) and (3.10). The boundary conditions are the algebraic property (3.8) and definitions (3.9) and (3.10). □

Lemma 2. *If there is any $g_{j,i}(\theta) = 1$, the auxiliary matrices involved are as follows*

$$Z_{j,i,p+1}(\tau) = J_{j,i,p}(\tau),$$

so the system (3.11,3.12) can be reduced.

Proof. It is easy to see that

$$\int_{-h}^{0} U(\tau+\theta+(p+1)h)d\theta = \int_{-h}^{0} U(\tau-\theta+ph)d\theta.$$

□

Lemma 3. *The following equalities are satisfied by any solutions of (3.11,3.12)*

$$\begin{aligned} Z_{j,i,p}(0) &= \int_0^h g_{j,i}(\theta-h)Y_{p-1}(\theta)d\theta, \quad Z_{j,i,p}(h) = \int_0^h g_{j,i}(\theta-h)Y_p(\theta)d\theta, \\ J_{j,i,p}(0) &= \int_0^h g_{j,i}(-\theta)Y_p(\theta)d\theta, \quad J_{j,i,p}(h) = \int_0^h g_{j,i}(-\theta)Y_{p+1}(\theta)d\theta. \end{aligned}$$

Proof. For $Z_{j,i,0}(0)$ and $J_{j,i,0}(0)$ the relations hold trivially. Moreover,

$$\begin{aligned} Z_{0,0,1}(0) = Z_{0,0,0}(h) &= Z_{0,0,0}(0) + \int_0^h [g_{0,0}(\theta-h)Y_0(\theta) - g_{0,0}(\theta-h)Y_{-1}(\theta)d\theta] \\ &= \int_0^h g_{0,0}(\theta-h)Y_0(\theta)d\theta, \end{aligned}$$

and the same applies when , $0 < j < m-1$, $0 \le i \le k_j$, $\quad -j \le p \le (m-1)-j$. In the other cases,

$$\begin{aligned} J_{0,0,1}(0) = J_{0,0,0}(h) &= J_{0,0,0}(0) + \int_0^h [g_{0,0}(-\theta)Y_1(\theta) - g_{0,0}(-\theta)Y_0(\theta)d\theta] \\ &= \int_0^h g_{0,0}(-\theta)Y_1(\theta)d\theta, \end{aligned}$$

similarly when, $0 < j < m-1$, $0 \le i \le k_j$, $\quad -(m-j) \le p \le -1+j$. □

Corollary 1. *The solutions of the system of linear differential equations (3.11-3.12) satisfy*

$$\begin{aligned} Z_{j,i,p}(t) &= \int_0^t g_{j,i}(\theta-t)Y_p(\theta)d\theta + \int_t^h g_{j,i}(\theta-h-t)Y_{p-1}(\theta)d\theta, \\ J_{j,i,p}(t) &= \int_t^{2t} g_{j,i}(t-\theta)Y_p(\theta)d\theta - \int_t^{2t-h} g_{j,i}(t-\theta-h)Y_{p+1}(\theta)d\theta. \end{aligned}$$

We summarize the above results in the following theorem.

Theorem 1. *Consider a time-delay system in the form (3.1) with matrix kernels $G_j(\theta-jh)$ in the representation* (3.2) *satisfying the Lyapunov condition. The delay-free system of matrix equations (3.11) and the boundary conditions (3.12) has a solution with*

$$\begin{aligned} &Y_i(\tau), -m \le i \le m-1, \\ &Z_{j,i,p}(\tau), j = 0,1,\ldots,m-1, \quad 0 \le i \le k_j, \quad -j \le p \le (m-1)-j, \\ &J_{j,i,p}(\tau), j = 0,1,\ldots,m-1, \quad 0 \le i \le k_j, \quad -(m-j) \le p \le -1+j, \end{aligned}$$

and the Lyapunov matrix associated with a symmetric matrix W is $U(\tau) = Y_0(\tau)$, $\tau \in [0, h]$.

Corollary 2. *(Kharitonov, 2012), If boundary value problem (3.11), (3.12) admits a unique solution*

$$\{Y_{m-1}(\tau), Y_{m-1}(\tau), \ldots, Y_0(\tau), \ldots, Y_{-m}(\tau)\}, \quad \tau \in [0, h],$$

then there exists a unique Lyapunov matrix $U(\tau)$ associated with the matrix W, and the matrix is defined on $[0, H]$ by the equalities

$$U(\tau + jh) = Y_j(\tau), \quad \tau \in [0, h], \quad j = 0, 1, \ldots, m-1.$$

3.3 Illustrative example

In this section, an example validates the Lyapunov matrix construction. Using the Lyapunov matrix, and the stability conditions (A.6), the complete stability region of the system is shown on the space of previously defined parameters. A scalar case example is addressed in the publication (Juárez & Mondié, 2018a). When the system has repeated kernels, it is possible to reduce the dimension of the delay-free system of matrix equations, as shown in (Juárez & Mondié, 2018b).

Consider the delay linear system

$$\begin{aligned}\dot{x}(t) &= A_0 x(t) + A_1 x(t-h) + A_2 x(t-2h) + C_{0,0}\int_{-h}^{0} x(t+\theta)d\theta + C_{0,1}\int_{-h}^{0} \theta x(t+\theta)d\theta \\ &\quad + C_{1,0}\int_{-2h}^{-h} \theta e^{\theta} x(t+\theta)d\theta + C_{1,1}\int_{-2h}^{-h} e^{\theta} x(t+\theta)d\theta, \end{aligned} \tag{3.13}$$

$$\text{where} \qquad A_0 = \begin{bmatrix} -0.2 & 0.1 \\ 0.1 & a \end{bmatrix}, \; A_1 = \begin{bmatrix} -0.8 & 0 \\ 0 & b \end{bmatrix}, \; A_2 = \begin{bmatrix} 0 & 1 \\ 0 & 0 \end{bmatrix},$$

$$C_{0,0} = \begin{bmatrix} 0 & 0 \\ 0 & 0.3 \end{bmatrix}, \; C_{0,1} = \begin{bmatrix} 0 & 0 \\ 0 & 0.1 \end{bmatrix}, \; C_{1,0} = \begin{bmatrix} 0.2 & 0 \\ 0 & 0 \end{bmatrix}, \; C_{1,1} = \begin{bmatrix} 0.4 & 0 \\ 0 & 0 \end{bmatrix},$$

$$\text{then} \qquad \begin{aligned} &G_0(\theta) = C_{0,0} + \theta C_{0,1}, \\ &G_1(\theta - h) = \theta e^{\theta}(C_{1,0}e^{-h}) + e^{\theta}(C_{1,1}e^{-h}(1-h)) = \theta e^{\theta}\tilde{C}_{1,0} + e^{\theta}\tilde{C}_{1,1}, \end{aligned}$$

The number of auxiliary matrices is $2m(1 + \sum_{j=0}^{m-1}(k_j + 1)) = 4(1 + 2 + 2) = 20$. We have 4 auxiliary matrices

$$Y_1(\tau) = U(\tau + h), \quad Y_0(\tau) = U(\tau), \quad Y_{-1}(\tau) = U(\tau - h), \quad Y_{-2}(\tau) = U(\tau - 2h).$$

In accordance with (3.10), $j = 0, 1$, $k_0 = 1$ and $k_1 = 1$, 16 auxiliary matrices are defined as follows

$$
\begin{aligned}
Z_{0,i,p}(t) &= \int_{-h}^{0} g_{0,i}(\theta) U(t+\theta+ph) d\theta,\ 0 \le i \le 1,\ 0 \le p \le 1, \\
J_{0,i,p}(t) &= \int_{-h}^{0} g_{0,i}(\theta) U(t-\theta+ph) d\theta,\ 0 \le i \le 1,\ -2 \le p \le -1, \\
Z_{1,i,p}(t) &= \int_{-h}^{0} g_{1,i}(\theta) U(t+\theta+ph) d\theta,\ 0 \le i \le 1,\ -1 \le p \le 0, \\
J_{1,i,p}(t) &= \int_{-h}^{0} g_{1,i}(\theta) U(t-\theta+ph) d\theta,\ 0 \le i \le 1,\ -1 \le p \le 0,
\end{aligned}
$$

$$
\begin{aligned}
Z_{0,0,1}(\tau) &= \int_{-h}^{0} U(\tau+\theta+h) d\theta, \quad Z_{0,0,0}(\tau) = \int_{-h}^{0} U(\tau+\theta) d\theta, \\
J_{0,0,-1}(\tau) &= \int_{-h}^{0} U(\tau-\theta-h) d\theta, \quad J_{0,0,-2}(\tau) = \int_{-h}^{0} U(\tau-\theta-2h) d\theta, \\
Z_{0,1,1}(\tau) &= \int_{-h}^{0} \theta\, U(\tau+\theta+h) d\theta, \quad Z_{0,1,0}(\tau) = \int_{-h}^{0} \theta\, U(\tau+\theta) d\theta, \\
J_{0,1,-1}(\tau) &= \int_{-h}^{0} \theta\, U(\tau-\theta-h) d\theta, \quad J_{0,1,-2}(\tau) = \int_{-h}^{0} \theta\, U(\tau-\theta-2h) d\theta, \\
Z_{1,0,0}(\tau) &= \int_{-h}^{0} \theta e^{\theta} U(\tau+\theta) d\theta, \quad Z_{1,0,-1}(\tau) = \int_{-h}^{0} \theta e^{\theta}\, U(\tau+\theta-h) d\theta, \\
J_{1,0,0}(\tau) &= \int_{-h}^{0} \theta e^{\theta}\, U(\tau-\theta) d\theta, \quad J_{1,0,-1}(\tau) = \int_{-h}^{0} \theta e^{\theta}\, U(\tau-\theta-h) d\theta, \\
Z_{1,1,0}(\tau) &= \int_{-h}^{0} e^{\theta}\, U(\tau+\theta) d\theta, \quad Z_{1,1,-1}(\tau) = \int_{-h}^{0} e^{\theta}\, U(\tau+\theta-h) d\theta, \\
J_{1,1,0}(\tau) &= \int_{-h}^{0} e^{\theta}\, U(\tau-\theta) d\theta, \quad J_{1,1,-1}(\tau) = \int_{-h}^{0} e^{\theta}\, U(\tau-\theta-h) d\theta.
\end{aligned}
$$

In system (3.13) there is a scalar function $g_{0,0}(\theta) = 1$, therefore by Lemma 2, $Z_{0,0,0}(\tau) = J_{0,0,-1}(\tau)$, the number of auxiliary matrices is reduced to 19. By Lemma 1, we obtain the delay-free system of linear matrix differential equations,

$$
\begin{aligned}
Y_1'(\tau) &= Y_1(\tau)A_0 + Y_0(\tau)A_1 + Y_{-1}(\tau)A_2 + Z_{0,0,1}(\tau)C_{0,0} + Z_{0,1,1}(\tau)C_{0,1} \\
&+ Z_{1,0,0}(\tau)\tilde{C}_{1,0} + Z_{1,1,0}(\tau)\tilde{C}_{1,1} \\
Y_0'(\tau) &= Y_0(\tau)A_0 + Y_{-1}(\tau)A_1 + Y_{-2}(\tau)A_2 + Z_{0,0,0}(\tau)C_{0,0} + Z_{0,1,0}(\tau)C_{0,1} \\
&+ Z_{1,0,-1}(\tau)\tilde{C}_{1,0} + Z_{1,1,-1}(\tau)\tilde{C}_{1,1} \\
Y_{-1}'(\tau) &= -A_0^T Y_{-1}(\tau) - A_1^T Y_0(\tau) - A_2^T Y_1(\tau) - C_{0,0}^T Z_{0,0,0}(\tau) - C_{0,1}^T J_{0,1,-1}(\tau) \\
&- \tilde{C}_{1,0}^T J_{1,0,0}(\tau) - \tilde{C}_{1,1}^T J_{1,1,0}(\tau)
\end{aligned}
$$

$$\begin{aligned}
Y'_{-2}(\tau) &= -A_0^T Y_{-2}(\tau) - A_1^T Y_{-1}(\tau) - A_2^T Y_0(\tau) - C_{0,0}^T J_{0,0,-2}(\tau) - C_{0,1}^T J_{0,1,-2}(\tau) \\
&- \tilde{C}_{1,0}^T J_{1,0,-1}(\tau) - \tilde{C}_{1,1}^T J_{1,1,-1}(\tau) \\
Z'_{0,0,1}(\tau) &= Y_1(\tau) - Y_0(\tau) \\
Z'_{0,0,0}(\tau) &= Y_0(\tau) - Y_{-1}(\tau) \\
J'_{0,0,-2}(\tau) &= -Y_{-2}(\tau) + Y_{-1}(\tau) \\
Z'_{0,1,1}(\tau) &= hY_0(\tau) - Z_{0,0,1}(\tau) \\
Z'_{0,1,0}(\tau) &= hY_{-1}(\tau) - Z_{0,0,0}(\tau) \\
J'_{0,1,-1}(\tau) &= -hY_0(\tau) + Z_{0,0,0}(\tau) \\
J'_{0,1,-2}(\tau) &= -hY_{-1}(\tau) + J_{0,0,-2}(\tau) \qquad (3.14) \\
Z'_{1,0,0}(\tau) &= he^{-h}Y_{-1}(\tau) - Z_{1,0,0}(\tau) - Z_{1,1,0}(\tau) \\
Z'_{1,0,-1}(\tau) &= he^{-h}Y_{-2}(\tau) - Z_{1,0,-1}(\tau) - Z_{1,1,-1}(\tau) \\
J'_{1,0,0}(\tau) &= -he^{-h}Y_1(\tau) + J_{1,0,0}(\tau) + J_{1,1,0}(\tau) \\
J'_{1,0,-1}(\tau) &= -he^{-h}Y_0(\tau) + J_{1,0,-1}(\tau) + J_{1,1,-1}(\tau) \\
Z'_{1,1,0}(\tau) &= Y_0(\tau) - e^{-h}Y_{-1}(\tau) - Z_{1,1,0}(\tau) \\
Z'_{1,1,-1}(\tau) &= Y_{-1}(\tau) - e^{-h}Y_{-2}(\tau) - Z_{1,1,-1}(\tau) \\
J'_{1,1,0}(\tau) &= -Y_0(\tau) + e^{-h}Y_1(\tau) + J_{1,1,0}(\tau) \\
J'_{1,1,-1}(\tau) &= -Y_{-1}(\tau) + e^{-h}Y_0(\tau) + J_{1,1,-1}(\tau). \qquad (3.15)
\end{aligned}$$

According to (3.12), the boundary conditions are,

$$\begin{aligned}
Y_1(0) &= Y_0(h) \\
Y_0(0) &= Y_{-1}(h) \\
Y_{-1}(0) &= Y_{-2}(h) \\
Z_{0,0,1}(0) &= Z_{0,0,0}(h) \\
Z_{0,1,1}(0) &= Z_{0,1,0}(h) \\
Z_{1,0,0}(0) &= Z_{1,0,-1}(h) \\
Z_{1,1,0}(0) &= Z_{1,1,-1}(h) \\
Z_{0,0,0}(0) &= J_{0,0,-2}(h) \\
J_{0,1,-1}(0) &= J_{0,1,-2}(h) \\
J_{1,0,0}(0) &= J_{1,0,-1}(h) \\
J_{1,1,0}(0) &= J_{1,1,-1}(h)
\end{aligned}
\qquad
\begin{aligned}
Z_{0,1,0}(0) &= J_{0,1,-1}^T(h) \\
Z_{1,0,-1}(0) &= J_{1,0,0}^T(h) \\
Z_{1,1,-1}(0) &= J_{1,1,0}^T(h) \\
Z_{0,0,0}(0) &= \int_0^h Y_{-1}(\theta)d\theta \\
Z_{0,1,0}(0) &= \int_0^h (\theta - h)Y_{-1}(\theta)d\theta \\
Z_{1,0,0}(0) &= \int_0^h (\theta - h)e^{\theta-h}Y_{-1}(\theta)d\theta \\
Z_{1,1,0}(0) &= \int_0^h e^{\theta-h}Y_{-1}(\theta)d\theta
\end{aligned}$$

$$\begin{aligned}
A_0^T Y_0(0) + Y_0(0)A_0 + A_1^T Y_0(h) + Y_{-1}(0)A_1 + A_2^T Y_1(h) + Y_{-2}(0)A_2 \\
+Z_{0,0,0}(0)C_{0,0} + Z_{0,1,0}(0)C_{0,1} + Z_{1,0,-1}(0)\tilde{C}_{1,0} + Z_{1,1,-1}(0)\tilde{C}_{1,1} \\
+C_{0,0}^T Z_{0,0,0}(h) + C_{0,1}^T J_{0,1,-1}(h) + \tilde{C}_{1,0}^T J_{1,0,0}(h) + \tilde{C}_{1,1}^T J_{1,1,0}(h) &= -W. \quad (3.16)
\end{aligned}$$

To write the delay-free system of differential equations (3.15) in vector form, we apply Kronecker product of matrices, see Appendix D. System (3.15) can be represented as

$$\dot{R}(\tau) = LR(\tau),$$

where L is a constant matrix of dimension (76×76), and

$$\begin{aligned}
R(\tau) = [&y_1(\tau),\ y_0(\tau),\ y_{-1}(\tau),\ y_{-2}(\tau),\ z_{0,0,1}(\tau),\ z_{0,0,0}(\tau),\ j_{0,0,-2}(\tau),\ z_{0,1,1}(\tau),\ z_{0,1,0}(\tau), \\
&j_{0,1,-1}(\tau),\ j_{0,1,-2}(\tau),\ z_{1,0,0}(\tau),\ z_{1,0,-1}(\tau),\ j_{1,0,0}(\tau),\ j_{1,0,-1}(\tau),\ z_{1,1,0}(\tau),\ z_{1,1,-1}(\tau), \\
&j_{1,1,0}(\tau),\ j_{1,1,-1}(\tau)]^T.
\end{aligned}$$

It follows that

$$R(\tau) = e^{L\tau}R(0).$$

The boundary condition (3.16) can be rewritten with the help of appropriate matrices N and M as

$$\left[M + Ne^{Lh}\right] R(0) = \begin{bmatrix} 0 \\ -w \end{bmatrix},$$

and it follows that

$$R(\tau) = e^{L\tau}[M + Ne^{Lh}]^{-1} \begin{bmatrix} 0 \\ -w \end{bmatrix}. \quad (3.17)$$

We construct $U(\tau)$ using (3.17) for $h = 0.1$, and $W = \begin{pmatrix} 1 & 0 \\ 0 & 1 \end{pmatrix}$. For $a = 5$ and $b = -9.5$, the elements of $U(\tau) = Y_0(\tau)$ and $U(\tau + h) = Y_1(\tau)$ $\tau \in [0, 0.1]$ are shown in Figure 3.1.

The Lyapunov matrix is used to find the exact stability region of system (3.13) in the space of parameters (a, b) with the help of the necessary condition (A.6). The region where this condition holds is depicted on Figures 3.2 and 3.3, for $r = 2$ and $r = 6$, respectively. It is worthy of mention that no further improvement is obtained for greater r. Continuous lines correspond to the exact stability boundaries obtained using the D-partition method Neimark (1949).

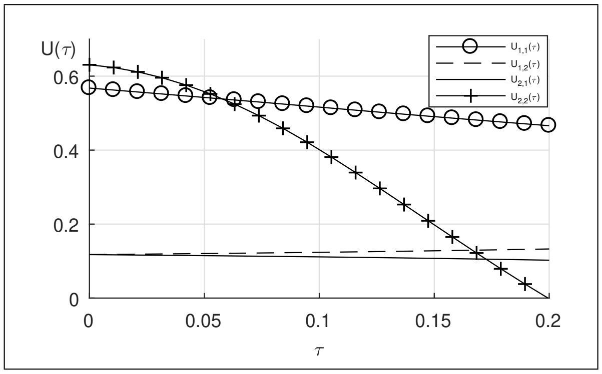

Figure 3.1: Matrix $U(\tau)$ elements.

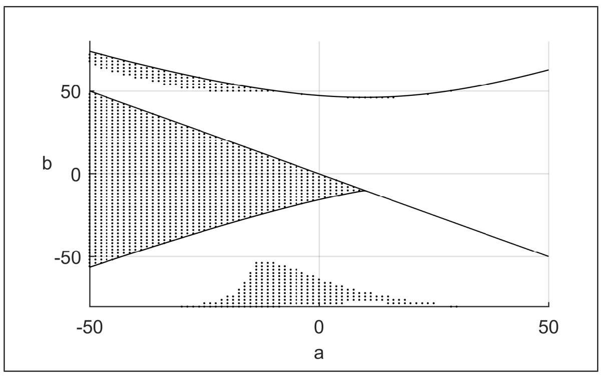

Figure 3.2: Stability chart (a, b), $r = 2$.

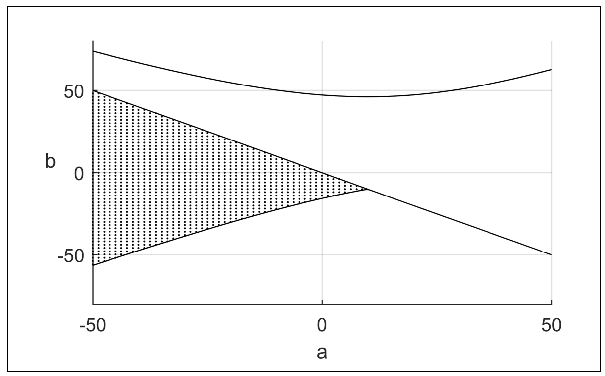

Figure 3.3: Stability chart (a, b), $r = 6$.

3.4 Conclusions

A method to compute the Lyapunov matrix of multiple distributed time-delay system with piecewise function kernel is presented. It consists in finding the solution of a delay-free system of ordinary differential equations subject to boundary conditions. The Lyapunov matrix allows us to test stability of the system. An academic example illustrates the results of the approach.

Chapter 4

Dynamic predictive control strategy

In this chapter, the dynamic predictive control strategy is explained. This technique is applied to systems with both state/input delays. Up to now, the stability of the closed-loop was studied in (Kharitonov, 2015), and its robust stability analysis in (Rodríguez-Guerrero, Kharitonov & Mondié, 2016). A time-domain analysis strategy for systems with state/input delays under dynamic predictive controllers is important because it allows considering not only constant unknown uncertainties in the delay or parameters, but also those that are time-varying. The result is obtained by rewritting the linear system with state/input delays in closed-loop with the dynamic controller as an extended system with distributed delays, which gives rise to a compact system representation. As a result, it is possible to carry out the analysis using the methodology developed in chapter 3.

4.1 System with state/input delays

Consider the system with state and input delays

$$\dot{x}(t) = A_0 x(t) + A_1 x(t-h) + Bu(t-\tau), \tag{4.1}$$

where $h > 0$, $\tau > 0$ and the matrices $A_0,\ A_1 \in \mathbb{R}^{n\times n}$, $B \in \mathbb{R}^{n\times m}$. The delays are assumed to satisfy $h < \tau$. Let the initial function be $\varphi \in\ PC([-h,0],\mathbb{R}^n)$. If matrices F_0 and F_1 that assign a desired closed-loop are known, we apply to system (4.1) the predictor control law

$$u(t) = F_0 x(t+\tau) + F_1 x(t+\tau-h), \tag{4.2}$$

the resulting closed-loop system is

$$\dot{x}(t) = (A_0 + BF_0)x(t) + (A_1 + BF_1)x(t-h), \tag{4.3}$$

where $F_0,\ F_1$ are matrices such that (4.3) is exponentially stable. The predictor-based control (4.2), explained in (Kharitonov, 2014), is given by the integral equation

$$
\begin{aligned}
u(t) = & \int_{-\tau}^{0} F_0 K(-\theta) B u(t+\theta) d\theta + \int_{-\tau}^{-h} F_1 K(-h-\theta) B u(t+\theta) d\theta \\
& + \int_{-h}^{0} F_0 K(\tau-\theta-h) A_1 x(t+\theta) d\theta + \int_{-h}^{0} F_1 K(\tau-\theta-2h) A_1 x(t+\theta) d\theta \\
& + [F_0 K(\tau) + F_1 K(\tau-h)] x(t),
\end{aligned}
\tag{4.4}
$$

where $K(t)$ is the fundamental matrix of system (4.1) and satisfies

$$
\dot{K}(t) = K(t)A_0 + K(t-h)A_1, \quad t \geq 0 \tag{4.5}
$$

with the initial conditions $K(0) = 0_{n\times n},\ t < 0,\ K(0) = I$.
An additional initial function condition is required for the control law. Let $u(t) = \psi(t),\ t \in [-\tau, 0]$, where $\psi \in PC([-\tau, 0], \mathbb{R}^m)$.
The implementation problem of the control (4.4) requires the replacement of the integral terms by a difference equation, that results in a neutral type closed-loop system that may loose stability. In the case without state delay, where only the input delay is considered, the contribution in (Mondié & Michiels, 2003) introduces a filter in the control input in order to avoid such instability possibility.
For the case of state and input delays, Kharitonov (2015) introduces the dynamic predictor-based control law described by

$$
\begin{aligned}
\dot{u}(t) = & (G + F_0 B) u(t) + F_1 B u(t-h) + Q(\tau) x(t) + \int_{\tau}^{0} Q(-\xi) B u(t+\xi) d\xi \\
& + \int_{-h}^{0} Q(\tau - h - \theta) A_1 x(t+\theta) d\theta,
\end{aligned}
\tag{4.6}
$$

where $G \in \mathbb{R}^{m\times m}$, $F_0,\ F_1 \in \mathbb{R}^{m\times n}$, $Q(t) \in \mathbb{R}^{m\times n}$ and

$$
Q(t) = (F_0 A_0 - G F_0) K(t) + F_1 A_1 K(t-2h) + (F_0 A_1 + F_1 A_0 - G F_1) K(t-h),
$$

and $K(t)$ is the fundamental matrix which satisfies the delay differential equation (4.5).
In contrast with the simple preditor control law (4.4), the closed-loop system formed by system (4.1) and the dynamic predictor control law (4.6) is of retarded type and exponentially stable.

Theorem 2. *(Kharitonov, 2015). The characteristic function $q(s)$ of the closed-loop system (4.1), (4.6) is given by the formula*

$$q(s) = det[sI_{n\times n} - (A_0 + BF_0) - e^{-sh}(A_1 + BF_1)] \times det[sI_{n\times n} - G].$$

Corollary 3. *(Kharitonov, 2015). Let the matrices F_0 and F_1 choices insure exponential stability of system (4.3). The closed-loop system (4.1), (4.6) is exponentially stable if G is a Hurwitz matrix.*

As we see above, the implementation problem was solved and the stability analysis was addressed in the frequency domain framework. In the present work, we exploit the advantages that provides the time-domain framework, in particular, the extension of the robust stability analysis to time-varying uncertainties in parameters and/or delays.
The extended system representation of the closed-loop system (4.1), (4.6) in the time-domain is

$$\begin{bmatrix} \dot{x}(t) \\ \dot{u}(t) \end{bmatrix} = \begin{bmatrix} A_0 & 0_{n\times m} \\ Q(\tau) & G + F_0 B \end{bmatrix} \begin{bmatrix} x(t) \\ u(t) \end{bmatrix} + \begin{bmatrix} A_1 & 0_{n\times m} \\ 0_{m\times n} & F_1 B \end{bmatrix} \begin{bmatrix} x(t-h) \\ u(t-h) \end{bmatrix}$$
$$+ \begin{bmatrix} 0_{n\times n} & B \\ 0_{m\times n} & 0_{m\times m} \end{bmatrix} \begin{bmatrix} x(t-\tau) \\ u(t-\tau) \end{bmatrix} + \int_{-\tau}^{0} G(\theta) \begin{bmatrix} x(t+\theta) \\ u(t+\theta) \end{bmatrix} d\theta. \tag{4.7}$$

Defining $z(t) = [x(t) \quad u(t)]^T$, we represent system (4.7) in the compact form

$$\dot{z}(t) = \mathcal{A}_0 z(t) + \mathcal{A}_1 z(t-h) + \mathcal{A}_2 z(t-\tau) + \int_{-\tau}^{0} G(\theta) z(t+\theta) d\theta, \tag{4.8}$$

with

$$\mathcal{A}_0 = \begin{bmatrix} A_0 & 0_{n\times m} \\ Q(\tau) & G + F_0 B \end{bmatrix}, \ \mathcal{A}_1 = \begin{bmatrix} A_1 & 0_{n\times m} \\ 0_{m\times n} & F_1 B \end{bmatrix}, \ \mathcal{A}_2 = \begin{bmatrix} 0_{n\times n} & B \\ 0_{m\times n} & 0_{m\times m} \end{bmatrix},$$

and

$$G(\theta) = \begin{cases} \begin{bmatrix} 0_{n\times n} & 0_{n\times m} \\ Q(\tau - h - \theta)A_1 & Q(-\theta)B \end{bmatrix}, & \theta \in [-h, 0], \\ \begin{bmatrix} 0_{n\times n} & 0_{n\times m} \\ 0_{m\times n} & Q(-\theta)B \end{bmatrix}, & \theta \in [-\tau, -h], \end{cases}$$

where, $\mathcal{A}_0, \ \mathcal{A}_1, \ \mathcal{A}_2, \ G(\theta) \in R^{(n+m)\times(n+m)}$.
Note that the state-space representation of system (4.7) in the above compact representation is a distributed time-delay system with piecewise function kernel.

Our aim is to find the stability regions in the space of parameters of system (4.8) using the Lyapunov matrix approach introduced in the previous chapter. In the case of commensurate delays, where the delays are h, $\tau = jh$ and j is a natural number, it is always possible to prove stability of system (4.8) if this satisfies the Lyapunov condition.

4.2 Lyapunov matrix construction

For simplicity we consider $\tau = 2h$, then system (4.8) can be written into the form

$$\dot{z}(t) = \sum_{j=0}^{2} \mathcal{A}_j z(t - jh) + \sum_{j=0}^{1} \int_{-h}^{0} G_j(\theta) z(t + \theta - jh) d\theta, \tag{4.9}$$

where,

$$G_0(\theta) = \begin{bmatrix} 0_{n\times n} & 0_{n\times p} \\ Q(h-\theta)A_1 & Q(-\theta)B \end{bmatrix}, \quad G_1(\theta - h) = \begin{bmatrix} 0_{n\times n} & 0_{n\times p} \\ 0_{p\times n} & Q(-\theta+h)B \end{bmatrix}.$$

At this point, we do not know the number of matrix components of the terms $G_0(\theta)$ and $G_1(\theta - h)$. To address this problem, we represent the kernel in a general form,

$$G_j(\theta) = \sum_{i=0}^{k_j} g_{j,i}(\theta) C_{j,i},$$

then,

$$G_0(\theta) = \sum_{i=0}^{k_0} g_{0,i}(\theta) C_{0,i}, \qquad G_1(\theta - h) = \sum_{i=0}^{k_1} g_{1,i}(\theta) C_{1,i},$$

where $g_{0,i}(\theta),\ g_{1,i}(\theta)$ are scalar functions and $C_{0,i},\ C_{1,i} \in R^{(n+m)\times(n+m)}$. The scalar functions g are assumed to satisfy

$$g'_{j,i}(\theta) = \sum_{k=0}^{k_j} \alpha_{j,i}^{k} g_{j,k}, \quad j = 0, 1.$$

The system (4.9) has two concentrated delays and two distributed delays. In accordance with (Kharitonov, 2012), in this case, the matrix $U(\tau)$ associated with a symmetric matrix $W > 0$ satisfies:

- the dynamic property for $\tau > 0$,

$$U'(\tau) = \sum_{j=0}^{2} U(\tau - jh) \mathcal{A}_j + \sum_{j=0}^{1} \int_{-h}^{0} U(\tau + \theta - jh) G_j(\theta) d\theta, \tag{4.10}$$

- the symmetric property for $\tau \geq 0$,

$$U(-\tau) = U^T(\tau), \tag{4.11}$$

- the algebraic property,

$$U'(+0) - U'(-0) = -W. \tag{4.12}$$

From (4.10) and (4.11), the dynamic property for $\tau < 0$,

$$U'(\tau) = -[U'(-\tau)]^T = -\sum_{j=0}^{2} \mathcal{A}_j^T U(\tau + jh) - \sum_{j=0}^{1} [G_j(\theta)]^T \int_{-h}^{0} U(\tau - \theta + jh) d\theta. \tag{4.13}$$

The algebraic property can be rewritten as,

$$-W = \sum_{j=0}^{2} \left[U(-jh)\mathcal{A}_j + \mathcal{A}_j^T U(jh)\right] + \sum_{j=0}^{1} \left[\int_{-h}^{0} U(\theta - jh) G_j(\theta) d\theta \right.$$
$$\left. + [G_j(\theta)]^T \int_{-h}^{0} U(-\theta + jh) d\theta \right]. \tag{4.14}$$

4.3 Illustrative example

In this section we present a scalar example of the dynamic predictor control, illustrate the Lyapunov matrix construction, and validate the obtained results.
Consider the scalar linear distributed system with state and input delays and dynamic predictor control

$$\begin{aligned}\dot{x}(t) &= a_0 x(t) + a_1 x(t-h) + bu(t-2h)\\ \dot{u}(t) &= (g + f_0 b)u(t) + f_1 bu(t-h) + Q(\tau)x(t) + \int_{-h}^{0} Q(h-\theta) a_1 x(t+\theta) d\theta\\ &+ \int_{-2h}^{0} Q(-\theta) bu(t+\theta) d\theta,\end{aligned} \tag{4.15}$$

where, $Q(t) = (f_0 a_0 - g f_0)k(t) + f_1 a_1 k(t-2h) + (f_0 a_1 + f_1 a_0 - g f_1)k(t-h)$.
We define $z(t) = [x(t) \quad u(t)]^T$, then (4.15) can be represented in a compact form as

$$\begin{aligned}\dot{z}(t) &= A_0 z(t) + A_1 z(t-h) + A_2 z(t-\tau) + \int_{-h}^{0} G_0(\theta) z(t+\theta) d\theta\\ &+ \int_{-h}^{0} G_1(\theta - h) z(t + \theta - h) d\theta,\end{aligned} \tag{4.16}$$

$$\text{where,}\quad A_0=\begin{bmatrix} a_0 & 0 \\ Q(\tau) & g+f_0b \end{bmatrix},\ A_1=\begin{bmatrix} a_1 & 0 \\ 0 & f_1b \end{bmatrix},\ A_2=\begin{bmatrix} 0 & b \\ 0 & 0 \end{bmatrix},$$

$$G_0(\theta)=\begin{bmatrix} 0 & 0 \\ Q(h-\theta)a_1 & Q(-\theta)b \end{bmatrix},\ G_1(\theta-h)=\begin{bmatrix} 0 & 0 \\ 0 & Q(-\theta+h)b \end{bmatrix}.$$

Now, we calculate the kernels $G_0(\theta)$ and $G_1(\theta-h)$ by assessing the function $Q(t)$. The main challenge for obtaining the term $Q(t)$ reduces to the solution of the fundamental matrix $K(t)$ in the intervals $[0,h]$ and $[h,\tau]$. In the interval $t\in[0,h]$ the fundamental matrix solution is,

$$K(t)=e^{a_0t}.$$

For $t\in[h,\tau]$, we have,

$$K(t)=e^{a_0t}[1+a_1e^{-a_0h}(t-h)],$$

then

$$G_0(\theta)=\theta e^{-a_0\theta}C_{0,0}+e^{-a_0\theta}C_{0,1},$$

$$\begin{aligned}
\text{with}\quad & C_{0,0}=\begin{bmatrix} 0 & 0 \\ c_1a_1 & 0 \end{bmatrix},\ C_{0,1}=\begin{bmatrix} 0 & 0 \\ c_2a_1 & c_3b \end{bmatrix},\\
& c_1=(gf_0-f_0a_0)a_1,\\
& c_2=\left[(f_0a_0-gf_0)e^{a_0h}+(f_0a_1+f_1a_0-gf_1)\right],\\
& c_3=(f_0a_0-gf_0),
\end{aligned}$$

$$G_1(\theta-h)=\theta e^{-a_0\theta}C_{1,0}+e^{-a_0\theta}C_{1,1},$$

$$\begin{aligned}
\text{with}\quad & C_{1,0}=\begin{bmatrix} 0 & 0 \\ 0 & c_4b \end{bmatrix},\ C_{1,1}=\begin{bmatrix} 0 & 0 \\ 0 & c_5b \end{bmatrix},\\
& c_4=(gf_0-f_0a_0)a_1,\\
& c_5=\left[(f_0a_0-gf_0)e^{a_0h}+(f_0a_1+f_1a_0-gf_1)\right].
\end{aligned}$$

Finally the extended system is,

$$\begin{aligned}
\dot{z}(t)&=A_0z(t)+A_1z(t-h)+A_2z(t-2h)+\int_{-h}^{0}\theta e^{-a_0\theta}C_{0,0}z(t+\theta)d\theta\\
&+\int_{-h}^{0}e^{-a_0\theta}C_{0,1}z(t+\theta)d\theta+\int_{-h}^{0}\theta e^{-a_0\theta}C_{1,0}z(t+\theta-h)d\theta+\int_{-h}^{0}e^{-a_0\theta}C_{1,1}z(t+\theta-h)d\theta.
\end{aligned}\tag{4.17}$$

4.3.1 Lyapunov matrix construction

To construct the Lyapunov matrix, we obtain first the delay-free system of matrix equations. We define 4 auxiliary matrices corresponding to multiple constant delays,

$$Y_1(\tau) = U(\tau + h), \quad Y_0(\tau) = U(\tau), \quad Y_{-1}(\tau) = U(\tau - h), \quad Y_{-2}(\tau) = U(\tau - 2h). \tag{4.18}$$

Note that the distributed terms of system (4.17) have repeated kernels, hence the corresponding auxiliary matrices can be reduced. Both kernels G_0 and G_1 have two similar scalar functions, hence $g_{0,0}(\theta) = g_{1,0}(\theta)$ and $g_{0,1}(\theta) = g_{1,1}(\theta)$. As $g_{0,0}(\theta) = g_{1,0}(\theta) = \theta e^{-a_0\theta}$, we define the following auxiliary matrices

$$\begin{aligned}
Z_{0,1}(\tau) &= \int_{-h}^{0} \theta e^{-a_0\theta} U(\tau + \theta + h) d\theta, \quad J_{0,0}(\tau) = \int_{-h}^{0} \theta e^{-a_0\theta} U(\tau - \theta) d\theta, \\
Z_{0,0}(\tau) &= \int_{-h}^{0} \theta e^{-a_0\theta} U(\tau + \theta) d\theta, \quad J_{0,-1}(\tau) = \int_{-h}^{0} \theta e^{-a_0\theta} U(\tau - \theta - h) d\theta, \\
Z_{0,-1}(\tau) &= \int_{-h}^{0} \theta e^{-a_0\theta} U(\tau + \theta - h) d\theta, \quad J_{0,-2}(\tau) = \int_{-h}^{0} \theta e^{-a_0\theta} U(\tau - \theta - 2h) d\theta.
\end{aligned} \tag{4.19}$$

As $g_{0,1}(\theta) = g_{1,1}(\theta) = e^{-a_0\theta}$, the auxiliary matrices are

$$\begin{aligned}
Z_{1,1}(\tau) &= \int_{-h}^{0} e^{-a_0\theta} U(\tau + \theta + h) d\theta, \quad J_{1,0}(\tau) = \int_{-h}^{0} e^{-a_0\theta} U(\tau - \theta) d\theta, \\
Z_{1,0}(\tau) &= \int_{-h}^{0} e^{-a_0\theta} U(\tau + \theta) d\theta, \quad J_{1,-1}(\tau) = \int_{-h}^{0} e^{-a_0\theta} U(\tau - \theta - h) d\theta, \\
Z_{1,-1}(\tau) &= \int_{-h}^{0} e^{-a_0\theta} U(\tau + \theta - h) d\theta, \quad J_{1,-2}(\tau) = \int_{-h}^{0} e^{-a_0\theta} U(\tau - \theta - 2h) d\theta.
\end{aligned} \tag{4.20}$$

The subscripts of the matrices $Z_{i,j}$ and $J_{i,j}$ reveal the following: the first subscript indicates the $i - th$ term of the scalar function of G and the second indicates the advancement or delay h times with regard to the matrix U. Once the auxiliary matrices are defined, we obtain the delay-free system of auxiliary matrices.

Lemma 4. *Let $U(\tau)$ the Lyapunov matrix of system (4.16), associated with a symmetric matrix W. Then the auxiliary matrices (4.18), (4.19) and 4.20) satisfy the delay-free* *system of linear differential equations,*

$$
\begin{cases}
Y_i'(\tau) = \sum_{j=0}^{2} Y_{i-j}(\tau)A_j + \sum_{j=0}^{1}\left[Z_{j,i}(\tau)C_{0,j} + Z_{j,(i-1)}(\tau)C_{1,j}\right], \quad 0 < i < 1, \\
Y_i'(\tau) = -\sum_{j=0}^{2} A_j^T Y_{i+j}(\tau) - \sum_{j=0}^{1}\left[C_{0,j}^T J_{j,i}(\tau) + C_{1,j}^T J_{j,i+1}(\tau)\right], \quad 2 < i < -1, \\
Z_{0,i}'(\tau) = he^{a_0 h}Y_{i-1}(\tau) - Z_{1,i}(\tau) + a_0 Z_{0,i}(\tau), \quad -1 < i < 1, \\
J_{0,i}'(\tau) = -he^{a_0 h}Y_{i+1}(\tau) + J_{1,i}(\tau) - a_0 J_{0,i}(\tau), \quad -2 < i < 0, \\
Z_{1,i}'(\tau) = Y_i(\tau) - e^{a_0 h}Y_{i-1}(\tau) + a_0 Z_{1,i}(\tau), \quad -1 < i < 1, \\
J_{1,i}'(\tau) = e^{a_0 h}Y_{i+1}(\tau) - Y_i(\tau) - a_0 J_{1,i}(\tau), \quad -2 < i < 0,
\end{cases}
\tag{4.21}
$$

and the boundary conditions,

$$
\begin{cases}
Y_i(0) = Y_{i-1}(h), \quad -1 < i < 1, \\
Z_{0,i}(0) = Z_{0,i-1}(h), \quad 0 < i < 1, \\
J_{0,i}(0) = J_{0,i-1}(h), \quad -1 < i < 0, \\
Z_{1,i}(0) = Z_{1,i-1}(h), \quad 0 < i < 1, \\
J_{1,i}(0) = J_{1,i-1}(h), \quad -1 < i < 0, \\
Z_{0,-1}(0) = J_{0,0}^T(h), \\
Z_{1,-1}(0) = J_{1,0}^T(h), \\
J_{0,-2}(0) = Z_{0,1}^T(h), \\
J_{1,-2}(0) = Z_{1,1}^T(h), \\
Z_{0,0}(0) = \int_0^h (\theta - h)e^{-a_0(\theta-h)}Y_{-1}(\theta)d\theta, \\
Z_{1,0}(0) = \int_0^h e^{-a_0(\theta-h)}Y_{-1}(\theta)d\theta, \\
J_{0,0}(0) = -\int_0^h \theta e^{a_0\theta}Y_0(\theta)d\theta, \\
J_{1,0}(0) = \int_0^h e^{a_0\theta}Y_0(\theta)d\theta, \\
\sum_{j=0}^{2}\left[Y_{-j}(0)A_j + A_j^T Y_{j-1}(h)\right] + \sum_{j=0}^{1}\left[\sum_{i=0}^{1} Z_{i,-j}(0)C_{j,i} + \sum_{i=0}^{1} C_{j,i}^T J_{i,j-1}(h)\right] = -W.
\end{cases}
\tag{4.22}
$$

Proof. Equations (4.21), come from (4.10), (4.13), (4.18), (4.19) and (4.20). Boundary conditions (4.22) come from (4.18), (4.19) and (4.20) and the algebraic property (4.14). □

We apply (4.21) to obtain the delay-free system of linear matrix differential equations in terms of the auxiliary matrices

$$
\begin{aligned}
Y_1'(\tau) &= Y_1(\tau)A_0 + Y_0(\tau)A_1 + Y_{-1}(\tau)A_2 + Z_{0,1}(\tau)C_{0,0} \\
&\quad + Z_{1,1}(\tau)C_{0,1} + Z_{0,0}(\tau)C_{1,0} + Z_{1,0}(\tau)C_{1,1}, \\
Y_0'(\tau) &= Y_0(\tau)A_0 + Y_{-1}(\tau)A_1 + Y_{-2}(\tau)A_2 + Z_{0,0}(\tau)C_{0,0} \\
&\quad + Z_{1,0}(\tau)C_{0,1} + Z_{0,-1}(\tau)C_{1,0} + Z_{1,-1}(\tau)C_{1,1},
\end{aligned}
$$

$$
\begin{aligned}
Y'_{-1}(\tau) &= -A_0^T Y_{-1}(\tau) - A_1^T Y_0(\tau) - A_2^T Y_1(\tau) \\
&\quad -C_{0,0}^T J_{0,-1}(\tau) - C_{0,1}^T J_{1,-1}(\tau) - C_{1,0}^T J_{0,0}(\tau) \\
&\quad -C_{1,1}^T J_{1,0}(\tau), \\
Y'_{-2}(\tau) &= -A_0^T Y_{-2}(\tau) - A_1^T Y_{-1}(\tau) - A_2^T Y_0(\tau) \\
&\quad -C_{0,0}^T J_{0,-2}(\tau) - C_{0,1}^T J_{1,-2}(\tau) - C_{1,0}^T J_{0,-1}(\tau) \\
&\quad -C_{1,1}^T J_{1,-1}(\tau), \\
Z'_{0,1}(\tau) &= he^{a_0 h} Y_0(\tau) - Z_{1,1}(\tau) + a_0 Z_{0,1}(\tau) \\
Z'_{0,0}(\tau) &= he^{a_0 h} Y_{-1}(\tau) - Z_{1,0}(\tau) + a_0 Z_{0,0}(\tau) \\
Z'_{0,-1}(\tau) &= he^{a_0 h} Y_{-2}(\tau) - Z_{1,-1}(\tau) + a_0 Z_{0,-1}(\tau) \\
J'_{0,0}(\tau) &= -he^{a_0 h} Y_1(\tau) + J_{1,0}(\tau) - a_0 J_{0,0}(\tau) \\
J'_{0,-1}(\tau) &= -he^{a_0 h} Y_0(\tau) + J_{1,-1}(\tau) - a_0 J_{0,-1}(\tau) \\
J'_{0,-2}(\tau) &= -he^{a_0 h} Y_{-1}(\tau) + J_{1,-2}(\tau) - a_0 J_{0,-2}(\tau) \\
Z'_{1,1}(\tau) &= Y_1(\tau) - e^{a_0 h} Y_0(\tau) + a_0 Z_{1,1}(\tau) \\
Z'_{1,0}(\tau) &= Y_0(\tau) - e^{a_0 h} Y_{-1}(\tau) + a_0 Z_{1,0}(\tau) \\
Z'_{1,-1}(\tau) &= Y_{-1}(\tau) - e^{a_0 h} Y_{-2}(\tau) + a_0 Z_{1,-1}(\tau) \\
J'_{1,0}(\tau) &= e^{a_0 h} Y_1(\tau) - Y_0(\tau) - a_0 J_{1,0}(\tau) \\
J'_{1,-1}(\tau) &= e^{a_0 h} Y_0(\tau) - Y_{-1}(\tau) - a_0 J_{1,-1}(\tau) \\
J'_{1,-2}(\tau) &= e^{a_0 h} Y_{-1}(\tau) - Y_{-2}(\tau) - a_0 J_{1,-2}(\tau).
\end{aligned}
\tag{4.23}
$$

According to equation (4.22), the boundary conditions are,

$$
\begin{aligned}
Y_1(0) &= Y_0(h) \\
Y_0(0) &= Y_{-1}(h) \\
Y_{-1}(0) &= Y_{-2}(h) \\
Z_{0,1}(0) &= Z_{0,0}(h) \\
Z_{0,0}(0) &= Z_{0,-1}(h) \\
J_{0,0}(0) &= J_{0,-1}(h) \\
J_{0,-1}(0) &= J_{0,-2}(h) \\
Z_{1,1}(0) &= Z_{1,0}(h)
\end{aligned}
\qquad
\begin{aligned}
Z_{1,0}(0) &= Z_{1,-1}(h) \\
J_{1,0}(0) &= J_{1,-1}(h) \\
J_{1,-1}(0) &= J_{1,-2}(h) \\
Z_{0,-1}(0) &= J_{0,0}^T(h) \\
Z_{1,-1}(0) &= J_{1,0}^T(h) \\
J_{0,-2}(0) &= Z_{0,1}^T(h) \\
J_{1,-2}(0) &= Z_{1,1}^T(h)
\end{aligned}
$$

$$
\begin{aligned}
A_0^T Y_0(0) + Y_0(0)A_0 + A_1^T Y_0(h) + Y_{-1}(0)A_1 & \\
+A_2^T Y_1(h) + Y_{-2}(0)A_2 + Z_{0,0}(0)C_{0,0} + C_{0,0}^T J_{0,-1}(h) & \\
+Z_{1,0}(0)C_{0,1} + C_{0,1}^T J_{1,-1}(h) + Z_{0,-1}(0)C_{1,0} + C_{1,0}^T J_{0,0}(h) & \\
+Z_{1,-1}(0)C_{1,1} + C_{1,1}^T J_{1,0}(h) &= -W. \qquad (4.24)
\end{aligned}
$$

To write the delay-free system of differential equations (4.23) in vector form, we use Kronecker products of matrices, see Appendix D. The vectorization of system (4.23) is $\dot{R}(\tau) = LR(\tau)$ where

$$
\begin{aligned}
R(\tau) = [&y_1(\tau),\ y_0(\tau),\ y_{-1}(\tau),\ y_{-2}(\tau),\ z_{0,1}(\tau),\ z_{0,0}(\tau),\ z_{0,-1}(\tau),\ j_{0,0}(\tau),\ j_{0,-1}(\tau),\\
&j_{0,-2}(\tau),\ z_{1,1}(\tau),\ z_{1,0}(\tau),\ z_{1,-1}(\tau),\ j_{1,0}(\tau),\ j_{1,-1}(\tau),\ j_{1,-2}(\tau)]^T.
\end{aligned}
$$

$R(\tau)$ is such that $R(\tau) = e^{L\tau}R(0)$, and it follows from the boundary condition (4.24) that

$$
\left[M + Ne^{Lh}\right] R(0) = \begin{bmatrix} 0 \\ -w \end{bmatrix},
$$

$$
R(\tau) = e^{L\tau}[M + Ne^{Lh}]^{-1} \begin{bmatrix} 0 \\ -w \end{bmatrix}. \qquad (4.25)
$$

Next, we construct the Lyapunov matrix $U(\tau)$ using (4.25) for $h = 1$, $a_0 = 0.2$, $a_1 = 0.8$, $b = 1$, $g = -2$ and $W = \begin{pmatrix} 1 & 0 \\ 0 & 1 \end{pmatrix}$. The elements of $U(\tau) = Y_0(\tau)$ and $U(\tau + h) = Y_1(\tau)$ defined in the interval $\tau \in [0, 1]$ for $(k_0, k_1) = (0.25, -2)$, are shown in Figure 4.1. After obtaining the Lyapunov matrix, the necessary condition (A.6) is applied to find the stability region of system (4.17) in the space of parameters (f_0, f_1). The regions where this condition holds for $r = 1$ and $r = 4$, respectively, are depicted on Figures 4.2 and 4.3. No further improvement is obtained for greater r.

4.3.2 Verification

For verification, we compare the regions on Figures 4.2 and 4.3, analyzing the closed-loop of the original scalar delay linear system (4.15) but using the simple predictor control law (4.2) when $\tau = 2h$, as follows

$$
\begin{aligned}
\dot{x}(t) &= a_0 x(t) + a_1 x(t-h) + bu(t-2h),\\
u(t) &= f_0 x(t+2h) + f_1 x(t+2h-h), \qquad (4.26)
\end{aligned}
$$

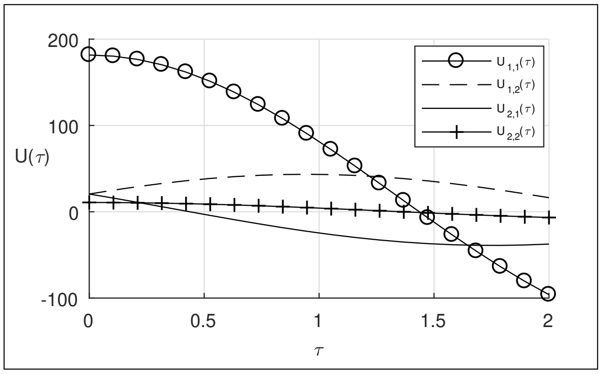

Figure 4.1: Matrix $U(\tau)$ elements, system (4.17) .

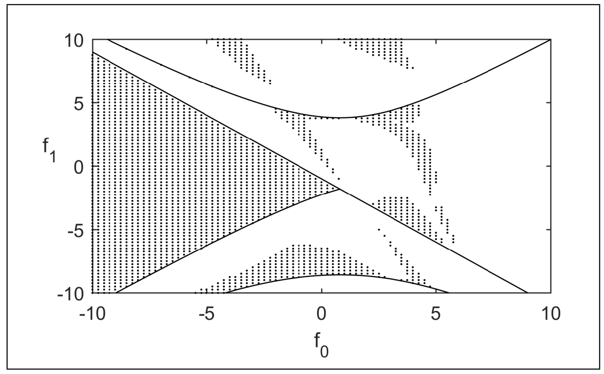

Figure 4.2: Necessary condition (A.6) satisfied for system (4.17), $r = 1$.

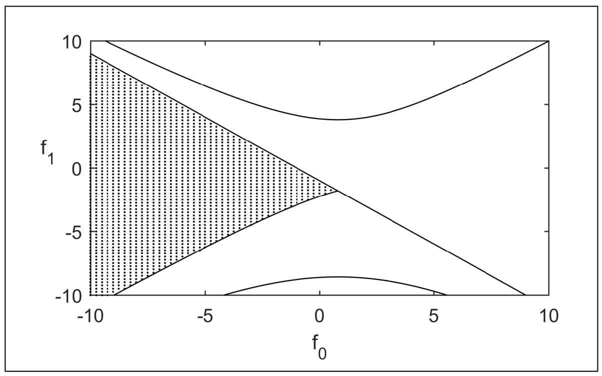

Figure 4.3: Exact stability region for system (4.17), $r = 4$.

then the closed-loop of (4.26) replacing $a_0 = 0.2$ and $a_1 = 0.8$ and $b = 1$ is a system only with state delay

$$\dot{x}(t) = (0.2 + f_0)x(t) + (0.8 + f_1)x(t - h). \tag{4.27}$$

Note that the predictor control law has compensated the input delay of the system, but as we mentioned at the beginning, the problem is the control $u(t)$ implementation. In conclusion the system that we analyze in the time-domain with the dynamic predictor control law is equivalent to system (4.27). The stability chart of this system can be obtained using the necessary conditions (A.6) and is depicted on Figure 4.4. As expected, stability regions from Figures 4.3 and 4.4 are similar. In other words, using the dynamic predictor control law produces the same stability region obtained by applying the predictor control law, and at the same time, solves the implementation problem.

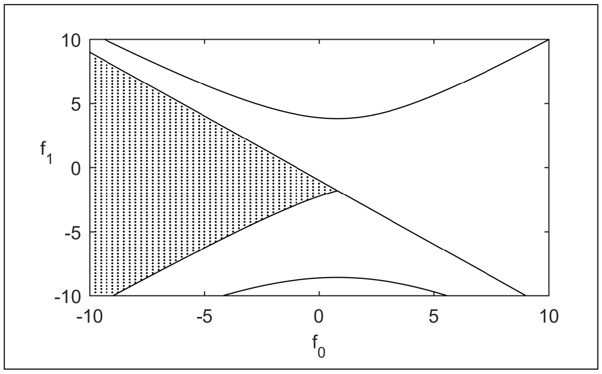

Figure 4.4: Stability region, system (4.27), $r = 6$.

4.4 Conclusions

We have presented the extended system representation of the dynamic predictor controller for systems with input and state delays. Moreover, a method to construct the Lyapunov matrix of these systems in closed-loop with the dynamic predictive controller, is described. This matrix allows us to find the stability region of the closed-loop. The region obtained is consistent with that produced by a simple predictor control law. The main advantage of using the dynamic version is to solve the implementation problem. It is worthy of mention that a multivariable example is presented in (Juárez, Mondié & Kharitonov, 2020), and that a $\sigma-$stabilization example for this controller is given in (Juárez & Mondié, 2019).

Chapter 5

Robust stability analysis

To address the robust stability analysis of linear systems with only pointwise delays, the reader is referred to Appendix C. This chapter is devoted to the robust stability analysis of systems with multiple pointwise and distributed delays subjected to matrix parameters and delays uncertainties. Exact robust stability conditions expressed in terms of the delay Lyapunov matrix are given. The obtained conditions extend to the above mentioned class of systems the results achieved by (Alexandrova & Zhabko, 2018; Medvedeva, 2015; Medvedeva & Zhabko, 2015) based on functionals with simple quadratic derivative in the instantaneous state (Huang, 1989). Some illustrative examples are presented.

5.1 Problem statement

We consider a delay linear nominal system of the form

$$\dot{x}(t) = \sum_{k=0}^{m} A_k x(t - h_k) + \sum_{j=1}^{m} \int_{-h_j}^{0} G_j(\theta) x(t + \theta) d\theta, \tag{5.1}$$

where A_k, $k = \overline{0, m}$, are constant $n \times n$ matrices, the constant delays satisfy $0 = h_0 < h_1 < \ldots < h_m = h$, and $G_j(\theta)$, $j = \overline{1, m}$, are continuous matrix-valued functions defined for $\theta \in [-h_j, 0]$. We denote by $x(t, \varphi)$ the solution of system (5.1) with a given initial function $\varphi(\theta)$, $\theta \in [-h, 0]$, and

$$x_t(\varphi) : \theta \to x(t + \theta, \varphi),\ \theta \in [-h, 0]\,,$$

the restriction of the solution $x(t, \varphi)$ to the interval $[t - h, t]$. If the initial function is not crucial, the argument φ is dropped. In this work, we address the following problems:

Problem 1. Consider the following perturbed system

$$\dot{y}(t) = \sum_{k=0}^{m} (A_k + \Delta_k)\, y(t-h_k) + \sum_{j=1}^{m} \int_{-h_j}^{0} (G_j(\theta) + \delta_j(\theta))\, y(t+\theta) d\theta. \tag{5.2}$$

The nominal system (5.1) is assumed to be asymptotically stable and the matrices $\Delta_k,\ k = \overline{0,m}$, and $\delta_j(\theta)$, $j = \overline{1,m}$, are time-invariant uncertainties of the system matrices and kernel functions, respectively. The problem is to find the bounds

$$\|\Delta_k\| \leq \rho_k, \quad \|\delta_j(\theta)\| \leq \tilde{\rho}_j,$$

such that system (5.2) remains asymptotically stable.

Problem 2. Consider the following perturbed system

$$\dot{y}(t) = \sum_{k=0}^{m} A_k y(t - h_k - \eta_k) + \sum_{j=1}^{m} \int_{-h_j-\eta_j}^{0} G_j(\theta) y(t+\theta) d\theta. \tag{5.3}$$

The nominal system (5.1) is assumed to be asymptotically stable and the constant perturbations η_k, $k = \overline{0,m}$, are uncertainties of the system delays. The restrictions $\eta_k \geq -h_k$ insure that system (5.3) is of retarded type. The problem is to find conditions on the perturbations η_k under which the perturbed system (5.3) remains asymptotically stable.

5.2 Preliminary results

In this section, we remind some concepts of the Lyapunov-Krasovskii framework for distributed delay systems (Huang, 1989; Kharitonov, 2012). The functional given by

$$\begin{aligned}
v(\varphi) &= \varphi^T(0)U(0)\varphi(0) + 2\varphi^T(0) \sum_{j=1}^{m} \int_{-h_j}^{0} U(-\theta - h_j) A_j \varphi(\theta) d\theta \\
&+ \sum_{k=1}^{m}\sum_{j=1}^{m} \int_{-h_k}^{0} \varphi^T(\theta_1) A_k^T \int_{-h_j}^{0} U(\theta_1 + h_k - \theta_2 - h_j) A_j \varphi(\theta_2) d\theta_2 d\theta_1 \\
&+ 2\varphi^T(0) \sum_{j=1}^{m} \int_{-h_j}^{0} \int_{-h_j}^{\theta} U(\xi - \theta) G_j(\xi) d\xi \varphi(\theta) d\theta
\end{aligned}$$

$$\begin{aligned}
&+ 2\sum_{j=1}^{m} \int_{-h_j}^{0} \varphi^T(\theta_1) A_j^T \sum_{k=1}^{m} \int_{-h_k}^{0} \int_{-h_k}^{\theta_2} U(h_j + \theta_1 - \theta_2 + \xi) G_k(\xi) \varphi(\theta_2) d\xi d\theta_2 d\theta_1 \\
&+ \sum_{j=1}^{m}\sum_{k=1}^{m} \int_{-h_j}^{0} \varphi^T(\theta_1) \int_{-h_k}^{0} \int_{-h_j}^{\theta_1} G_j^T(\xi_1) \int_{-h_k}^{\theta_2} U(\theta_1 - \theta_2 - \xi_1 + \xi_2) G_k(\xi_2) d\xi_2 d\xi_1 \varphi(\theta_2) d\theta_2 d\theta_1,
\end{aligned} \tag{5.4}$$

has time derivative along the solutions of system (5.1) of the form

$$\frac{dv(x_t)}{dt} = -x^T(t)Wx(t), \quad t \geq 0, \tag{5.5}$$

where $W > 0$. The matrix $U(\tau)$, $\tau \in [-h, h]$, is called the Lyapunov matrix associated with matrix W and is known to exist and to be unique if system (5.1) satisfies the Lyapunov condition (the characteristic equation of (5.1) has no roots s_0 and $-s_0$ simultaneously). For $\tau \geq 0$, this matrix is solution of the following matrix equation, also called dynamic property

$$U'(\tau) = \sum_{j=0}^{m} U(\tau - h_j)A_j + \sum_{j=1}^{m} \int_{-h_j}^{0} U(\tau + \theta)G_j(\theta)d\theta,$$

and satisfies the symmetry property

$$U(\tau) = U^T(-\tau),$$

and the algebraic property

$$-W = \sum_{j=0}^{m} \left[U(-h_j)A_j + A_j^T U(h_j)\right] + \sum_{j=1}^{m} \left(\int_{-h_j}^{0} U(\theta)G_j(\theta)d\theta + \int_{-h_j}^{0} G_j^T(\theta)U(-\theta)d\theta \right).$$

5.3 Robust stability conditions

In this section, we present robust stability bounds for Problems 1 and 2. We apply the novel approach (Alexandrova & Zhabko, 2018; Medvedeva, 2015; Medvedeva & Zhabko, 2015) where a simple Lyapunov-Krasovskii functional with derivative (5.5) is used, and the integral bound for the derivative of the functional along the solutions of the uncertain system is constructed. Let us define the following constants:

$$M = \max_{\tau \in [0,h]} \|U(\tau)\|, \quad K = \sum_{k=0}^{m} \|A_k\|, \quad g_j = \max_{\theta \in [-h_j, 0]} \|G_j(\theta)\|, \ j = \overline{1, m},$$

$$\beta = \sum_{k=1}^{m} \|A_k\| h_k, \quad \gamma = \sum_{k=1}^{m} g_k h_k^2, \quad \alpha = 1 + \beta + \gamma, \quad P = \rho_0 + \sum_{k=1}^{m} (\rho_k + \tilde{\rho}_k h_k),$$

$$N = \sum_{k=0}^{m} \|A_k\| |\eta_k|, \quad \lambda = \sum_{j=1}^{m} g_j |\eta_j|, \quad \mu = \sum_{j=1}^{m} g_j (h_j + \eta_j), \quad h_\eta = \max_{k=\overline{0,m}} \{h_k + \eta_k\},$$

$$H = \max\{h, h_\eta\}.$$

It is worthy of mention that the fact that $M = \max_{\tau \in [0,h]} \|U(\tau)\| = \|U(0)\|$ proved (Egorov & Mondié, 2015) for asymptotically stable systems with multiple concentrated delays, is also true for systems of the form (5.1).

5.3.1 Uncertainties in the system matrices

The first step in finding bounds on matrix parameters uncertainties is to compute the time-derivative of functional (5.4) along the solutions of system (5.2),

$$\frac{dv(y_t)}{dt} = -y^T(t)Wy(t) + l(y_t), \quad t \geq 0, \tag{5.6}$$

where

$$l(y_t) = 2\left[\sum_{k=0}^{m} \Delta_k y(t-h_k) + \sum_{j=1}^{m} \int_{-h_j}^{0} \delta_j(\theta) y(t+\theta) d\theta\right]^T \Big[U(0)y(t) +$$
$$\sum_{l=1}^{m} \int_{-h_l}^{0} U(-s-h_l)A_l y(t+s)ds + \sum_{l=1}^{m} \int_{-h_l}^{0} \int_{-h_l}^{s} U(\xi-s)G_l(\xi)d\xi y(t+s)ds\Big].$$

First, we estimate the summands of the functional $l(y_t)$:

$$J_{11} = 2\left[\sum_{k=0}^{m} \Delta_k y(t-h_k)\right]^T U(0)y(t) \leq M\sum_{k=0}^{m} \rho_k \left\|y(t)\right\|^2 + M\sum_{k=0}^{m} \rho_k \left\|y(t-h_k)\right\|^2,$$

$$J_{12} = 2\left[\sum_{k=0}^{m} \Delta_k y(t-h_k)\right]^T \sum_{l=1}^{m} \int_{-h_l}^{0} U(-s-h_l)A_l y(t+s)ds \leq M\beta\sum_{k=0}^{m} \rho_k \left\|y(t-h_k)\right\|^2$$
$$+ M\sum_{k=0}^{m} \rho_k \sum_{l=1}^{m} \|A_l\| \int_{-h_l}^{0} \left\|y(t+\theta)\right\|^2 d\theta,$$

$$J_{13} = 2\left[\sum_{k=0}^{m} \Delta_k y(t-h_k)\right]^T \sum_{l=1}^{m} \int_{-h_l}^{0} \int_{-h_l}^{s} U(\xi-s)G_l(\xi)d\xi\, y(t+s)ds \leq M\gamma\sum_{k=0}^{m} \rho_k \left\|y(t-h_k)\right\|^2$$
$$+ M\sum_{k=0}^{m} \rho_k \sum_{l=1}^{m} g_l h_l \int_{-h_l}^{0} \left\|y(t+\theta)\right\|^2 d\theta,$$

$$J_{21} = 2\left[\sum_{j=1}^{m} \int_{-h_j}^{0} \delta_j(\theta)y(t+\theta)d\theta\right]^T U(0)y(t) \leq M\sum_{j=1}^{m} \tilde{\rho}_j h_j \left\|y(t)\right\|^2$$
$$+ M\sum_{j=1}^{m} \tilde{\rho}_j \int_{-h_j}^{0} \left\|y(t+\theta)\right\|^2 d\theta,$$

$$J_{22} = 2\left[\sum_{j=1}^{m} \int_{-h_j}^{0} \delta_j(\theta)y(t+\theta)d\theta\right]^T \sum_{l=1}^{m} \int_{-h_l}^{0} U(-s-h_l)A_l y(t+s)ds$$
$$\leq M\beta\sum_{j=1}^{m} \tilde{\rho}_j \int_{-h_j}^{0} \left\|y(t+\theta)\right\|^2 d\theta + M\sum_{j=1}^{m} \tilde{\rho}_j h_j \sum_{l=1}^{m} \|A_l\| \int_{-h_l}^{0} \left\|y(t+\theta)\right\|^2 d\theta,$$

$$J_{23} = 2\left[\sum_{j=1}^{m}\int_{-h_j}^{0}\delta_j(\theta)y(t+\theta)d\theta\right]^T\sum_{l=1}^{m}\int_{-h_l}^{0}\int_{-h_l}^{s}U(\xi-s)G_l(\xi)d\xi\, y(t+s)ds$$
$$\leq M\gamma\sum_{j=1}^{m}\tilde{\rho}_j\int_{-h_j}^{0}\|y(t+\theta)\|^2 d\theta + M\sum_{j=1}^{m}\tilde{\rho}_j h_j\sum_{l=1}^{m}g_l h_l\int_{-h_l}^{0}\|y(t+\theta)\|^2 d\theta.$$

Summarizing, we obtain the following upper bound for $l(y_t)$:

$$l(y_t) \leq (L_0+\rho_0 L_1)\|y(t)\|^2 + L_1\sum_{k=1}^{m}\rho_k\|y(t-h_k)\|^2 + \sum_{j=1}^{m}\Big((\|A_j\|+g_j h_j)L_0+\tilde{\rho}_j L_1\Big)$$
$$\times\int_{-h_j}^{0}\|y(t+\theta)\|^2 d\theta, \tag{5.7}$$

where $L_0 = PM$, $L_1 = \alpha M$.

Next, we present a technical lemma that is instrumental in the robustness proof.

Lemma 5. *The functional $l(y_t)$ satisfies the inequality*

$$\int_0^t l(y_s)ds \leq L\left(\int_0^t\|y(s)\|^2 ds + \int_{-h}^{0}\|y(s)\|^2 ds\right),$$

where $L = 2\alpha PM$.

Proof. Integrating each summand of the right-hand side of (5.7) yields

$$\int_0^t\|y(s-h_k)\|^2 ds \leq \int_{-h_k}^{t-h_k}\|y(s)\|^2 ds \leq \int_0^t\|y(s)\|^2 ds + \int_{-h}^{0}\|y(s)\|^2 ds, \quad k=\overline{1,m},$$
$$\int_0^t\int_{-h_j}^{0}\|y(s+\theta)\|^2 d\theta ds = \int_{-h_j}^{0}\int_{\theta}^{t+\theta}\|y(s)\|^2 ds d\theta$$
$$\leq h_j\left(\int_0^t\|y(s)\|^2 ds + \int_{-h}^{0}\|y(s)\|^2 ds\right), \quad j=\overline{1,m},$$

hence

$$\int_0^t l(y_s)ds \leq (\alpha L_0 + PL_1)\int_0^t\|y(s)\|^2 ds + \left((\alpha-1)L_0 + L_1\sum_{k=1}^{m}(\rho_k+\tilde{\rho}_k h_k)\right)$$
$$\times\int_{-h}^{0}\|y(s)\|^2 ds,$$

and the lemma is proved. □

The following result reveals the phylosophy of the proof which is at the junction of frequency and time domain techniques.

Lemma 6. *Let system* (5.1) *satisfy the Lyapunov condition. Then, if*

$$P = \rho_0 + \sum_{k=1}^{m} (\rho_k + \tilde{\rho}_k h_k) < \frac{\lambda_{min}(W)}{2\alpha M}, \tag{5.8}$$

where $\alpha = 1 + \sum_{j=1}^{m} \left(\|A_j\| h_j + g_j h_j^2 \right)$, *and* $M = \|U(0)\|$, *then system* (5.2) *has no eigenvalues on the imaginary axis.*

Proof. The idea of the proof is borrowed from (Alexandrova, 2018). As the Lyapunov condition is assumed to be satisfied, the functional v exists. Integrating both sides of equality (5.6) from 0 to t_1, $t_1 \geq 0$, along the solutions of system (5.2) yields

$$v(y_{t_1}(\varphi)) - v(\varphi) = -\int_0^{t_1} \left[y^T(s) W y(s) - l(y_s) \right] ds,$$

or

$$\int_0^{t_1} y^T(s) W y(s) ds - \int_0^{t_1} l(y_s) ds = v(\varphi) - v(y_{t_1}(\varphi)).$$

Lemma 5 implies that

$$(\lambda_{min}(W) - L) \int_0^{t_1} \|y(s)\|^2 ds - L \int_{-h}^{0} \|y(s)\|^2 ds \leq v(\varphi) - v(y_{t_1}(\varphi)). \tag{5.9}$$

Assume by contradiction that a crossing of the imaginary axis occur, namely $s = 0$ or $s = \pm j\beta$.

For $s = 0$, this implies that there exists a constant solution of (5.2), i.e. $y(t) = c$, $t \geq -h$, where c is a non zero vector. Substitution of this solution into inequality (5.9) gives

$$(\lambda_{min}(W) - L) t_1 \|c\|^2 - Lh \|c\|^2 \leq 0.$$

Clearly, in view of the fact that condition (5.8) implies $\lambda_{min}(W) - L > 0$, the left-hand side becomes positive for a large enough t_1, which leads to a contradiction.

For $s = \pm j\beta$, $\beta > 0$, it follows that there exists a solution of the form $y(t) = \cos(\beta t) c_1 - \sin(\beta t) c_2$, $t \geq -h$, where $c_1, c_2 \in \mathbb{R}^n$, with at least one of them non zero. Let $t_1 = 2\pi k/\beta$, $k \in \mathbb{N}$, and observe that $y_{t_1}(\varphi) \equiv \varphi$. Substituting this solution into (5.9), we obtain

$$(\lambda_{min}(W) - L) \left(\|c_1\|^2 + \|c_2\|^2 \right) \frac{\pi k}{\beta} - \psi \leq 0,$$

where

$$\psi = \frac{L}{\beta} \left\{ \|c_1\|^2 \left(\frac{\beta h}{2} + \frac{\sin(2\beta h)}{4} \right) + \|c_2\|^2 \left(\frac{\beta h}{2} - \frac{\sin(2\beta h)}{4} \right) + c_1^T c_2 \sin^2(\beta h) \right\}.$$

As ψ is finite, the left-hand side of the previous inequality becomes positive for sufficiently large k, thus we arrive again at a contradiction, and the result is proved. □

Our main result on matrix parameters uncertainties follows immediately.

Theorem 3. *Assume system* (5.1) *to be asymptotically stable. Then if the disturbances in system* (5.2) *satisfy the condition* (5.8), *then the perturbed system* (5.2) *is asymptotically stable.*

Proof. By the continuity properties of the roots of time-delay systems of retarded type, with respect to matrix parameters, roots at the right-hand side of the complex plane can occur only if for some parameters values, the imaginary axis is crossed. As this possibility is ruled out by condition (5.8) we conclude that the system (5.2) remains stable. □

5.3.2 Uncertainties in the system delays

In order to address the case of delays uncertainty, system (5.3) is first transformed by using the Newton-Leibniz formula,

$$\begin{aligned}\dot{y}(t) &= \sum_{k=0}^{m} A_k y(t-h_k) + \left(\sum_{k=0}^{m} A_k y(t-h_k-\eta_k) - \sum_{k=0}^{m} A_k y(t-h_k) \right)\\ &+ \sum_{j=1}^{m} \int_{-h_j-\eta_j}^{0} G_j(\theta) y(t+\theta) d\theta,\\ &= \sum_{k=0}^{m} A_k y(t-h_k) + \sum_{k=0}^{m} A_k \int_{-h_k}^{-h_k-\eta_k} \dot{y}(t+\theta) d\theta + \sum_{j=1}^{m} \int_{-h_j}^{0} G_j(\theta) y(t+\theta) d\theta\\ &+ \sum_{j=1}^{m} \int_{-h_j-\eta_j}^{-h_j} G_j(\theta) y(t+\theta) d\theta.\end{aligned}$$

Substituting $\dot{y}(t+\theta)$ from (5.3), we get

$$\begin{aligned}\dot{y}(t) &= \sum_{k=0}^{m} A_k y(t-h_k) + \sum_{j=1}^{m} \int_{-h_j}^{0} G_j(\theta) y(t+\theta) d\theta + \sum_{k=0}^{m} A_k\\ &\times \int_{-h_k}^{-h_k-\eta_k} \left\{ \sum_{j=0}^{m} A_j y(t+\theta-h_j-\eta_j) \right\} d\theta + \sum_{k=0}^{m} A_k\\ &\times \int_{-h_k}^{-h_k-\eta_k} \left\{ \sum_{j=1}^{m} \int_{-h_j-\eta_j}^{0} G_j(s) y(t+\theta+s) ds \right\} d\theta + \sum_{j=1}^{m} \int_{-h_j-\eta_j}^{-h_j} G_j(\theta) y(t+\theta) d\theta, \quad t \geq H.\end{aligned}$$

The time derivative of functional (5.4) along the solutions of system (5.3) is

$$\frac{dv(y_t)}{dt} = -y^T(t) W y(t) + l(y_t), \quad t \geq H,$$

where

$$
\begin{aligned}
l(y_t) = 2 &\left[\sum_{k=0}^{m} \sum_{j=0}^{m} A_k A_j \int_{-h_k}^{-h_k-\eta_k} y(t+\theta-h_j-\eta_j) d\theta + \sum_{k=0}^{m} \sum_{j=1}^{m} A_k \int_{-h_k}^{-h_k-\eta_k} \int_{-h_j-\eta_j}^{0} \right. \\
&\left. \times G_j(s) y(t+\theta+s) ds d\theta + \sum_{j=1}^{m} \int_{-h_j-\eta_j}^{-h_j} G_j(\theta) y(t+\theta) d\theta \right]^T \left[U(0) y(t) \right. \\
&\left. + \sum_{l=1}^{m} \int_{-h_l}^{0} U(-s-h_l) A_l y(t+s) ds + \sum_{l=1}^{m} \int_{-h_l}^{0} \int_{-h_l}^{s} U(\xi - s) G_l(\xi) d\xi y(t+s) ds \right].
\end{aligned}
$$

The estimation of each summand of the functional $l(y_t)$ gives

$$
\begin{aligned}
I_{11} &= 2 \left[\sum_{k=0}^{m} \sum_{j=0}^{m} A_k A_j \int_{-h_k}^{-h_k-\eta_k} y(t+\theta-h_j-\eta_j) d\theta \right]^T U(0) y(t) \leq MKN \left\| y(t) \right\|^2 \\
&+ M \sum_{k=0}^{m} \|A_k\| \sum_{j=0}^{m} \|A_j\| \left| \int_{-h_k-\eta_k-h_j-\eta_j}^{-h_k-h_j-\eta_j} \left\| y(t+\theta) \right\|^2 d\theta \right|, \\
I_{12} &= 2 \left[\sum_{k=0}^{m} \sum_{j=0}^{m} A_k A_j \int_{-h_k}^{-h_k-\eta_k} y(t+\theta-h_j-\eta_j) d\theta \right]^T \sum_{l=1}^{m} \int_{-h_l}^{0} U(-s-h_l) A_l y(t+s) ds \\
&\leq M\beta \sum_{k=0}^{m} \|A_k\| \sum_{j=0}^{m} \|A_j\| \left| \int_{-h_k-\eta_k-h_j-\eta_j}^{-h_k-h_j-\eta_j} \left\| y(t+\theta) \right\|^2 d\theta \right| + MKN \sum_{l=1}^{m} \|A_l\| \\
&\times \int_{-h_l}^{0} \left\| y(t+\theta) \right\|^2 d\theta, \\
I_{13} &= 2 \left[\sum_{k=0}^{m} \sum_{j=0}^{m} A_k A_j \int_{-h_k}^{-h_k-\eta_k} y(t+\theta-h_j-\eta_j) d\theta \right]^T \sum_{l=1}^{m} \int_{-h_l}^{0} \int_{-h_l}^{s} U(\xi - s) G_l(\xi) d\xi \\
&\times y(t+s) ds \leq M\gamma \sum_{k=0}^{m} \|A_k\| \sum_{j=0}^{m} \|A_j\| \left| \int_{-h_k-\eta_k-h_j-\eta_j}^{-h_k-h_j-\eta_j} \left\| y(t+\theta) \right\|^2 d\theta \right| \\
&+ MKN \sum_{l=1}^{m} g_l h_l \int_{-h_l}^{0} \left\| y(t+\theta) \right\|^2 d\theta, \\
I_{21} &= 2 \left[\sum_{k=0}^{m} \sum_{j=1}^{m} A_k \int_{-h_k}^{-h_k-\eta_k} \int_{-h_j-\eta_j}^{0} G_j(s) y(t+\theta+s) ds d\theta \right]^T U(0) y(t) \leq MN\mu \left\| y(t) \right\|^2 \\
&+ M \sum_{j=1}^{m} g_j \sum_{k=0}^{m} \|A_k\| \left| \int_{-h_k-\eta_k}^{-h_k} \int_{\theta-h_j-\eta_j}^{\theta} \left\| y(t+\xi) \right\|^2 d\xi d\theta \right|,
\end{aligned}
$$

$$
\begin{aligned}
I_{22} &= 2\left[\sum_{k=0}^{m}\sum_{j=1}^{m} A_k \int_{-h_k}^{-h_k-\eta_k}\int_{-h_j-\eta_j}^{0} G_j(s)y(t+\theta+s)dsd\theta\right]^T \sum_{l=1}^{m}\int_{-h_l}^{0} U(-\zeta-h_l)A_l \\
&\times y(t+\zeta)d\zeta \le M\beta\sum_{j=1}^{m} g_j \sum_{k=0}^{m}\|A_k\| \left|\int_{-h_k-\eta_k}^{-h_k}\int_{\theta-h_j-\eta_j}^{\theta} \|y(t+\xi)\|^2 d\xi d\theta\right| \\
&+ MN\mu\sum_{l=1}^{m}\|A_l\|\int_{-h_l}^{0}\|y(t+\theta)\|^2 d\theta, \\
I_{23} &= 2\left[\sum_{k=0}^{m}\sum_{j=1}^{m} A_k \int_{-h_k}^{-h_k-\eta_k}\int_{-h_j-\eta_j}^{0} G_j(s)y(t+\theta+s)dsd\theta\right]^T \sum_{l=1}^{m}\int_{-h_l}^{0}\int_{-h_l}^{\psi} U(\zeta-\psi) \\
&\times G_l(\zeta)d\zeta y(t+\psi)d\psi \le M\gamma\sum_{j=1}^{m} g_j \sum_{k=0}^{m}\|A_k\| \left|\int_{-h_k-\eta_k}^{-h_k}\int_{\theta-h_j-\eta_j}^{\theta} \|y(t+\xi)\|^2 d\xi d\theta\right| \\
&+ MN\mu\sum_{l=1}^{m} g_l h_l\int_{-h_l}^{0}\|y(t+\theta)\|^2 d\theta, \\
I_{31} &= 2\left[\sum_{j=1}^{m}\int_{-h_j-\eta_j}^{-h_j} G_j(\theta)y(t+\theta)d\theta\right]^T U(0)y(t) \le M\lambda\|y(t)\|^2 \\
&+ M\sum_{j=1}^{m} g_j\left|\int_{-h_j-\eta_j}^{-h_j}\|y(t+\theta)\|^2 d\theta\right|, \\
I_{32} &= 2\left[\sum_{j=1}^{m}\int_{-h_j-\eta_j}^{-h_j} G_j(\theta)y(t+\theta)d\theta\right]^T \sum_{l=1}^{m}\int_{-h_l}^{0} U(-s-h_l)A_l y(t+s)ds \le M\beta\sum_{j=1}^{m} g_j \\
&\times\left|\int_{-h_j-\eta_j}^{-h_j}\|y(t+\theta)\|^2 d\theta\right| + M\lambda\sum_{l=1}^{m}\|A_l\|\int_{-h_l}^{0}\|y(t+\theta)\|^2 d\theta,
\end{aligned}
$$

$$
\begin{aligned}
I_{33} &= 2\left[\sum_{j=1}^{m}\int_{-h_j-\eta_j}^{-h_j} G_j(\theta)y(t+\theta)d\theta\right]^T \sum_{l=1}^{m}\int_{-h_l}^{0}\int_{-h_l}^{s} U(\xi-s)G_l(\xi)d\xi y(t+s)ds \\
&\le M\gamma\sum_{j=1}^{m} g_j\left|\int_{-h_j-\eta_j}^{-h_j}\|y(t+\theta)\|^2 d\theta\right| + M\lambda\sum_{l=1}^{m} g_l h_l\int_{-h_l}^{0}\|y(t+\theta)\|^2 d\theta.
\end{aligned}
$$

In view of the above, we obtain the following upper bound for the functional $l(y_t)$,

$$
\begin{aligned}
l(y_t) &\le L_0\|y(t)\|^2 + L_0\sum_{l=1}^{m}(\|A_l\| + g_l h_l)\int_{-h_l}^{0}\|y(t+\theta)\|^2 d\theta + L_1\sum_{j=1}^{m} g_j \\
&\times\left|\int_{-h_j-\eta_j}^{-h_j}\|y(t+\theta)\|^2 d\theta\right| + L_1\sum_{k=0}^{m}\|A_k\|\sum_{j=0}^{m}\|A_j\|\left|\int_{-h_k-\eta_k-h_j-\eta_j}^{-h_k-h_j-\eta_j}\|y(t+\theta)\|^2 d\theta\right| \\
&+ L_1\sum_{k=0}^{m}\|A_k\|\sum_{j=1}^{m} g_j\left|\int_{-h_k-\eta_k}^{-h_k}\int_{\theta-h_j-\eta_j}^{\theta}\|y(t+\xi)\|^2 d\xi d\theta\right|, \qquad (5.10)
\end{aligned}
$$

where $L_0 = M\left(\lambda + (K+\mu)N\right),\ L_1 = \alpha M.$

Lemma 7. *The functional $l(y_t)$ satisfies the inequality*

$$\int_H^t l(y_s)ds \leq L\left(\int_H^t \|y(s)\|^2\, ds + \int_{-h_\eta}^H \|y(s)\|^2\, ds\right),$$

where $L = 2\alpha M\left(\lambda + (K+\mu)N\right).$

Proof. We integrate each term of the right-hand side of (5.10):

$$\int_H^t \int_{-h_l}^0 \|y(s+\theta)\|^2\, d\theta ds = \int_{-h_l}^0 \int_{H+\theta}^{t+\theta} \|y(s)\|^2\, dsd\theta \leq h_l\left(\int_H^t \|y(s)\|^2\, ds + \int_0^H \|y(s)\|^2\, ds\right).$$

Next, by the mean value theorem, we obtain

$$\int_H^t \left|\int_{-h_j-\eta_j}^{-h_j} \|y(s+\theta)\|^2\, d\theta\right| ds = |\eta_j| \int_H^t \|y(s-c_1)\|^2\, ds \leq |\eta_j|\left(\int_H^t \|y(s)\|^2\, ds\right.$$
$$\left. + \int_0^H \|y(s)\|^2\, ds\right),$$

where c_1 is a value between h_j and $h_j+\eta_j$. Similarly,

$$\int_H^t \left|\int_{-h_k-\eta_k-h_j-\eta_j}^{-h_k-h_j-\eta_j} \|y(s+\theta)\|^2\, d\theta\right| ds = |\eta_k| \int_H^t \|y(s-c_2)\|^2\, ds \leq |\eta_k|\left(\int_H^t \|y(s)\|^2\, ds\right.$$
$$\left. + \int_{-h_\eta}^H \|y(s)\|^2\, ds\right),$$

where c_2 is a value between $h_k+h_j+\eta_j$ and $h_k+\eta_k+h_j+\eta_j$. Finally,

$$\int_H^t \left|\int_{-h_k-\eta_k}^{-h_k} \int_{\theta-h_j-\eta_j}^{\theta} \|y(s+\xi)\|^2\, d\xi d\theta\right| ds = \left|\int_{-h_k-\eta_k}^{-h_k} \int_{\theta-h_j-\eta_j}^{\theta} \int_{H+\xi}^{t+\xi} \|y(s)\|^2\, dsd\xi d\theta\right|$$
$$\leq (h_j+\eta_j)\,|\eta_k|\left(\int_H^t \|y(s)\|^2\, ds + \int_{-h_\eta}^H \|y(s)\|^2\, ds\right).$$

Summarizing, we obtain

$$\int_H^t l(y_s)ds \leq \big(\alpha L_0 + (\lambda + (K+\mu)N)L_1\big) \int_H^t \|y(s)\|^2\, ds + \big((\alpha-1)L_0$$
$$+ (\lambda + (K+\mu)N)L_1\big) \int_{-h_\eta}^H \|y(s)\|^2\, ds,$$

and the lemma is proved. □

Lemma 8. *Let system* (5.1) *satisfy the Lyapunov condition. Then, if*

$$\lambda + (K+\mu)\,N = \sum_{j=1}^{m} g_j\,|\eta_j| + \left(K + \sum_{j=1}^{m} g_j(h_j+\eta_j)\right)\sum_{k=0}^{m} \|A_k\|\,|\eta_k| < \frac{\lambda_{min}(W)}{2\alpha M}, \quad (5.11)$$

where $\eta_k \geq -h_k$, $k = \overline{0,m}$, *then the perturbed system* (5.3) *has no eigenvalues on the imaginary axis.*

Proof. The proof of the result is similar to the proof of Lemma 7. □

Theorem 4. *Assume system* (5.1) *to be asymptotically stable. Then, if the delays uncertainties in system* (5.3) *satisfy condition* (5.11), *then the perturbed system* (5.3) *is asymptotically stable.*

Proof. The proof of the result is similar to the proof of Theorem 3. □

5.4 Iterative procedure

In order to improve our robust stability bounds, we propose an iterative procedure extending the one in (Alexandrova & Zhabko, 2018). For illustrative purposes, consider the case of matrix uncertainties of the following structure:

$$\begin{aligned} &\Delta_k = \rho_k I, \quad \rho_k = \lambda_k \rho, \quad k = \overline{0,m}, \\ &\delta_j(\theta) = \tilde{\rho}_j I, \quad \tilde{\rho}_j = \tilde{\lambda}_j \rho, \quad j = \overline{1,m}. \end{aligned} \quad (5.12)$$

Here, $\lambda_k \geq 0$ and $\tilde{\lambda}_j \geq 0$ are fixed, and $\rho \geq 0$ is a parameter. This structure can be interpreted as a "direction" in the space of uncertainties $\rho_0, \ldots, \rho_m, \tilde{\rho}_1, \ldots, \tilde{\rho}_m$. Define

$$\Lambda = \lambda_0 + \sum_{k=1}^{m} \left(\lambda_k + \tilde{\lambda}_k h_k\right),$$

and set a symmetric positive definite matrix W. For the computation of the Lyapunov matrix the reader is referred to (Juárez & Mondié, 2018a; Kharitonov, 2012), and Chapter 3.

Step 1. Consider a nominal asymptotically stable system (5.1). Compute the Lyapunov matrix associated with W, and calculate the bound

$$\bar{\rho} = \frac{\lambda_{min}(W)}{2\alpha M \Lambda} - \varepsilon.$$

Here, ε is an arbitrary positive value such that $\bar{\rho} > 0$. According to Theorem 3, the perturbed system (5.2) with uncertainties of the form (5.12) is asymptotically stable for $\rho \in [0, \bar{\rho}]$.

Step 2. Consider the new nominal system with

$$\tilde{A}_k = A_k + \lambda_k \bar{\rho} I, \quad \tilde{G}_j(\theta) = G_j(\theta) + \tilde{\lambda}_j \bar{\rho} I,$$

and go back to step 1. Proceed until the bound with desired precision is obtained.

After a number of steps, we get the sequence of bounds $\bar{\rho}_l > 0$, $l = 1, 2, \ldots$ found successively for different nominal systems, and the sequence of corresponding positive values ε_l. Similarly to (Alexandrova & Zhabko, 2018), it can be shown that if the sequence ε_l is chosen converging to zero as $l \to +\infty$, then the value $\sum_{k=1}^{l} \bar{\rho}_k$ converges to the exact critical value of the parameter ρ, as is confirmed by the examples in the next section. A similar procedure can be used for the uncertainties of different structure, or for delay uncertainties. Negative perturbations can be considered as well.

5.5 Illustrative Examples

In this section, we apply the iterative procedure to find robust stability bounds for three illustrative examples. The delay Lyapunov matrix is computed for $W = I$. With the purpose of evaluating the conservatism of the obtained bounds, we present first two examples for which the exact stability region can be depicted in the space of parameters. The isolated points indicate where the necessary and sufficient stability conditions expressed in terms of the delay Lyapunov matrix, presented in (Egorov, Cuvas & Mondié, 2017) are satisfied. The continuous lines correspond to stability boundaries obtained via the D-partition method (Neimark, 1949).

Example 1. Consider the delay linear distributed system (Feng & Lam, 2011)

$$\dot{x}(t) = A_0 x(t) + A_h \int_{-h_1}^{0} x(t+\theta) d\theta, \tag{5.13}$$

$$\text{where} \quad A_0 = \begin{pmatrix} a & 0 \\ 0.1 & -1.9 \end{pmatrix}, \quad A_h = \begin{pmatrix} -1 & 0 \\ -1 & -1 \end{pmatrix}.$$

We choose the nominal pair of parameters $(h_1, a) = (1.34, 1)$ in the stability region of system (5.13) depicted in Figure 5.1. We consider the following matrix perturbation

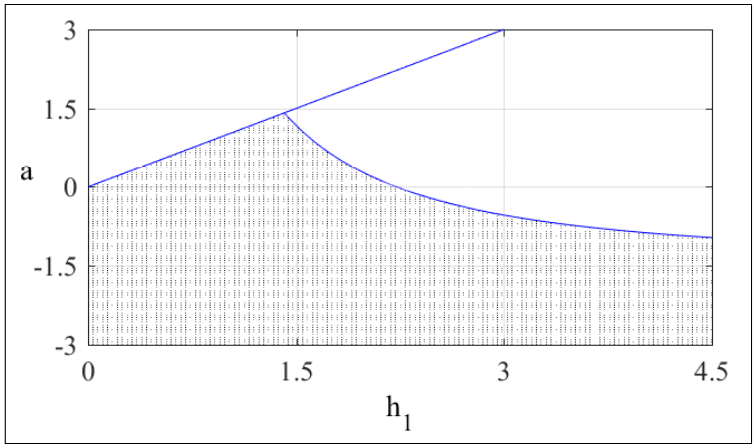

Figure 5.1: Stability region for system (5.13).

structure

$$\Delta_0 = \begin{pmatrix} \tilde{\Delta}_0 & 0 \\ 0 & 0 \end{pmatrix} \rightarrow \|\Delta_0\| = |\tilde{\Delta}_0| \leq \rho_0,$$

such that the parameter a is only affected by the perturbation. For $\varepsilon = 10^{-6}$, the iterative procedure based on Theorem 3 gives the upper bound $\tilde{\Delta}_0 \leq 0.3399$ after 500 iterations, while the exact stability region is $\tilde{\Delta}_0 < 0.34$.

Now, consider uncertainty in the delay. The perturbed system is

$$\dot{y}(t) = A_0 y(t) + A_h \int_{-h_1-\eta_1}^{0} y(t+\theta)d\theta.$$

We select the nominal pair of parameters $(h_1, a) = (1.195, 1.1226)$. For $\varepsilon = 10^{-7}$, the application of the iterative method based on Theorem 4 gives the stability interval $\eta_1 \in (-0.07230, 0.3251)$ after 165 and 400 iterations for the lower and upper bounds, respectively, while the exact stability interval is $\eta_1 \in (-0.07232, 0.3251)$.

Example 2. Consider the delay linear distributed system (Gouaisbaut & Ariba, 2009)

$$\dot{x}(t) = a_0 x(t) + \int_{-h}^{0} (1 + \theta + \theta^3) x(t+\theta) d\theta. \tag{5.14}$$

We take the nominal pair of parameters $(h, a_0) = (1, -0.5)$ in the stability region of system (5.14) depicted in Figure 5.2. The iterative application of Theorem 3, for $\varepsilon = 10^{-4}$, and after 100 iterations, provides the upper bound $\Delta_0 \leq 0.2499$, whereas that from the exact stability region is $\Delta_0 < 0.25$.

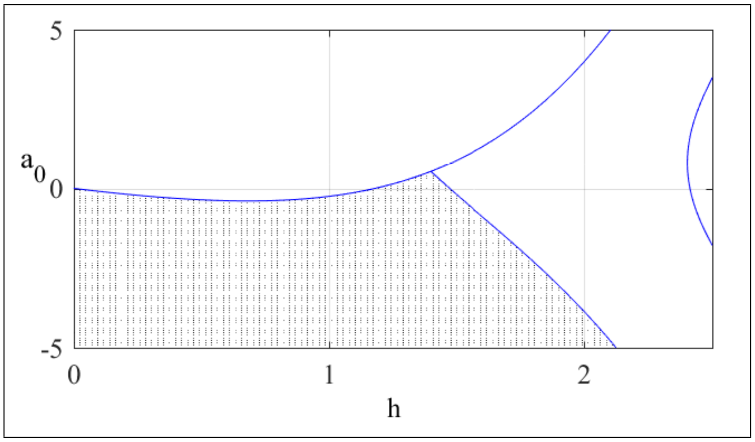

Figure 5.2: Stability region for system (5.14).

Consider now uncertainty in the delay. The delay perturbed system is

$$\dot{y}(t) = a_0 y(t) + \int_{-h-\eta_1}^{0} (1 + \theta + \theta^3) y(t+\theta) d\theta,$$

We choose the nominal pair of parameters $(h, a_0) = (1.4, 0.4)$. Applying the iterative method, for $\varepsilon = 10^{-7}$, we obtain after 200 iterations that the interval for the delay perturbation is $\eta_1 \in (-0.0463, 0.0155)$, whereas the exact stability region is $\eta_1 \in (-0.0470, 0.0157)$.

Next, we turn our attention to the robustness analysis case study of the dynamic predictor based control (Kharitonov, 2014) of systems with state and input delays. It is worthy of mention that the robustness analysis of these systems in closed-loop with predictor based control law is an intricate issue that has given rise to many proposals (truncated predictor (Zhou, Lin & Duan, 2012), sequential observer based predictors (Najafi, Hosseinnia, Sheikholeslam & Karimadini, 2013; Zhou, Liu & Mazenc, 2017), to name a few) whose aim is to circumvent the presence of the resulting coupled delay differential and integral equations. In contrast with these approaches, the dynamic predictor (Kharitonov, 2015) does not involve any approximation. It resorts to the introduction of stable dynamics, such that one ends up with an extended system with distributed delay. Clearly, our results are tailor-made to address the robustness of the closed-loop.

Example 3. Consider the delay linear system with both state and input delay (Kharitonov, 2014)

$$\dot{x}(t) = A_0 x(t) + A_1 x(t-h) + Bu(t-\tau) \tag{5.15}$$

in closed-loop with the dynamic predictor-based controller (Kharitonov, 2015)

$$
\begin{aligned}
\dot{u}(t) = (G + F_0 B)u(t) + F_1 Bu(t-h) + Q(\tau)x(t) + \int_{-\tau}^{0} Q(-\theta)Bu(t+\theta)d\theta \\
+ \int_{-h}^{0} Q(\tau - h - \theta)A_1 x(t+\theta)d\theta,
\end{aligned}
\tag{5.16}
$$

where $Q(t) = (F_0A_0 - GF_0)K(t) + F_1A_1K(t-2h) + (F_0A_1 + F_1A_0 - GF_1)K(t-h)$.

Here, $K(t)$ is the fundamental matrix of system (5.15)

$$
\begin{aligned}
\dot{K}(t) =& K(t)A_0 + K(t-h)A_1, \quad t \geq 0, \\
K(t) =& 0_{n\times n}, \ t < 0, \\
K(0) =& I.
\end{aligned}
$$

The perturbed version of (5.15) is assumed to be of the form

$$
\dot{y}(t) = (A_0 + \Delta_0)y(t) + (A_1 + \Delta_1)y(t-h) + (B + \Delta_B)u(t-\tau), \tag{5.17}
$$

where $\|\Delta_0\| \leq \rho_0$, $\|\Delta_1\| \leq \rho_1$, $\|\Delta_B\| \leq \rho_2$. The control law (5.16) is computed for the nominal system (5.15), but with the perturbed state $y(t)$ instead of $x(t)$, i.e.

$$
\begin{aligned}
\dot{u}(t) = (G + F_0 B)u(t) + F_1 Bu(t-h) + Q(\tau)y(t) + \int_{-\tau}^{0} Q(-\theta)Bu(t+\theta)d\theta \\
+ \int_{-h}^{0} Q(\tau - h - \theta)A_1 y(t+\theta)d\theta.
\end{aligned}
\tag{5.18}
$$

Matrices F_0, F_1 and G are chosen such that the nominal closed-loop system (5.17), (5.18) is exponentially stable. This system can be represented (Juárez, Mondié & Kharitonov, 2020) as an extended system with distributed delays of the form

$$
\dot{\tilde{z}}(t) = \sum_{j=0}^{2}(\mathcal{A}_j + \Lambda_j)\tilde{z}(t-h_j) + \sum_{j=1}^{2}\int_{-h_j}^{0} G_j(\theta)\tilde{z}(t+\theta)d\theta,
$$

with $\tilde{z}(t) = [y(t) \quad u(t)]^T$, delays $h_0 = 0$, $h_1 = h$, $h_2 = \tau$, and matrices

$$
\mathcal{A}_0 = \begin{bmatrix} A_0 & 0 \\ Q(\tau) & G + F_0 B \end{bmatrix}, \quad \mathcal{A}_1 = \begin{bmatrix} A_1 & 0 \\ 0 & F_1 B \end{bmatrix}, \quad \mathcal{A}_2 = \begin{bmatrix} 0 & B \\ 0 & 0 \end{bmatrix},
$$

$$G_1(\theta) = \begin{bmatrix} 0 & 0 \\ Q(\tau - h - \theta)A_1 & Q(-\theta)B \end{bmatrix}, \quad \in [-h, 0],$$

$$G_2(\theta) = \begin{cases} \begin{bmatrix} 0 & 0 \\ Q(\tau - h - \theta)A_1 & Q(-\theta)B \end{bmatrix}, \\ \theta \in [-h, 0], \\ \begin{bmatrix} 0 & 0 \\ 0 & Q(-\theta)B \end{bmatrix}, \\ \theta \in [-\tau, -h]. \end{cases}$$

The uncertain matrices are of the form

$$\Lambda_0 = \begin{bmatrix} \Delta_0 & 0 \\ 0 & 0 \end{bmatrix}, \ \Lambda_1 = \begin{bmatrix} \Delta_1 & 0 \\ 0 & 0 \end{bmatrix}, \ \Lambda_2 = \begin{bmatrix} 0 & \Delta_B \\ 0 & 0 \end{bmatrix}.$$

Observe that $\|\Lambda_0\| = \|\Delta_0\|$, $\|\Lambda_1\| = \|\Delta_1\|$, $\|\Lambda_2\| = \|\Delta_B\|$. In this example, we consider the nominal system (5.15) with

$$A_0 = \begin{bmatrix} 1 & 0 \\ 1 & 2 \end{bmatrix}, \ A_1 \begin{bmatrix} 1 & 0 \\ 2 & -1 \end{bmatrix}, \ B = \begin{bmatrix} 1 \\ 1 \end{bmatrix},$$

and delays $h = 0.1$, $\tau = 0.2$. The control law (5.16) is tuned using the necessary and sufficient stability conditions (Egorov, Cuvas & Mondié, 2017) which yield

$$F_0 = [-1, -2], \ F_1 = [10, -20], \ G = -0.5.$$

We choose the following perturbation structure for the uncertain matrices

$$\Delta_0 = \begin{bmatrix} a & 0 \\ 0 & a \end{bmatrix}, \ \Delta_1 = \begin{bmatrix} a & 0 \\ 0 & a \end{bmatrix}, \ \Delta_B = \begin{bmatrix} a \\ a \end{bmatrix}, \ a \in \mathbb{R},$$

therefore $\|\Delta_0\| = \|\Delta_1\| = |a|$, $\|\Delta_B\| = \sqrt{2}\,|a|$. Hence, Theorem 3 takes the form

$$|a| < \frac{\lambda_{min}(W)}{2\alpha M(2 + \sqrt{2})}.$$

For $\varepsilon = 10^{-7}$, we find that the perturbed closed-loop system is exponentially stable for $a \in (-0.8774, 0.1319)$ after 500 and 2000 iterations for the lower and upper bound, respectively.

5.6 Conclusions

In this chapter we have presented robust stability conditions for systems with multiple pointwise and distributed delays. Theorems 3 and 4 provide conditions that are highly effective when they are applied in an iterative manner, indicating convergence to the exact matrix and delay uncertainty intervals. It is worthy of mention we first approached this problem in (Juárez, Mondié & Kharitonov, 2020), using complete type functionals. As the obtained results were much more conservative than those presented here, they are omitted.

Chapter 6

Illustrative examples

In this chapter, the analysis and design tools introduced in Chapters 3 and 4 are applied to a number of problems concerning the vehicle platoons models developed in chapter 2. For simplicity, only chains of three and five vehicles are presented. The first example is based on model "A" with Connected Cruise Control (Qin, Gomez & Orosz, 2017). The simplicity of this model resides in the fact that is a delay linear system with only pointwise delays. Our aim is to understand the role the delay is playing in modifying the stability of the system. The second example uses model "B" with the Extended Cooperative Adaptive Cruise Control (Montanaro *et al.*, 2014). The objective is to illustrate how the input delay compensator improves the system response when it is transformed into a delay-free linear system. Finally, the last example shows a novel control strategy which is based on the human driver's memory effects modeled in (Sipahi & Niculescu, 2010). The results are validated by stability charts and numerical simulations. Finally, each section concludes with some comments.

6.1 Robust and $\sigma-$stability analysis for a platoon of vehicles with the Connected Cruise Control

Our first example involves a chain of three vehicles. Based on model "A" developed in Chapter 2, a detailed σ-stability analysis is carried out with special interest in the maximum exponential decay. With the help of the results in Appendix C, robust stability bounds with respect to matrix uncertainties are calculated.

In chain of vehicles, the stability can be studied as: *plant stability:* capacity of a vehicle to achieve the steady state while no disturbances occur, and *string stability:* the ability to attenuate disturbances of vehicles ahead. Due to the connectivity structure depicted in Figure 2.1, the communication signals are broadcasted downstream, and therefore any perturbation at the input will be amplified or reduced for the vehicles in this direction, affecting the string stability. It is assumed that this perturbation will be reflected directly within the dynamic of the tail vehicle.

In this work, we perform in the time-domain a *plant stability* analysis aiming at the determination of the maximal platoon exponential decay. In the case of *string stability*, the frequency domain approach has demonstrated to facilitate this analysis, see (Jin & Orosz, 2014; Qin, Gomez & Orosz, 2017; Zhang & Orosz, 2016). The stability analysis is performed by using the necessary stability conditions presented in Appendix A. Moreover, the calculation of the maximal platoon exponential decay, (see Appendix B) involves the dynamic response of all vehicles in the platoon. The objective is to determine the vehicle with the slowest response since this sets the highest achievable exponential decay of the entire platoon.

Modeling three vehicles with CCC approach. In this section, a plant stability analysis which includes σ-stability and robust stability for a platoon scenario with three vehicles, is presented. The scenarios with four and five vehicles are available in (Juárez, Mondié & Cuvas, 2018). The figures of this section represent σ-stability regions in the space of controller or system parameters. They are obtained as follows: At equidistant points of the space of parameters for different values of σ, the Lyapunov matrix is computed and tested using the stability conditions of Theorem 5. The guaranteed exponential decay color code is described in each figure.

The mathematical CCC-vehicle model (2.4) has a variety of control gains $\alpha_{i,i-1}$, $\beta_{i,j}$ to be selected, giving rise to a large number of independent parameters. To make the analysis tractable and considering previous results in (Zhang & Orosz, 2016), the same value for all control gains $\alpha_{i,i-1} = 0.6$, $\beta_{i,j} = 0.7$ and delays $h_{i,i-1} = h_{i,j} = h = 0.4$ is assumed, where $i = \overline{0, n}$ and $j = \overline{0, i-1}$, with exception of the control gains of the tail vehicle $\alpha_{n,n-1}$ and $\beta_{n,0}$ which are considered as free control parameters. In the first experiments all delays are fixed. Later, they are used as another control parameter, giving rise to a 3D stability chart of control parameters. In this scenario, and in accordance with Figure 6.1, vehicles one and two are CCC-equipped, and vehicle zero is only broadcasting data. As recommended in (Zhang & Orosz, 2016), we chose the equilibrium point at $d_i(t) = d^* = 20[m]$, which gives $V(d^*) = v_i(t) = v^* = 15[m/s]$ and $V'(d^*) = \pi/2$. Vehicle zero is the leader and its parameters are the input of the entire state-space representation of the platoon. Vehicles

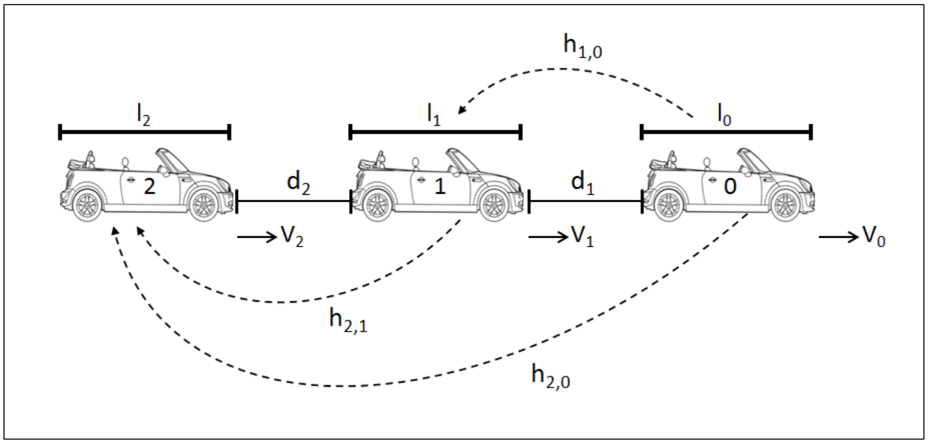

Figure 6.1: Three connected vehicles

one and two are described by (2.3), as follows:

$$\dot{\tilde{x}}_1(t) = A_0^1\tilde{x}_1(t) + A_{1,0}\tilde{x}_1(t-h_{1,0}) + B_{1,0}\tilde{x}_1(t-h_{1,0}) + C_{1,0}\tilde{x}_0(t-h_{1,0}) + D_0\tilde{x}_0(t),$$

$$\text{where} \quad A_0^1 = \begin{bmatrix} 0 & -1 \\ 0 & 0 \end{bmatrix}, \quad A_{1,0} = \begin{bmatrix} 0 & 0 \\ \psi_{1,0} & -\alpha_{1,0} \end{bmatrix}, \quad B_{1,0} = \begin{bmatrix} 0 & 0 \\ 0 & -\beta_{1,0} \end{bmatrix},$$
$$C_{1,0} = \begin{bmatrix} 0 & 0 \\ 0 & \beta_{1,0} \end{bmatrix}, \quad D_0 = \begin{bmatrix} 0 & 1 \\ 0 & 0 \end{bmatrix}, \quad \psi_{1,0} = \alpha_{1,0}V'(d^*),$$

$$\begin{aligned}\dot{\tilde{x}}_2(t) &= A_0^2\tilde{x}_2(t) + A_{2,1}\tilde{x}_2(t-h_{2,1}) + B_{2,0}\tilde{x}_2(t-h_{2,0}) + C_{2,0}\tilde{x}_0(t-h_{2,0}) \\ &\quad + B_{2,1}\tilde{x}_2(t-h_{2,1}) + C_{2,1}\tilde{x}_1(t-h_{2,1}) + D_0\tilde{x}_1(t),\end{aligned}$$

$$\text{where} \quad A_0^2 = \begin{bmatrix} 0 & -1 \\ 0 & 0 \end{bmatrix}, \quad A_{2,1} = \begin{bmatrix} 0 & 0 \\ \psi_{2,1} & -\alpha_{2,1} \end{bmatrix}, \quad B_{2,0} = \begin{bmatrix} 0 & 0 \\ 0 & -\beta_{2,0} \end{bmatrix},$$
$$C_{2,0} = \begin{bmatrix} 0 & 0 \\ 0 & \beta_{2,0} \end{bmatrix}, \quad B_{2,1} = \begin{bmatrix} 0 & 0 \\ 0 & -\beta_{2,1} \end{bmatrix}, \quad C_{2,1} = \begin{bmatrix} 0 & 0 \\ 0 & \beta_{2,1} \end{bmatrix},$$
$$D_1 = \begin{bmatrix} 0 & 1 \\ 0 & 0 \end{bmatrix}, \quad \psi_{2,1} = \alpha_{2,1}V'(d^*).$$

The head to tail model is given by (2.4)

$$\begin{aligned}
\begin{bmatrix} \dot{\tilde{x}}_1(t) \\ \dot{\tilde{x}}_2(t) \end{bmatrix} &= \begin{bmatrix} A_0^1 & 0_{2\times 2} \\ D_1 & A_0^2 \end{bmatrix} \begin{bmatrix} \tilde{x}_1(t) \\ \tilde{x}_2(t) \end{bmatrix} + \begin{bmatrix} A_{1,0}+B_{1,0} & 0_{2\times 2} \\ 0_{2\times 2} & 0_{2\times 2} \end{bmatrix} \begin{bmatrix} \tilde{x}_1(t-h_{1,0}) \\ \tilde{x}_2(t-h_{1,0}) \end{bmatrix} \\
&+ \begin{bmatrix} 0_{2\times 2} & 0_{2\times 2} \\ 0_{2\times 2} & B_{2,0} \end{bmatrix} \begin{bmatrix} \tilde{x}_1(t-h_{2,0}) \\ \tilde{x}_2(t-h_{2,0}) \end{bmatrix} + \begin{bmatrix} 0_{2\times 2} & 0_{2\times 2} \\ C_{2,1} & A_{2,1}+B_{2,1} \end{bmatrix} \begin{bmatrix} \tilde{x}_1(t-h_{2,1}) \\ \tilde{x}_2(t-h_{2,1}) \end{bmatrix} \\
&+ \begin{bmatrix} D_0 \\ 0_{2\times 2} \end{bmatrix} \tilde{x}_0(t) + \begin{bmatrix} C_{1,0} \\ 0_{2\times 2} \end{bmatrix} \tilde{x}_0(t-h_{1,0}) + \begin{bmatrix} 0_{2\times 2} \\ C_{2,0} \end{bmatrix} \tilde{x}_0(t-h_{2,0}) \\
&= \mathcal{A}_{0,0}x(t) + \mathcal{A}_{1,0}x(t-h_{1,0}) + \mathcal{A}_{2,0}x(t-h_{2,0}) + \mathcal{A}_{2,1}x(t-h_{2,1}) \\
&\quad + \mathcal{B}_0\tilde{x}_0(t) + \mathcal{B}_1\tilde{x}_0(t-h_{1,0}) + \mathcal{B}_2\tilde{x}_0(t-h_{2,0}).
\end{aligned}$$

The wireless communication delay is set to $h = h_{1,0} = h_{2,0} = h_{2,1} = 0.4$. Then, the following compact form in the variable $x(t) = [\tilde{x}_1(t) \quad \tilde{x}_2(t)]^T$ is obtained:

$$\dot{x}(t) = \mathcal{A}_{0,0}x(t) + \mathcal{A}_1 x(t-h) + \mathcal{B}_0\tilde{x}_0(t) + \mathcal{B}\tilde{x}_0(t-h), \tag{6.1}$$

$$\begin{aligned}
\text{where} \quad \mathcal{A}_1 &= \mathcal{A}_{1,0} + \mathcal{A}_{2,0} + \mathcal{A}_{2,1}, \quad \mathcal{B} = \mathcal{B}_1 + \mathcal{B}_2 \\
\mathcal{A}_{0,0} &= \begin{bmatrix} A_0^1 & 0_{2\times 2} \\ D_1 & A_0^2 \end{bmatrix}, \quad \mathcal{A}_1 = \begin{bmatrix} A_{1,0}+B_{1,0} & 0_{2\times 2} \\ C_{2,1} & B_{2,0}+A_{2,1}+B_{2,1} \end{bmatrix}, \\
\mathcal{B}_0 &= \begin{bmatrix} D_0 \\ 0_{2\times 2} \end{bmatrix}, \quad \mathcal{B} = \begin{bmatrix} C_{1,0} \\ C_{2,0} \end{bmatrix}.
\end{aligned}$$

In order to analyze plant stability and exponential stability of (6.1), input terms are omitted. By using the change of variable (B.1) to (6.1) and considering $z(t) = [\tilde{z}_1(t) \quad \tilde{z}_2(t)]^T$ we get the following representation:

$$\dot{z}(t) = [\mathcal{A}_{0,0} + \sigma I_{4\times 4}]\, z(t) + \mathcal{A}_1 e^{\sigma h} z(t-h). \tag{6.2}$$

In Figure 6.2, the stability chart of system (6.2) for different exponential decays, is depicted in the space of parameters $(\alpha_{2,1}, \beta_{2,0})$. Basically, this chart shows stability regions, which shrink as σ is increased. The space of parameters is explored on a grid, which include 6,400 equidistant points and the value σ is increased by 0.1, ranging from 0 to 1. The green region shows ordered pairs that produce the highest exponential decay as indicated in Figure 6.2. A finer search around $\sigma = 0.8$ is made, while this is increased by 0.00001. The maximal achieved exponential decay $\sigma = 0.81066$ (indicated by a circle in this figure and in the rest of the paper), occurs when $\alpha_{2,1} = 0.5$ and $\beta_{2,0} = 0.025$. At this point of the

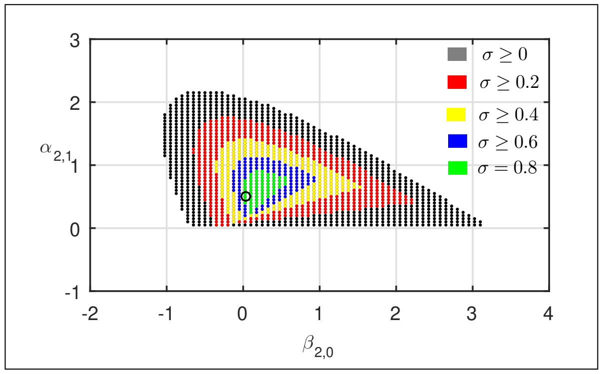

Figure 6.2: Stability chart $(\alpha_{2,1}, \beta_{2,0})$

space of parameters we have the best response of the platoon. Next, numerical simulations are carried out using the non-linear model in (2.1).

Numerical simulation. The initial velocities of the platoon in Figure 6.1 are chosen as follows: $v_0(0) = 15m/s$ as the constant velocity of vehicle zero or the leader and $v_1(0) = 20m/s$ and $v_2(0) = 10m/s$ for follower vehicles. On the gray region of Figure 6.2, the control parameters are tuned at the point $(-0.875, 1.5)$ which ensures $\sigma \in [0, 0.2)$.

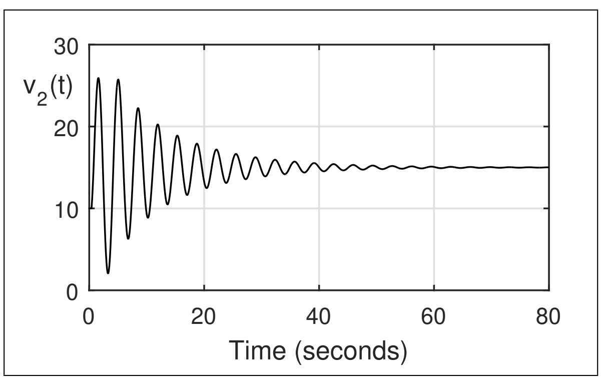

Figure 6.3: Velocity of the tail vehicle, $\sigma \in [0, 0.2)$

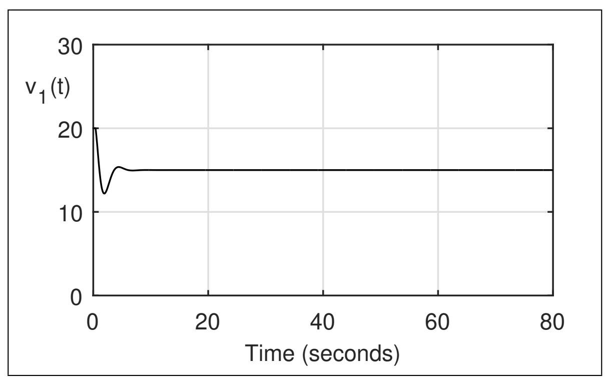

Figure 6.4: Velocity of the middle vehicle, $\sigma \in [0, 0.2)$

The velocity of the vehicle platoon is shown in Figures 6.3, and 6.4. As expected, it reaches the equilibrium velocity of the leader. Moreover, it is observed that the tail CCC-vehicle presents more oscillations than the one in the middle, so we conclude that the behavior of the tail vehicle is critical regarding plant stability under the selected parameters and connectivity structure. The dynamic of the headway between vehicles is also presented in Figures 6.5, and 6.6. From now on, only the tail vehicle behavior is shown because, according to the selected parameters and the direction of communication signals of the platoon, the tail vehicle is crucial for determining plant stability.

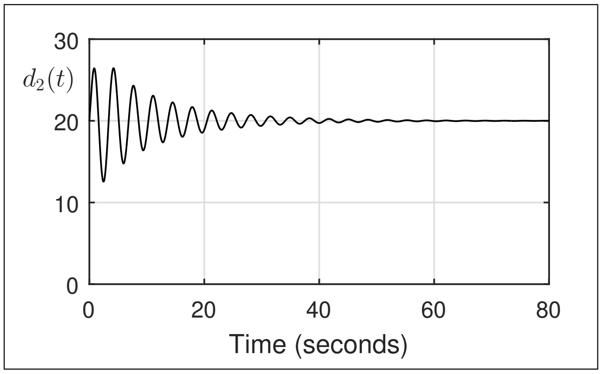

Figure 6.5: Headway between vehicle one and two, $\sigma \in [0, 0.2)$

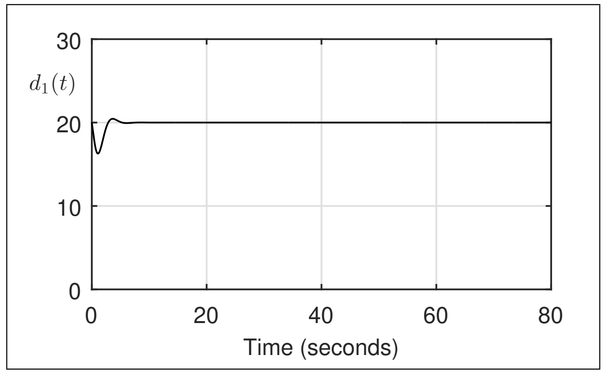

Figure 6.6: Headway between vehicle zero and one, $\sigma \in [0, 0.2)$

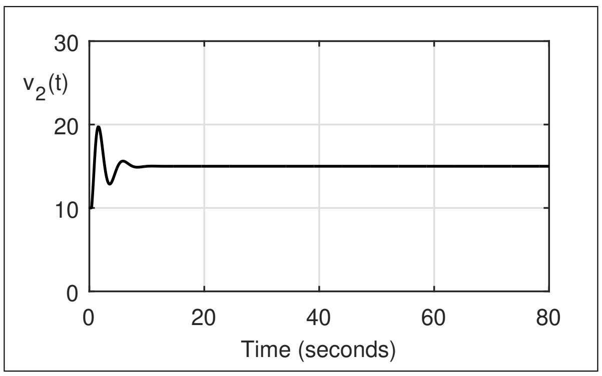

Figure 6.7: Velocity of the tail vehicle, $\sigma = 0.81066$

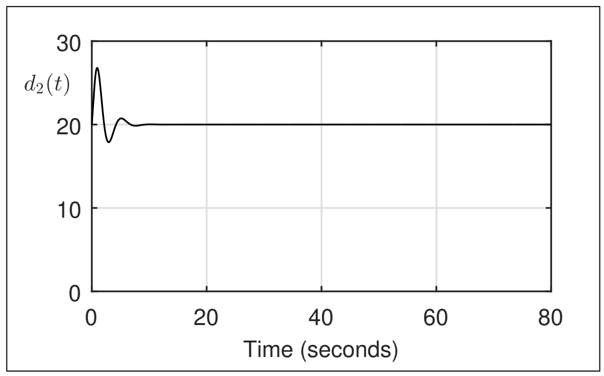

Figure 6.8: Headway between vehicle one and two, $\sigma = 0.81066$

Now, having in mind the above initial conditions and choosing in Figure 6.2 the point of maximal exponential decay $(0.025, 0.5)$, the velocity and headway of the tail vehicle are depicted in Figures 6.7, and 6.8. Note that, as expected, the oscillations reduce significantly. To summarize, after analyzing the platoon dynamics it is observed that the maximal exponential decay is bounded by the dynamic of the tail vehicle which has the slowest response.

We now consider the case where an unstable point close to the stability region on Figure 6.2 is chosen, specifically the pair $(-1, 0.5)$. The behavior of the tail vehicle is depicted in Figures 6.9, and 6.10. As expected, the platoon loses plant stability.

The time-domain approach also allows to consider the delay as a free parameter. Next, for the value of $\beta_{2,0} = 0.025$, which produces the maximal decay, the stability regions in the space of parameters $(\alpha_{2,1},\ h)$ are shown in Figure 6.11. The small circle corresponds to the parameters $h = 0.4$, $\alpha_{2,1} = 0.5$, $\beta_{2,0} = 0.025$, which produce the maximal exponential

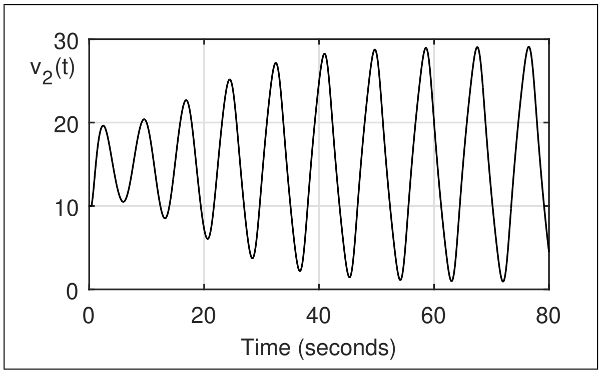

Figure 6.9: Velocity of the tail vehicle when an instability point is chosen

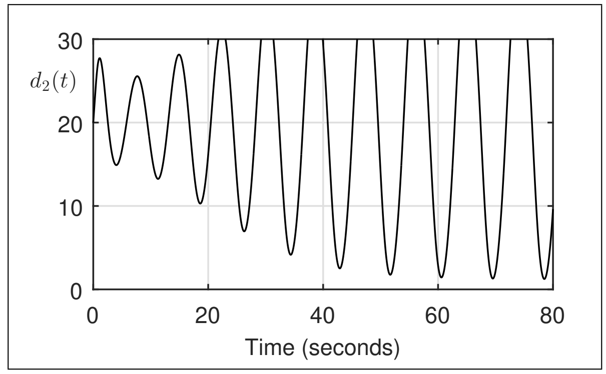

Figure 6.10: Headway between vehicle one and two when an instability point is chosen

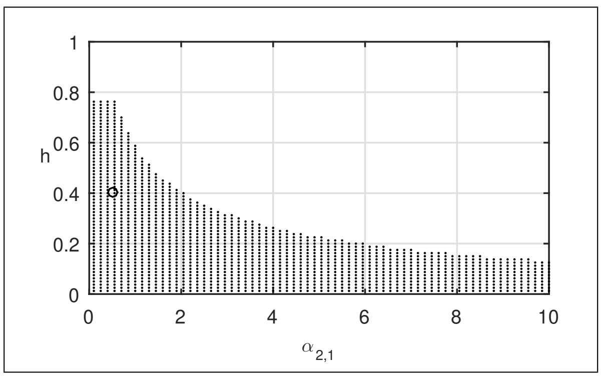

Figure 6.11: Stability chart $(\alpha_{2,1}, h)$

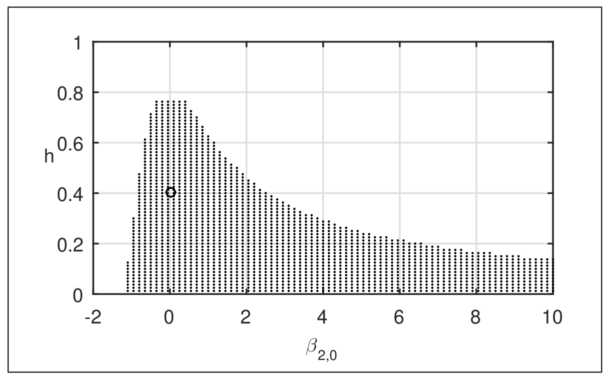

Figure 6.12: Stability chart $(\beta_{2,0}, h)$

decay when the delay is fixed. This indicates that there is some room for delay uncertainty. In another case, the parameter $\alpha_{2,1} = 0.5$ is selected and the stability region in the space of parameters $(\beta_{2,0},\ h)$ is depicted in Figure 6.12. Note that the delay can suffer some perturbations.

In Figures 6.11 and 6.12, it is possible to find the maximal exponential decay when a parameter is fixed.

There is special interest in exploring the behavior of the exponential decay of the platoon when the control gains of the tail vehicle as well as the communication delay are free design parameters in a 3D representation.

The delay Lyapunov matrix approach allows to depict 3D stability regions in the space of parameters $(\alpha_{2,1},\ \beta_{2,0},\ h)$. The region depicted in green in Figure 6.13 guarantees an exponential decay $\sigma = 0.8$. There is no configuration of parameters that results in an exponential decay larger than 0.81066. Therefore, a realistic delay value in platoon broadcasting considered in (Zhang & Orosz, 2016) is in line with the obtained maximal stability region.

The next step is to perform a robust stability analysis for the control parameter configuration achieving maximal exponential decay. Using (C.2) in (6.2), the delay Lyapunov matrix associated with $W = I$ is such that

$$\|U(0)\| = 4.887 \ > \|U(\tau)\| \ , \ \tau \in (0, 0.4].$$

Figure 6.14 shows the maximum value of the norm of the delay Lyapunov matrix. The equality

$$W_0 + \sum_{j=1}^{1} (W_j + h_j W_{1+j}) = W$$

is satisfied if we chose $W_0 = W_1 = W_2 = \frac{1}{2.4} I$, and it follows that $\lambda_{min} = \frac{1}{2.4}$. The inequality (C.2) gives the conservative stability bound

$$\sqrt{\|\Delta_0(t)\|^2 + \|\Delta_1(t)\|^2} < 0.02751.$$

The presented robustness time-domain results seem to be quite conservative. Nevertheless, their interest lie in the fact that they cover the case of time varying or non linear perturbations, contrasting with frequency domain robustness analysis that is restricted to constant unknown uncertainties.

To conclude this example, we answer the question: how our results compare with those obtained by frequency domain approaches?. In the frequency domain, the analysis

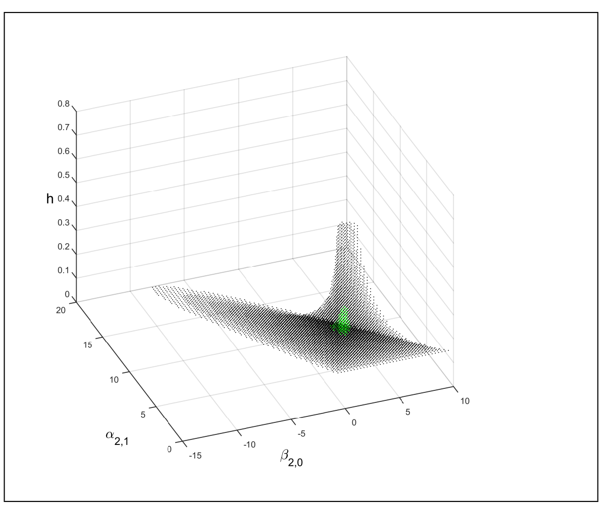

Figure 6.13: Stability chart $(\alpha_{2,1}, \beta_{2,0}, h)$

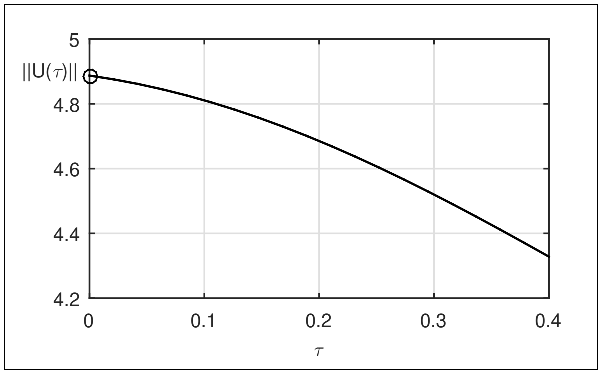

Figure 6.14: Norm of $U(\tau)$. The small circle is the maximum value.

consists in achieving stability regions for plant stability and string stability, then these are overlapped in one stability chart (Jin & Orosz, 2014; Qin, Gomez & Orosz, 2017). The next step is to select the best parameters guaranteeing stability at the equilibrium while the perturbations at the input are reduced.
In this work is carried out a plant stability analysis focused at finding the best parameters that ensure the maximal exponential decay. It is assumed that the best choice of control parameters are related to those for string stability. A direct comparison between both approaches is not feasible because of the particular connection of vehicles of the platoon; this does not exclude the possibility of making a comparison in future work.
Finally, it is noteworthy that only were considered in the analysis delay magnitudes greater than 0.15 because smaller values do not correspond to a realistic situation.

In conclusion, a general framework for time-domain analysis of a CCC scheme is presented. The analysis is based on the linearized models of a particular connectivity structure. We addressed in particular the choice of the parameters ensuring stability for a given or maximal platoon exponential decay. It is demonstrated that the maximal platoon exponential decay is bounded by the dynamic of the tail vehicle. The stability charts indicate that when delay increases, the stability region shrinks. Finally, the robust stability properties of the closed-loop are also analyzed.

6.2 Input delay compensation for a platoon of vehicles with Extended Cooperative Adaptive Cruise Control

In a scenario of five vehicles, this academic example shows the input delay compensation of the model "B" developed in Chapter 2 in closed-loop with the Extended Cooperative Adaptive Cruise Control. The compensator is the dynamic predictive controller proposed in Chapter 4. Our aim is not only to apply the strategy to input delays of stable systems, but also for instable ones.
The dynamic predictor-based controller design for system (2.8) is depicted in Figure 6.15. Matrix C is a identity $(n \times n)$ matrix. Note that the control law requires the errors e_i and velocities v_i of the fleet which are available with delay h. The information of the control law in the interval $[t-h, t]$ is also necessary. The control law applied in the interval $t \in [0, h]$ is a result of the initial condition $\psi(t)$; for $t \geq h$ the dynamic predictor-based control strategy enters into action, as explained in (Kharitonov, 2014). Under this control law, we consider

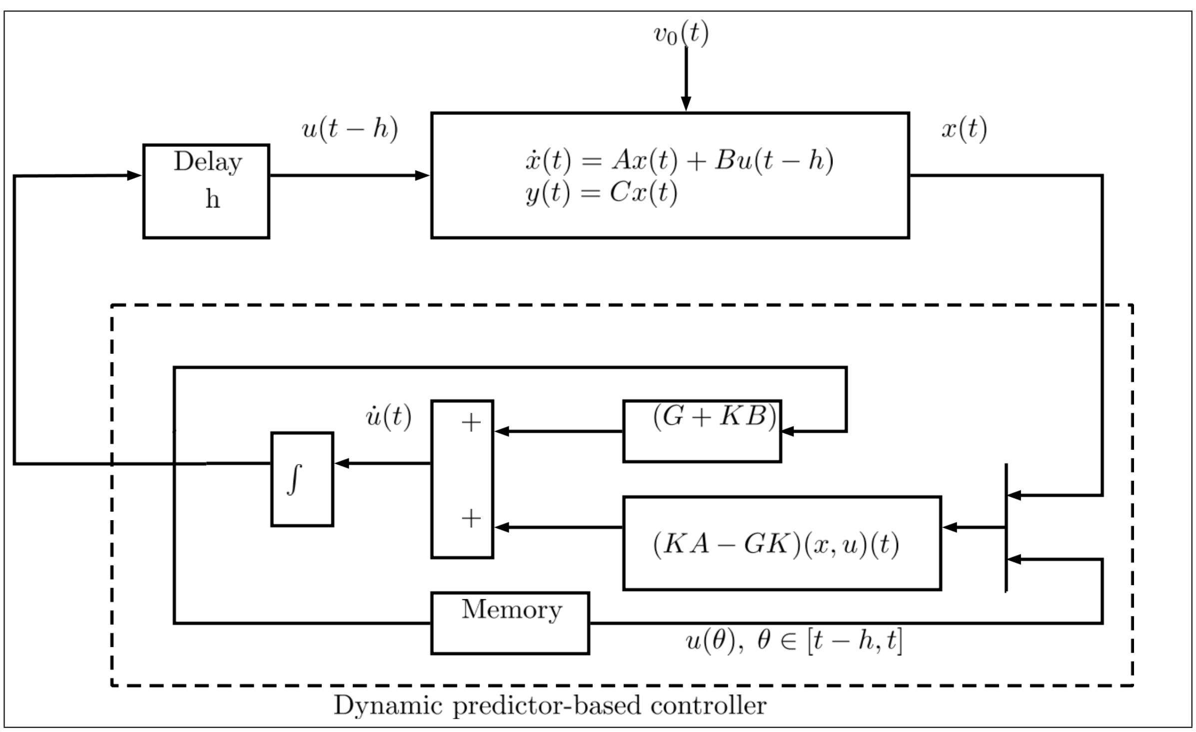

Figure 6.15: Block diagram representation of system (2.8) in closed-loop with the dynamic predictor-based controller.

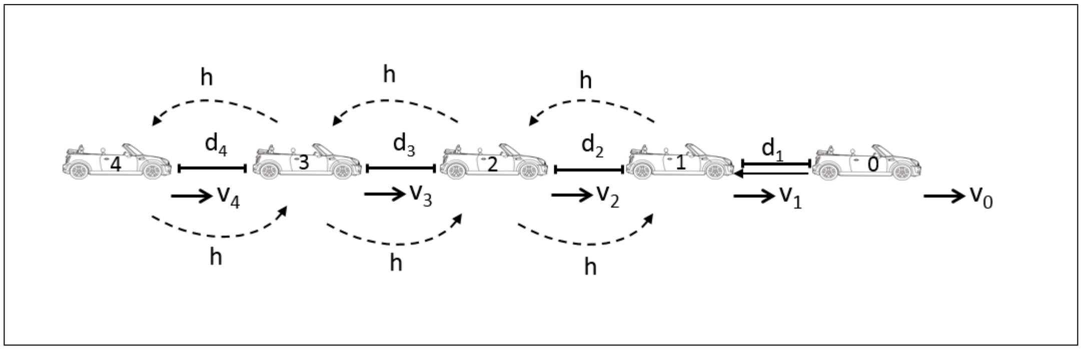

Figure 6.16: Network wireless communication structure

a fleet of 4 vehicles following a leader (vehicle 0), as depicted in Figure 6.16. Dotted arrows indicate the direction of the wireless information transmitted by each vehicle. The continuous arrow between the leader and vehicle 1 which has better sensor equipment, depicts instantaneous transmission. We first obtain the fleet dynamics by using (2.5) and (2.6). Introducing the variable $x(t) = [e_1(t)\ v_1(t)\ e_2(t)\ v_2(t)\ e_3(t)\ v_3(t)\ e_4(t)\ v_4(t)]$, and according to (2.8), the dynamic of the fleet is described by the following matrices

$$A = \begin{bmatrix} 0 & -1 & 0 & 0 & 0 & 0 & 0 & 0 \\ 0 & 0 & 0 & 0 & 0 & 0 & 0 & 0 \\ 0 & 1 & 0 & -1 & 0 & 0 & 0 & 0 \\ 0 & 0 & 0 & 0 & 0 & 0 & 0 & 0 \\ 0 & 0 & 0 & 1 & 0 & -1 & 0 & 0 \\ 0 & 0 & 0 & 0 & 0 & 0 & 0 & 0 \\ 0 & 0 & 0 & 0 & 0 & 1 & 0 & -1 \\ 0 & 0 & 0 & 0 & 0 & 0 & 0 & 0 \end{bmatrix},\ B = \begin{bmatrix} -p & 0 & 0 & 0 \\ 1 & 0 & 0 & 0 \\ 0 & -p & 0 & 0 \\ 0 & 1 & 0 & 0 \\ 0 & 0 & -p & 0 \\ 0 & 0 & 1 & 0 \\ 0 & 0 & 0 & -p \\ 0 & 0 & 0 & 1 \end{bmatrix},\ D = \begin{bmatrix} 0 \\ 1/p \\ 0 \\ 0 \\ 0 \\ 0 \\ 0 \\ 0 \end{bmatrix}.$$

For simplicity, we consider equal time headway $p_i = p$, $i = 1, ..., 4$. The control strategy is given by

$$u(t-h) = Kx(t),$$

where

$$K = \begin{bmatrix} \frac{k_1}{p} & \frac{-1}{p} & \frac{k_{12}}{p} & 0 & 0 & 0 & 0 & 0 \\ \frac{k_{21}}{p} & \frac{1}{p} & \frac{k_2}{p} & \frac{-1}{p} & \frac{k_{23}}{p} & 0 & 0 & 0 \\ 0 & 0 & \frac{k_{32}}{p} & \frac{1}{p} & \frac{k_3}{p} & \frac{-1}{p} & \frac{k_{34}}{p} & 0 \\ 0 & 0 & 0 & 0 & \frac{k_{43}}{p} & \frac{1}{p} & \frac{k_4}{p} & \frac{-1}{p} \end{bmatrix},$$

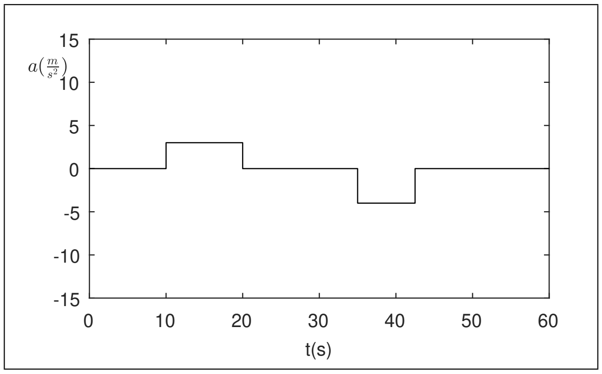

Figure 6.17: Acceleration of the leader vehicle.

the closed-loop system (2.8) with the predictor-based control is then

$$\dot{x}(t) = (A + BK)x(t) + Dv_0(t).$$

To overcome the implementation problem, we use the dynamic predictor-based control depicted on Figure 6.15. We choose stabilizing gain values for the parameters k_i and k_{ij}. In the extended cooperative adaptive cruise control strategy in (Montanaro, Tufo, Fiengo, di Bernardo, Salvi & Santini, 2014) it is suggested that the neighboring vehicles gains have to satisfy the relation $k_{ij} = k/(g_i + 1)$ with g_i being the degree of the vehicle considered as node i (i.e $g_i = \sum_{j=1}^{4} a_{ij}$). Therefore we choose scalar gain values

$$\begin{aligned} k_1 &= k_2 = k_3 = k_4 = 3, \\ k_{12} &= k_{43} = \frac{3}{2} = 1.5, \\ k_{21} &= k_{23} = k_{32} = k_{34} = 1. \end{aligned}$$

Finally, we choose the Hurwitz matrix G as follows

$$G = \begin{bmatrix} -50 & 0 & 0 & 0 \\ 0 & -50 & 0 & 0 \\ 0 & 0 & -50 & 0 \\ 0 & 0 & 0 & -50 \end{bmatrix}.$$

Numerical simulation. Consider a homogeneous platoon of vehicles of length $L_i = 5m$. In concordance with (Bekiaris-Liberis, Roncoli & Papageorgiou, 2017), we change the velocity $v_0(t)$ of the leader according to the acceleration $\dot{v}_0(t) = a_0(t)$, as depicted in Figure

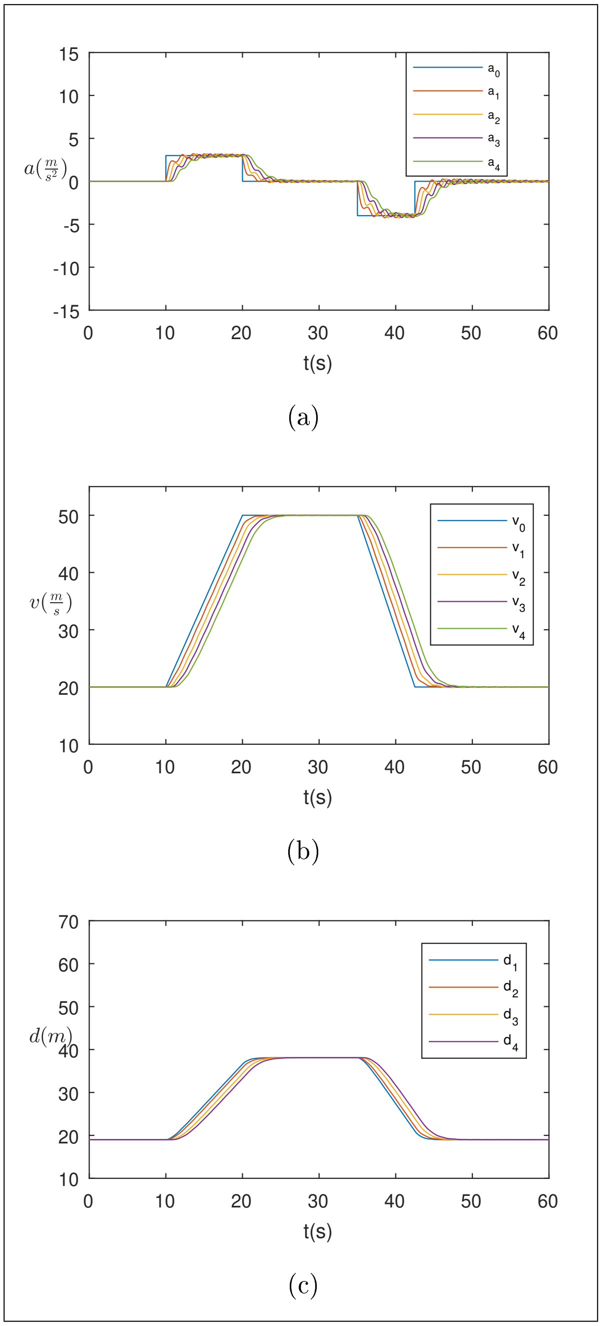

Figure 6.18: a) Acceleration, b) velocity and c) spacing among four vehicles following a leader without input delay compensation. Delay $h = 0.23s$

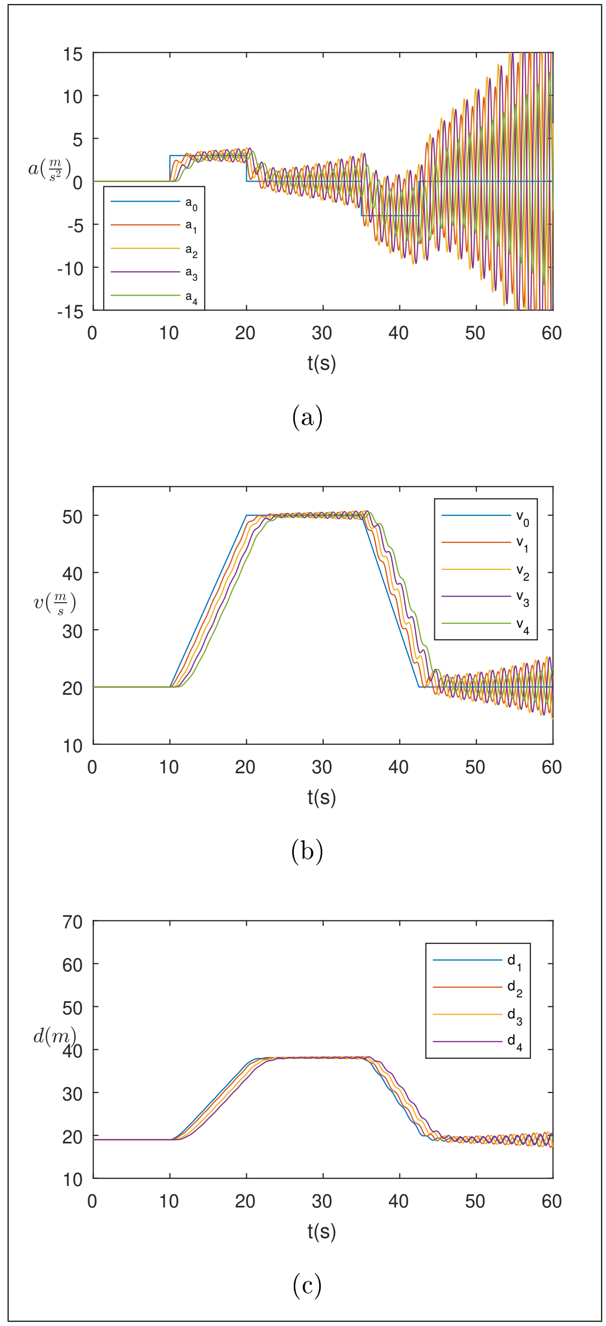

Figure 6.19: a) Acceleration, b) velocity and c) spacing among four vehicles following a leader without input delay compensation. Delay $h = 0.245s$.

6.17, and we take the time headway as $p = 2/\pi$. Next, we simulate system (2.8) with the above defined matrices which represents the fleet dynamics in two possible cases: 1) without compensating the input delay , 2) applying the dynamic predictor-based control

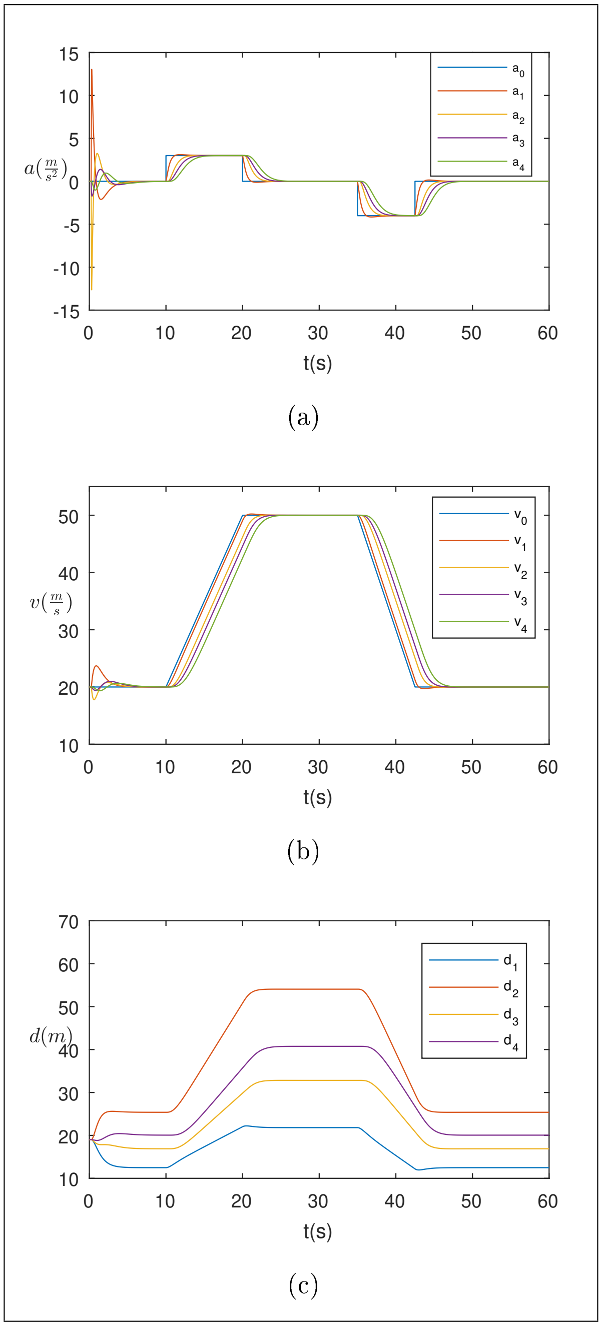

Figure 6.20: a) Acceleration, b) velocity and c) spacing among four vehicles following a leader when the dynamic predictor-based controller is applied. Delay $h = 0.245s$

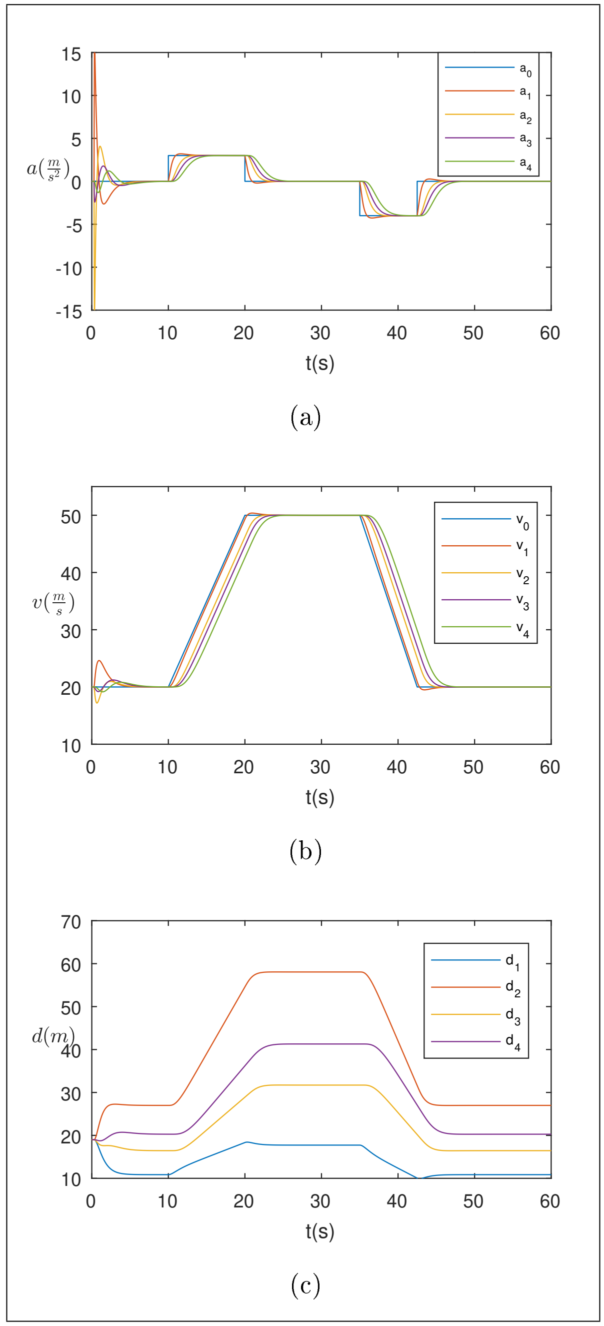

Figure 6.21: a) Acceleration, b) velocity and c) spacing among four vehicles following a leader when the dynamic predictor-based controller is applied. Delay $h = 0.3s$

law on Figure 6.15. The figures of this section show the system response described by a) acceleration and b) velocity, numbered from 0 to 4, and the c) spacing, numbered from

1 to 4. In all cases, the parameter tunning of the previous section is employed. In Figure 6.18 we present the response for a delay $h = 0.23s$ for the non compensated control. Encouraged by these results, the delay is increased to $h = 0.245s$. The system response depicted in Figure 6.19, shows that the stability is lost. When the dynamic predictor-based scheme is applied to system (2.8) with this same delay $h = 0.245s$, we observe in Figure 6.20, that the a) acceleration, b) velocity and c) spacing of the fleet oscillate but all signals remain stable. An observed disadvantage is that some large transients in the acceleration appear in the early seconds, as shown in Figures 6.20 and 6.21. In a realistic situation, they should be taken into account and should be limited. Another disadvantage is that a steady state error is present in the spacing among vehicles d, as depicted in Figures 6.20 and 6.21. This is due to the introduction of the predictor-based controller as explained in (Bekiaris-Liberis, Roncoli & Papageorgiou, 2017). The significant reduction of the inter-vehicle spacing can dramatically minimize the security distance, resulting in safety problems. As seen in Figure 6.21 the dynamic controller is able to manage larger delays as, for example $h = 0.3s$.

In conclusion, the presented results show that applying dynamic predictor -based control laws to vehicle fleets, allows recovering the stability of the closed-loop for larger delays than uncompensated control laws. In this work, we study asymptotic stability of the steady state solution. An undesirable observed effect is the presence of a steady state error in the inter-vehicle spacing.

6.3 Modeling human memory effects for a platoon of vehicles with the Extended Cooperative Adaptive Cruise Control

In this example, the stability of a chain of three vehicles considering human driver's memory effects as distributed delays is studied. The ideas for modeling the human memory are borrowed from (Sipahi & Niculescu, 2010). The control strategy proposed in (Montanaro *et al.*, 2014) is modified such that the delayed wireless network as well as the local driver reaction ensure that all followers vehicles attain the velocity of the leader and a given spacing policy among vehicles. Our aim is to assist the driver by using the wireless information of the neighboring vehicles, so that the inter-vehicular distance is regulated.

The resulting closed-loop systems is a delay linear system with distributed delays, hence the analysis is done using the results of Chapter 3.
The inter-vehicle signal transmission network protocol is shown in Figure 6.22. The adjacency matrix corresponding to this fleet is

$$\mathcal{A} = \begin{pmatrix} a_{11} & a_{12} \\ a_{21} & a_{22} \end{pmatrix} = \begin{pmatrix} 0 & 1 \\ 1 & 0 \end{pmatrix},$$

by using equation (2.12), the tracking error is expressed as

$$\begin{aligned} \dot{e}_1(t) &= -\frac{k_1}{\xi_1}\int_{-\xi_1}^{0} e_1(t+\theta-h_1)d\theta - a_{12}k_{12}e_2(t-h_{12}(t)), \\ \dot{e}_2(t) &= -\frac{k_2}{\xi_2}\int_{-\xi_2}^{0} e_2(t+\theta-h_2)d\theta - a_{21}k_{21}e_1(t-h_{21}(t)), \end{aligned}$$

for simplicity, the delay values are assumed to be $h_{12}(t) = h_{21}(t) = h_1 = h_2 = h$, $\xi_1 = \xi_2 = 2h$, and the network gains $k_{12} = k_{21} = 2.5$. Let $e(t) = [e_1(t) \quad e_2(t)]^T$, then the dynamic behavior of the fleet is

$$\dot{e}(t) = Ae(t-h) + \int_{-2h}^{0} G\, e(t+\theta-h)d\theta, \tag{6.3}$$

where

$$A = \begin{bmatrix} 0 & -2.5 \\ -2.5 & 0 \end{bmatrix}, \quad G = \begin{bmatrix} -\frac{k_1}{2h} & 0 \\ 0 & -\frac{k_2}{2h} \end{bmatrix},$$

the variables k_1 and k_2 are design parameters. Note that the above system has one concentrated delay and one distributed delay. The integral term defines the maximum delay H being equal to $3h$.

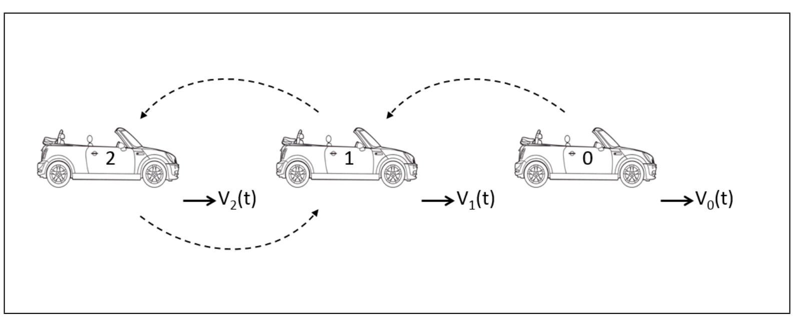

Figure 6.22: Communication network structure of the fleet.

6.3.1 Stability Analysis

In this section we construct the delay Lyapunov matrix of system (6.3) applying the methodology proposed in (Juárez & Mondié, 2018a), (Juárez & Mondié, 2018c). This matrix allows to test the stability of system (6.3) by means of the exponential stability criterion (A.6). At first, we define six auxiliary matrices corresponding to the multiple constant delays,

$$Y_i(\tau) = U(\tau + ih), \quad i = -3, -2, -1, 0, 1, 2,$$

because of kernel G in equation (6.3) is a scalar matrix, we define the following auxiliary matrices,

$$Z_{0,j}(\tau) = \int_{-2h}^{0} U(\tau + \theta + jh)d\theta, \quad j = -1, 0, 1,$$
$$J_{0,j}(\tau) = \int_{-2h}^{0} U(\tau - \theta + jh)d\theta, \quad j = -2, -1, 0.$$

Lemma 9. *(Juárez & Mondié, 2018a) There is equivalence between the auxiliary matrices $Z_{0,j}$ and $J_{0,j}$, hence these can be reduced.*

Proof. We apply a change of variable as follows

$$\int_{-2h}^{0} U(\tau - \theta + ph)d\theta = \int_{-2h}^{0} U(\tau + \theta + (ph + 2h))d\theta,$$
$$\text{with} \quad p = -2, -1.$$

□

By Lemma 9, we find some auxiliary matrix equivalences as follows

$$J_{0,-1}(\tau) = Z_{0,1}(\tau),$$
$$\int_{-2h}^{0} U(\tau - \theta - h)d\theta = \int_{-2h}^{0} U(\tau + \theta + h)d\theta,$$
$$J_{0,-2}(\tau) = Z_{0,0}(\tau),$$
$$\int_{-2h}^{0} U(\tau - \theta - 2h)d\theta = \int_{-2h}^{0} U(\tau + \theta)d\theta,$$

then, the auxiliary matrices corresponding to the kernel G are

$$Z_{0,1}(\tau) = \int_{-2h}^{0} U(\tau + \theta + h)d\theta, \quad Z_{0,0}(\tau) = \int_{-2h}^{0} U(\tau + \theta)d\theta,$$
$$Z_{0,-1}(\tau) = \int_{-2h}^{0} U(\tau + \theta - h)d\theta, \quad J_{0,0}(\tau) = \int_{-2h}^{0} U(\tau - \theta)d\theta.$$

The delay-free system of linear auxiliary matrix differential equations is

$$
\begin{aligned}
Y_2'(\tau) &= Y_1(\tau)A + Z_{0,1}(\tau)G, & Y_{-3}'(\tau) &= -A^T Y_{-2}(\tau) - G^T Z_{0,0}(\tau),\\
Y_1'(\tau) &= Y_0(\tau)A + Z_{0,0}(\tau)G, & Z_{0,1}'(\tau) &= Y_1(\tau) - Y_{-1}(\tau),\\
Y_0'(\tau) &= Y_{-1}(\tau)A + Z_{0,-1}(\tau)G, & Z_{0,0}'(\tau) &= Y_0(\tau) - Y_{-2}(\tau),\\
Y_{-1}'(\tau) &= -A^T Y_0(\tau) - G^T J_{0,0}(\tau), & Z_{0,-1}'(\tau) &= Y_{-1}(\tau) - Y_{-3}(\tau),\\
Y_{-2}'(\tau) &= -A^T Y_{-1}(\tau) - G^T Z_{0,1}(\tau), & J_{0,0}'(\tau) &= Y_2(\tau) - Y_0(\tau).
\end{aligned}
\tag{6.4}
$$

The boundary conditions are,

$$
\begin{aligned}
Y_2(0) &= Y_1(h), & Z_{0,0}(0) &= \int_0^{2h} Y_{-2}(\theta)d\theta,\\
Y_1(0) &= Y_0(h), & Z_{0,-1}(0) &= J_{0,0}^T(h),\\
Y_0(0) &= Y_{-1}(h), & J_{0,0}(0) &= \int_0^{2h} Y_0(\theta)d\theta,\\
Y_{-1}(0) &= Y_{-2}(h), & A^T Y_0(h) &+ Y_{-1}(0)A+\\
Y_{-2}(0) &= Y_{-3}(h), & Z_{0,-1}(0)G &+ G^T J_{0,0}(h) = -W.\\
Z_{0,1}(0) &= Z_{0,0}(h), & &
\end{aligned}
\tag{6.5}
$$

To solve the delay-free system of auxiliary matrix differential equations (6.4) with the boundary conditions (6.5), we apply Kronecker product of matrices to obtain a vectorized form. Then, system (6.4) is expressed as $\dot{R}(\tau) = LR(\tau)$ where

$$
\begin{aligned}
R(\tau) = [&y_2(\tau),\ y_1(\tau),\ y_0(\tau),\ y_{-1}(\tau),\ y_{-2}(\tau),\ y_{-3}(\tau),\\
&z_{0,1}(\tau),\ z_{0,0}(\tau),\ z_{0,-1}(\tau),\ j_{0,0}(\tau)]^T.
\end{aligned}
$$

$R(\tau)$ is such that $R(\tau) = e^{L\tau}R(0)$, and it follows from the boundary condition (6.5) that

$$
\left[M + Ne^{Lh}\right] R(0) \quad = \quad \begin{bmatrix} 0 \\ -w \end{bmatrix},
$$

$$
R(\tau) = e^{L\tau}[M + Ne^{Lh}]^{-1} \begin{bmatrix} 0 \\ -w \end{bmatrix}. \tag{6.6}
$$

Due to space limitations, the real matrices L, M and N which are obtained from the vectorization process are omitted. We define a constant symmetric positive definite matrix

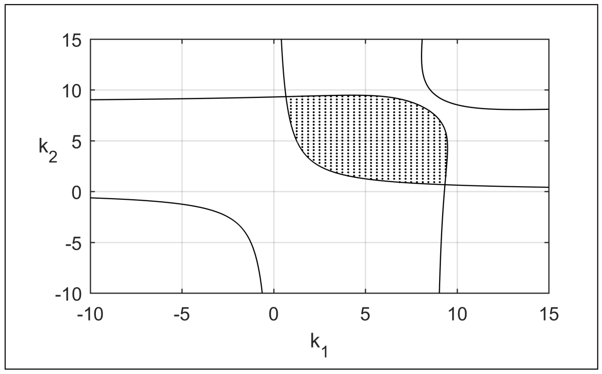

Figure 6.23: Stability chart (k_1, k_2).

$W = \begin{pmatrix} 1 & 0 \\ 0 & 1 \end{pmatrix}$ and obtain the delay Lyapunov matrix $U(\tau)$ using (6.6), this matrix is equivalent to $U(\tau + ih) = Y_i(\tau)$, $\tau \in [0, h]$.

The stability chart in Figure 6.23 shows the stability region in the space of design parameters (k_1, k_2) where system (6.3) is stable when the delays are equal to $h = 0.1s$. We define an eighty by eighty points region inside the stability chart (k_1, k_2). At each ordered pair a delay Lyapunov-Krasovskii type functional is defined by the corresponding Lyapunov matrix. We test the stability of system (6.3) using the exponential stability criterion (A.6). The dotted area in Figure 6.23, describing the space of parameters of the reaction human gains (k_1, k_2) correspond to points where the fleet is stable when the communication network delay $0.1s$ and the human memory window is $0.2s$. It is important to keep in mind that gains k_1 and k_2 belong to the drivers 1 and 2, respectively. Finally, the lines in Figure 6.23 are obtained applying the D-partition method in the frequency domain introduced in (Neimark, 1949).

6.3.2 Numerical results

At first, we define the length of each vehicle as 5 m. At time $t = 0$ the initial positions of the vehicles are $r_0(0) = 40m$, $r_1(0) = 20m$, and $r_2(0) = 0m$, to avoid collision. The constant speed of the leader is $v_0(0) = 20m/s$ and the initial velocities of the followers are $v_1(0) = 19m/s$ and $v_2(0) = 21m/s$. The reference distance $\hat{d}(t)$ is defined by the speed of the leader and for the parameters δ_i and p_i. These parameters have to be taken into account according to the vehicle properties as brake system, engine controllers, to name a few, as recommended in (Montanaro, Tufo, Fiengo, di Bernardo, Salvi & Santini, 2014). In this example we choose $\delta_i = 3m$ and $p_i = 0.8s$. In this way, the safe distance is $\hat{d}_i(t) = 3 + 0.8 * 20 = 19m$. Finally, we select the ordered pair $(k_1, k_2) = (3, 3)$ in the stable region in Figure 6.23, notice that one could search for pairs of gains in the space of parameters leading to less oscillatory response. The numerical results are shown in Figures 6.24-6.28.

As expected, it is shown in Figure 6.24 that the errors $e_1(t)$, $e_2(t)$ of the closed-loop (6.3) go to zero. Figure 6.25 shows that there is no collision while the velocities of the followers reach the leader velocity in Figure 6.26. Note that the control action is appropriate in steady-state, as depicted in Figure 6.27. Finally, the inter-vehicle distances are shown in Figure 6.28. The distance between vehicles $1, 0$ and $2, 1$ are refereed as d_1 and d_2, respectively. As calculated, all the fleet reaches the safe inter-vehicular distance equal to $19m$.

In conclusion, a control strategy involving the driver's memory effects as delayed reaction and decisions in a platoon of vehicles, is presented. To this aim, a model based

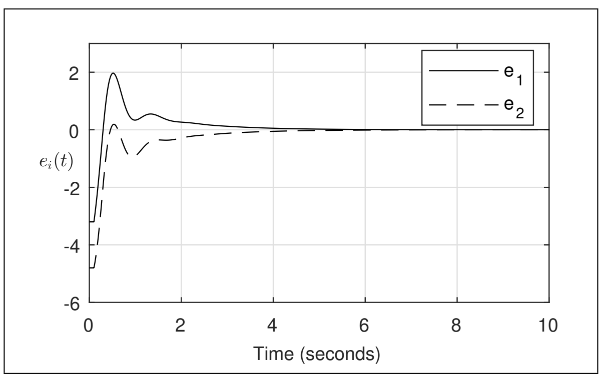

Figure 6.24: Error dynamics of the fleet in Figure 6.22

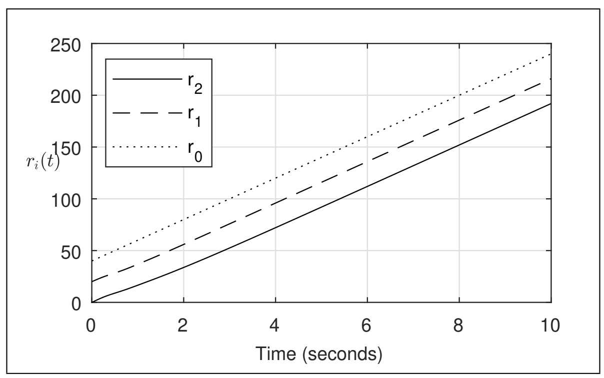

Figure 6.25: Position dynamics of the fleet in Figure 6.22

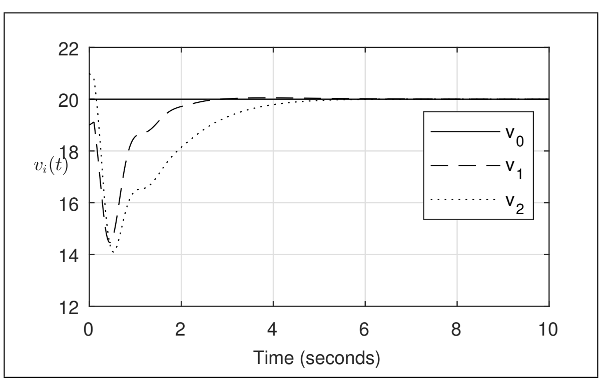

Figure 6.26: Velocity dynamics of the fleet in Figure 6.22

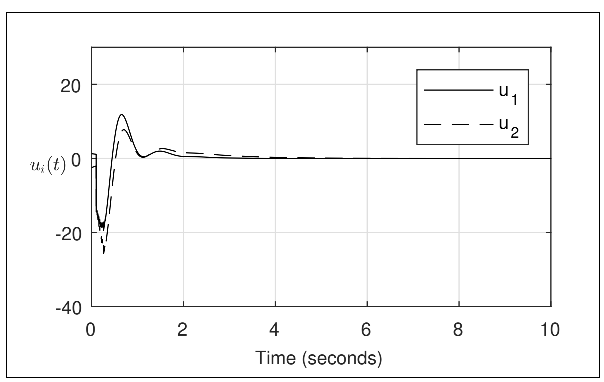

Figure 6.27: Control action dynamics of the fleet in Figure 6.22

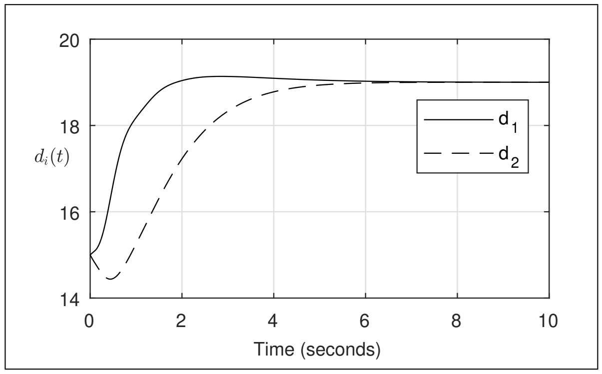

Figure 6.28: Inter-vehicle distances.

in the extended cooperative adaptive cruise control and distributed delays is developed. It is addressed a scenario of three vehicles and is also presented its stability chart which ensures the exponential stability of the fleet in a defined region. A measure of the driver's aggressiveness can be represented by the design parameters (k_1, k_2) of the chart. The stability analysis is carried out in the time-domain by using Lyapunov-Krasovskii functionals. This new information can be useful in designing new automated vehicle controllers.

6.4 Conclusions

In this chapter we have applied existing and new results developed in this thesis for the stability and robustness analysis of pointwise and distributed delay systems to platoons of vehicles, showing that these tools may be useful in designing and tuning new automated vehicle controllers.

Chapter 7

Conclusions and future work

This thesis introduces three mathematical tools in the time-domain for linear systems with multiple concentrated and distributed delays. The first one allows the construction of the delay Lyapunov matrix, the second gives a methodology for the application of the dynamic predictive controller, and the last one presents novel robust stability conditions. Most of the developed approaches are applied to traffic systems models through simulation results.

7.1 Theoretical contributions

Our research was motivated by the modeling and control of vehicle platoons. We introduced tree models based on the recent strategies CCC, CACC, and ECACC. The main delays corresponding to the inter-vehicle communications and the driver's memory effects, gave rise to linear systems with multiple concentrated and distributed delays. This lead us to one of the main contribution of the thesis, which is the development of theoretical tools for the analysis and control of systems having such delays.

The main contributions of this research work encompass the three following theoretical contributions.

First. A methodology for the construction of the delay Lyapunov matrix for linear systems with multiple concentrated and distributed delays. This result leads the reader to the definition of a delay-free system of matrix equations which is instrumental in obtaining the delay Lyapunov matrix. Among other applications, this matrix is crucial for proving stability. Fairly general kernels in the distributed term are considered. It is worthy of mention that the approach is restricted to the case of commensurate delays.

Second. A methodology for the delay compensation for linear systems with multiple concentrated and distributed delays is presented. The insight on delay compensation resides in applying dynamic predictive controllers. While in general the delay compensation has been successfully achieved by using approximated methods as sub-predictors, nested predictors to mention a few, the approach adopted in this thesis allows an exact delay compensation as well as the robust stability analysis of matrix parameters and delays perturbations.

Third. Robust stability conditions for linear systems with multiple concentrated and distributed delays are obtained. Based on Lyapunov-Krasovskii functionals which are not of complete type, these results allow to obtain exact stability bounds for matrix parameters and delay perturbations.

7.2 Future work

Finally, further research directions include additional topics, as itemized below

- For the CCC model "A", future work includes the study of the effects of changing connectivity structures, the theoretical analysis of the robustness with respect to delays, and the validation of the tuning choices on an experimental vehicle platoon platform.

- In the dynamic predictive controller applied to ECACC model "B", a steady state error in the inter-vehicle spacing is present. Future research includes analyzing strategies to overcome this issue as well as the study of string stability of the platoon.

- For the robust stability conditions of Chapter 6, future research directions include extending the present results that are restricted to unknown, but constant uncertainties, to time varying or non-linear perturbations. These robustness conditions will be applied in the next future to the vehicle platoon models.

- It is worth noting that the methods described in this thesis are not restricted to problems of traffic systems. Future research includes applying the methods to general linear systems with multiple concentrated and distributed delays. In the same vein, the dynamic predictive controller can be used for compensating state and input delays of linear systems.

- For the vehicle platoon with the human memory control strategy (Model "C"), future work includes the study of the robust stability, using the exact stability bounds of Chapter 6.

Considering the positive impact of delay modeling in traffic systems, further improvement of delayed strategies for cutting jams and preventing accidents presents a worthwhile challenge.

Appendix A

Delay systems and time-domain stability conditions

The purpose of this appendix is to introduce the reader to the mathematical representation of systems with concentrated and distributed delays, and to remind the Lyapunov-Krasovskii framework necessary stability conditions in terms of the Lyapunov matrix which are used in our work.

A.1 Systems with multiple concentrated delays

Consider a linear system of the form

$$\dot{x}(t) = \sum_{j=0}^{m} \mathcal{A}_j x(t - h_j), \quad t \geq 0, \tag{A.1}$$

where $\mathcal{A}_0, \ldots, \mathcal{A}_m$ are constant real $n \times n$ matrices, and $0 = h_0 < h_1 < \ldots < h_m = H$ are the delays. The initial functions φ are taken from $PC([-H, 0], \mathbb{R}^n)$. The restriction of the solution $x(t, \varphi)$ of system (A.1) on the interval $[t - H, t]$ is denoted by

$$x_t(\varphi) : \theta \to x(t + \theta, \varphi), \quad \theta \in [-H, 0].$$

To prove stability of system (A.1) a complete type Lyapunov-Krasovskii functional is provided:

$$\begin{aligned} v(\varphi) &= \varphi^T(0)U(0)\varphi(0) + \sum_{j=1}^{m} 2\varphi^T(0) \int_{-h_j}^{0} U^T(\theta + h_j)\mathcal{A}_j\varphi(\theta)d\theta \\ &+ \sum_{k=1}^{m}\sum_{j=1}^{m} \int_{-h_k}^{0} \varphi^T(\theta_1)\mathcal{A}_k^T \left(\int_{-h_j}^{0} U(\theta_1 + h_k - \theta_2 - h_j)\mathcal{A}_j\varphi(\theta_2)d\theta_2 \right) d\theta_1 \\ &+ \sum_{j=1}^{m} \int_{-h_j}^{0} \varphi^T(\theta)(W_j + (\theta + h_j)W_{m+j})\varphi(\theta)d\theta, \end{aligned} \tag{A.2}$$

$W_j > 0$, $j = \overline{0, 2m}$, with $W_0 + \sum_{j=1}^{m}(W_j + h_jW_{m+j}) = W$.
Then, by using the delay Lyapunov matrix $U(\tau)$ Kharitonov (2012), $\tau \in \mathbb{R}$, we determine the stability.

In the monograph Kharitonov (2012), the delay Lyapunov matrix of system (A.1), associated to a positive definite matrix W, is the matrix valued continuous function solution of the boundary value problem:

$$U'(\tau) = \sum_{j=0}^{m} U(\tau - h_j)\mathcal{A}_j, \quad \tau \geq 0, \tag{A.3}$$

$$U(\tau) = U^T(-\tau), \quad \tau \geq 0, \tag{A.4}$$

$$\sum_{j=0}^{m} \left[U(-h_j)\mathcal{A}_j + \mathcal{A}_j^T U(h_j)\right] = -W. \tag{A.5}$$

These equations admit a unique solution when the system satisfies the Lyapunov condition (the characteristic equation of (A.1) has no eigenvalues that are symmetric with respect to the origin of the complex plane). In the case of commensurate delays, $h_j = jh$, h is the *basic delay*, the matrix $U(\tau)$ can be constructed via the semianalytic method which provides a solution to (A.3-A.5) by computing a matrix exponential Kharitonov (2012). Necessary stability conditions formulated exclusively in terms of the delay Lyapunov matrix were introduced in Egorov & Mondié (2014):

Theorem 5. *Egorov & Mondié (2014) If system (A.1) is exponentially stable, then*

$$K_r(\tau_1, ..., \tau_r) = \{U(-\tau_i + \tau_j)\}_{i,j=1}^{r} > 0,$$

where $\tau_k \in [0, H]$, $k = \overline{1, r}$, $\tau_i \neq \tau_j$ *if* $i \neq j$, *and* r *is a natural number.*

A.2 Necessary and sufficient stability conditions for systems with distributed delays

Theorem 6. Egorov et al. (2017) *System (A.1) is exponentially stable if and only if the Lyapunov condition holds and for every natural number $r \geq 2$,*

$$\left\{ U\left(\frac{j-i}{r-1}H\right)\right\}_{i,j=1}^{r} > 0. \tag{A.6}$$

Moreover, if the Lyapunov condition holds and system (A.1) is unstable, there exists r such that

$$\left\{ U\left(\frac{j-i}{r-1}H\right)\right\}_{i,j=1}^{r} \ngtr 0.$$

Appendix B

Stabilization based on σ-stability analysis

In this appendix we present the change of variable that needs to be done to stabilize the delay system with a prescribed exponential decay. The control parameters are tuned so that closed-loop σ-stability is achieved. Of course, the largest possible decay is of special interest.

σ-Stability analysis. For the linear system (A.1) the change of variable,

$$z(t) = e^{\sigma t} x(t) \tag{B.1}$$

is such that the stability of the linear system

$$\dot{z}(t) = [\mathcal{A}_0 + \sigma I]\, z(t) + \sum_{j=1}^{m} \mathcal{A}_j e^{\sigma h_j} z(t - h_j)$$

is equivalent to the σ-stability of (A.1).

Appendix C

Robust stability conditions

In this appendix robust stability conditions for systems with multiple concentrated delays are presented. In specific, time-variant matrix perturbations are considered.

Robust stability. Consider a perturbed system of the form

$$\dot{y}(t) = \sum_{j=0}^{m}(A_j + \Delta_j(t))y(t - h_j) \tag{C.1}$$

where, $\Delta_j(t),\ j = \overline{0,m}$ are continuous bounded matrix valued functions on $[0,\infty)$. Its robust stability can be assessed by the following result:

Theorem 7. *Kharitonov (2012) Let system (A.1) be exponentially stable. The perturbed system (C.1) remains exponentially stable for any $t \geq 0$ if it satisfies*

$$\|\Delta(t)\| = \sqrt{\sum_{j=0}^{m}\|\Delta_j(t)\|^2} < \frac{\lambda_{min}}{2\nu}\left(1 + \sum_{j=1}^{m} h_j a_j^2\right)^{-\frac{1}{2}} \tag{C.2}$$

where

$$a_j = \|A_j\|,\ j = \overline{0,m}, \qquad \lambda_{min} = \min_{0\leq j\leq 2m}\{\lambda_{min}(W_j)\},$$
$$\nu \ = \ \max_{\tau\in[0,H]}\|U(\tau)\|.$$

The value of ν is found by using the results in Egorov & Mondié (2015).

Appendix D

Kronecker product of matrices

In this appendix the definition of the Kronecker product of matrices is reminded. The operation allows to express a system of matrix differential equations in vector form.

Kronecker product. Let Q be a $n \times n$ matrix, and let $vec(Q) = q$ be a $n^2 \times 1$ vector that includes the stacked columns of Q. The operation

$$vec(AQB) = (B^T \otimes A)vec(Q),$$

$$with \quad B^T \otimes A = \begin{bmatrix} b_{1,1}A & b_{2,1}A & \dots & b_{n,1}A \\ b_{1,2}A & b_{2,2}A & \dots & b_{n,2}A \\ \vdots & \vdots & & \vdots \\ b_{1,n}A & b_{2,n}A & \dots & b_{n,n}A \end{bmatrix},$$

is a $n^2 \times n^2$ matrix called the Kronecker product of matrices A and B.

Bibliography

Administration, N. H. T. S. *et al.* (2016). 2015 motor vehicle crashes: overview. *Traffic safety facts research note* **2016**, 1–9.

Alexandrova, I. V. (2018). New robustness bounds for neutral type delay systems via functionals with prescribed derivative. *Applied Mathematics Letters* **76**, 34–39.

Alexandrova, I. V. & Zhabko, A. P. (2018). A new LKF approach to stability analysis of linear systems with uncertain delays. *Automatica* **91**, 173–178.

Aliseyko, A. N. (). Lyapunov matrices for a class of systems with exponential kernel. *St Petersburg State University* .

Aliseyko, A. N. (2019). Lyapunov matrices for a class of time-delay systems with piecewise-constant kernel. *International Journal of Control* **92**(6), 1298–1305.

Bando, M., Hasebe, K., Nakanishi, K. & Nakayama, A. (1998). Analysis of optimal velocity model with explicit delay. *Physical Review E* **58**(5), 5429.

Bekiaris-Liberis, N., Roncoli, C. & Papageorgiou, M. (2017). Predictor-based adaptive cruise control design. *IEEE Transactions on Intelligent Transportation Systems* .

Bellman, R. E. & Cooke, K. L. (1963). Differential-difference equations .

Bose, A. & Ioannou, P. A. (2003). Analysis of traffic flow with mixed manual and semiautomated vehicles. *IEEE Transactions on Intelligent Transportation Systems* **4**(4), 173–188.

Caveney, D. (2010). Cooperative vehicular safety applications. *IEEE Control Systems* **30**(4), 38–53.

Chandler, R. E., Herman, R. & Montroll, E. W. (1958). Traffic dynamics: studies in car following. *Operations research* **6**(2), 165–184.

Cuvas, C., Mondié, S. & Ochoa, G. (2015). Distributed delay systems with truncated gamma distribution: instability regions. *IFAC-PapersOnLine* **48**(12), 239–244.

Desjardins, C. & Chaib-Draa, B. (2011). Cooperative adaptive cruise control: A reinforcement learning approach. *IEEE Transactions on intelligent transportation systems* **12**(4), 1248–1260.

Egorov, A. V., Cuvas, C. & Mondié, S. (2017). Necessary and sufficient stability conditions for linear systems with pointwise and distributed delays. *Automatica* **80**, 218–224.

Egorov, A. V. & Mondié, S. (2014). Necessary stability conditions for linear delay systems. *Automatica* **50**(12), 3204–3208.

Egorov, A. V. & Mondié, S. (2015). The delay Lyapunov matrix in robust stability analysis of time-delay systems. *Proceedings of the 12th IFAC Workshop on Time Delay Systems,* **48**(12), 245–250.

Feng, Z. & Lam, J. (2011). Integral partitioning approach to stability analysis and stabilization of distributed time delay systems. *Proceedings of the 18th World Congress The International Federation of Automatic Control Milano , Italy* **44**(1), 5094–5099.

Gouaisbaut, F. & Ariba, Y. (2009). Delay range stability of distributed time delay systems. *6th IFAC Symposium on Robust Control Design, Haifa, Israel* **42**(6), 225–230.

Hajdu, D., Zhang, L., Insperger, T. & Orosz, G. (2016). Robust stability analysis for connected vehicle systems .

Hale, J. K. & Lunel, S. M. V. (2013). *Introduction to functional differential equations*, vol. 99. Springer Science & Business Media.

Helbing, D. (2001). Traffic and related self-driven many-particle systems. *Reviews of modern physics* **73**(4), 1067.

Helbing, D. & Treiber, M. (1998). Gas-kinetic-based traffic model explaining observed hysteretic phase transition. *Physical Review Letters* **81**(14), 3042.

HUANG, W. (1989). Generalization of Liapunov's theorem in a linear delay system. *Journal of Mathematical Analysis and Applications* **142**(1), 83–94.

IOANNOU, P. A. & CHIEN, C.-C. (1993). Autonomous intelligent cruise control. *IEEE Transactions on Vehicular technology* **42**(4), 657–672.

JIN, I. G. & OROSZ, G. (2014). Dynamics of connected vehicle systems with delayed acceleration feedback. *Transportation Research Part C: Emerging Technologies* **46**, 46–64.

JIN, I. G. & OROSZ, G. (2015). Optimized connected cruise control with time delay. *IFAC-PapersOnLine* **48**(12), 468–473.

JUÁREZ, L. & MONDIÉ, S. (2018a). Lyapunov matrices for the stability analysis of a multiple distributed time-delay system with piecewise-function kernel. *IEEE Conference on Decision and Control* , 6216–6221.

JUÁREZ, L. & MONDIÉ, S. (2018b). Lyapunov matrices for the stability analysis of a multiple distributed time-delay system with repeated piecewise function kernel. *Memorias del Congreso Nacional de Control Automático* .

JUÁREZ, L. & MONDIÉ, S. (2018c). Lyapunov matrices for the stability analysis of a system with state and input delays and dynamic predictor control. In: *2018 15th International Conference on Electrical Engineering, Computing Science and Automatic Control (CCE)*. IEEE.

JUÁREZ, L. & MONDIÉ, S. (2019). Dynamic predictor-based controls: a time-domain stability analysis. *IEEE Latin America Transactions* **17**(07), 1207–1213.

JUÁREZ, L., MONDIÉ, S. & CUVAS, C. (2018). Connected cruise control of a car platoon: A time-domain stability analysis. *Proceedings of the Institution of Mechanical Engineers, Part I: Journal of Systems and Control Engineering* **232**(6), 672–682.

JUÁREZ, L., MONDIÉ, S. & KHARITONOV, V. L. (2020). Dynamic predictor for systems with state and input delay: A time-domain robust stability analysis. *International Journal of Robust and Nonlinear Control* .

KENNEY, J. B. (2011). Dedicated short-range communications (DSRC) standards in the united states. *Proceedings of the IEEE* **99**(7), 1162–1182.

Kharitonov, V. L. (2006). Lyapunov matrices for a class of time delay systems. *Systems & Control Letters* **55**(7), 610–617.

Kharitonov, V. L. (2012). *Time-delay systems: Lyapunov functionals and matrices.* Springer Science & Business Media.

Kharitonov, V. L. (2014). An extension of the prediction scheme to the case of systems with both input and state delay. *Automatica* **50**(1), 211–217.

Kharitonov, V. L. (2015). Predictor-based controls: the implementation problem. *Differential Equations* **51**(13), 1675–1682.

Kharitonov, V. L. & Zhabko, A. P. (2001). Lyapunov-Krasovskii approach to robust stability of time delay systems. *IFAC Proceedings Volumes* **34**(13), 477–481.

Kolmanovskii, V. (1967). Application of the Liapunov method to linear systems with lag: PMM. *Journal of Applied Mathematics and Mechanics* **31**(5), 959–963.

Krasovskii, N. (1956). On the application of the second method of Lyapunov for equations with time delays. *Prikl. Mat. Mekh* **20**(3), 315–327.

Li, N. I. & Orosz, G. (2016). Dynamics of heterogeneous connected vehicle systems. *IFAC-PapersOnLine* **49**(10), 171–176.

Medvedeva, I. V. (2015). Exponential estimates for solutions of linear systems with distributed delay. *Proceedings of 2015 International Conference "Stability and Control Processes" in Memory of VI Zubov,* , 285–287.

Medvedeva, I. V. & Zhabko, A. P. (2015). A novel approach to robust stability analysis of linear time-delay systems. *Proceedings of the 12th IFAC Workshop on Time Delay Systems,* **48**(12), 233–238.

Milanés, V., Shladover, S. E., Spring, J., Nowakowski, C., Kawazoe, H. & Nakamura, M. (2014). Cooperative adaptive cruise control in real traffic situations. *IEEE Trans. Intelligent Transportation Systems* **15**(1), 296–305.

Mondié, S. & Michiels, W. (2003). Finite spectrum assignment of unstable time-delay systems with a safe implementation. *IEEE Transactions on Automatic Control* **48**(12), 2207–2212.

MONTANARO, U., TUFO, M., FIENGO, G., DI BERNARDO, M., SALVI, A. & SANTINI, S. (2014). Extended cooperative adaptive cruise control. In: *Intelligent Vehicles Symposium Proceedings, 2014 IEEE*. IEEE.

NAJAFI, M., HOSSEINNIA, S., SHEIKHOLESLAM, F. & KARIMADINI, M. (2013). Closed-loop control of dead time systems via sequential sub-predictors. *International Journal of Control* **86**(4), 599–609.

NAUS, G. J., VUGTS, R. P., PLOEG, J., VAN DE MOLENGRAFT, M. J. & STEINBUCH, M. (2010). String-stable CACC design and experimental validation: A frequency-domain approach. *IEEE Transactions on vehicular technology* **59**(9), 4268–4279.

NEIMARK, J. (1949). D-subdivisions and spaces of quasi-polynomials. *Prikladnaya Matematika i Mekhanika* **13**(5), 349–380.

OROSZ, G. (2016). Connected cruise control: modelling, delay effects, and nonlinear behaviour. *Vehicle System Dynamics* **54**(8), 1147–1176.

OROSZ, G., KRAUSKOPF, B. & WILSON, R. E. (2005). Bifurcations and multiple traffic jams in a car-following model with reaction-time delay. *Physica D: Nonlinear Phenomena* **211**(3-4), 277–293.

OROSZ, G., WILSON, R. E. & KRAUSKOPF, B. (2004). Global bifurcation investigation of an optimal velocity traffic model with driver reaction time. *Physical Review E* **70**(2), 026207.

OROSZ, G., WILSON, R. E. & STÉPÁN, G. (2010). Traffic jams: dynamics and control.

PIPES, L. A. (1953). An operational analysis of traffic dynamics. *Journal of applied physics* **24**(3), 274–281.

QIN, W. B., GOMEZ, M. M. & OROSZ, G. (2017). Stability and frequency response under stochastic communication delays with applications to connected cruise control design. *IEEE Trans. Intelligent Transportation Systems* **18**(2), 388–403.

RAJAMANI, R. & ZHU, C. (2002). Semi-autonomous adaptive cruise control systems. *IEEE Transactions on Vehicular Technology* **51**(5), 1186–1192.

RODRÍGUEZ-GUERRERO, L., KHARITONOV, V. L. & MONDIÉ, S. (2016). Robust stability of dynamic predictor based control laws for input and state delay systems. *Systems & Control Letters* **96**, 95–102.

Rothery, R., Gartner, N., Messner, C. & Rathi, A. (1998). Traffic flow theory. *Transportation Research Board Special Report* **165**.

Sepulcre, M. & Gozalvez, J. (2012). Experimental evaluation of cooperative active safety applications based on V2V communications. In: *Proceedings of the ninth ACM international workshop on Vehicular inter-networking, systems, and applications*. ACM.

Shladover, S. E. (1991). Longitudinal control of automotive vehicles in close-formation platoons. *Journal of dynamic systems, measurement, and control* **113**(2), 231–241.

Sipahi, R., Atay, F. M. & Niculescu, S.-I. (2007). Stability of traffic flow behavior with distributed delays modeling the memory effects of the drivers. *SIAM Journal on Applied Mathematics* **68**(3), 738–759.

Sipahi, R. & Niculescu, S.-I. (2008). Chain stability in traffic flow with driver reaction delays. In: *American Control Conference, 2008*. IEEE.

Sipahi, R. & Niculescu, S.-I. (2009). Deterministic time-delayed traffic flow models: A survey. In: *Complex Time-Delay Systems*. Springer, pp. 297–322.

Sipahi, R. & Niculescu, S.-I. (2010). Stability of car following with human memory effects and automatic headway compensation. *Philosophical Transactions of the Royal Society of London A: Mathematical, Physical and Engineering Sciences* **368**(1928), 4563–4583.

Sipahi, R., Niculescu, S.-I. & Delice, I. I. (2009). Asymptotic stability of constant time headway driving strategy with multiple driver reaction delays. In: *American Control Conference, 2009. ACC'09*. IEEE.

Stankovic, S. S., Stanojevic, M. J. & Siljak, D. D. (2000). Decentralized overlapping control of a platoon of vehicles. *IEEE Transactions on Control Systems Technology* **8**(5), 816–832.

Suthaputchakun, C., Sun, Z. & Dianati, M. (2012). Applications of vehicular communications for reducing fuel consumption and CO2 emission: The state of the art and research challenges. *IEEE Communications Magazine* **50**(12).

Swaroop, D. (1997). String stability of interconnected systems: An application to platooning in automated highway systems .

Swaroop, D., Hedrick, J. K. & Choi, S. B. (2001). Direct adaptive longitudinal control of vehicle platoons. *IEEE Transactions on Vehicular Technology* **50**(1), 150–161.

Treiber, M. & Helbing, D. (1999). Macroscopic simulation of widely scattered synchronized traffic states. *Journal of Physics A: Mathematical and General* **32**(1), L17.

Treiber, M., Hennecke, A. & Helbing, D. (2000). Congested traffic states in empirical observations and microscopic simulations. *Physical review E* **62**(2), 1805.

Treiber, M., Kesting, A. & Helbing, D. (2006). Delays, inaccuracies and anticipation in microscopic traffic models. *Physica A: Statistical Mechanics and its Applications* **360**(1), 71–88.

Wang, J., Wang, J. & Wang, R. (2016). Trajectory replanning in V2V lane exchanging with consideration of driver preferences. In: *American Control Conference (ACC), 2016*. American Automatic Control Council (AACC).

Zhang, L. & Orosz, G. (2013). Designing network motifs in connected vehicle systems: delay effects and stability. In: *ASME 2013 Dynamic Systems and Control Conference*. American Society of Mechanical Engineers.

Zhang, L. & Orosz, G. (2016). Motif-based design for connected vehicle systems in presence of heterogeneous connectivity structures and time delays. *IEEE Transactions on Intelligent Transportation Systems* **17**(6), 1638–1651.

Zhou, B., Lin, Z. & Duan, G.-R. (2012). Truncated predictor feedback for linear systems with long time-varying input delays. *Automatica* **48**(10), 2387–2399.

Zhou, B., Liu, Q. & Mazenc, F. (2017). Stabilization of linear systems with both input and state delays by observer–predictors. *Automatica* **83**, 368–377.

Zhou, J. & Peng, H. (2005). Range policy of adaptive cruise control vehicles for improved flow stability and string stability. *IEEE Transactions on intelligent transportation systems* **6**(2), 229–237.